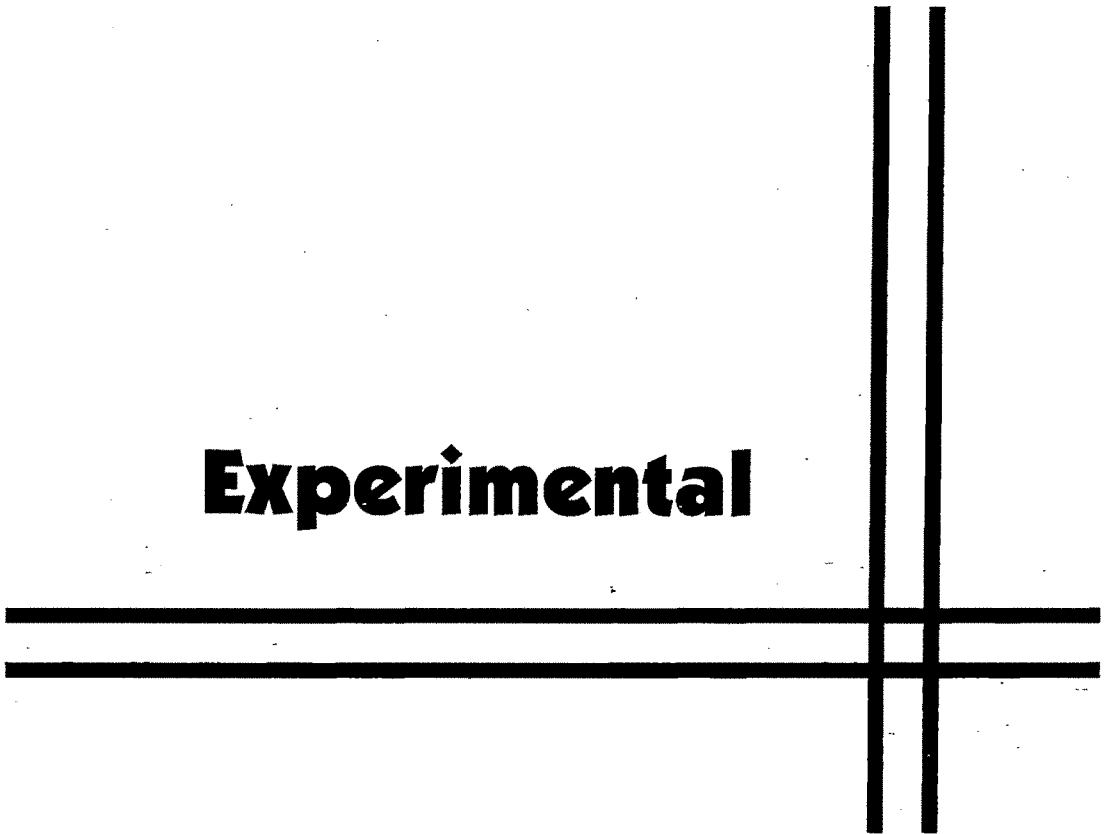
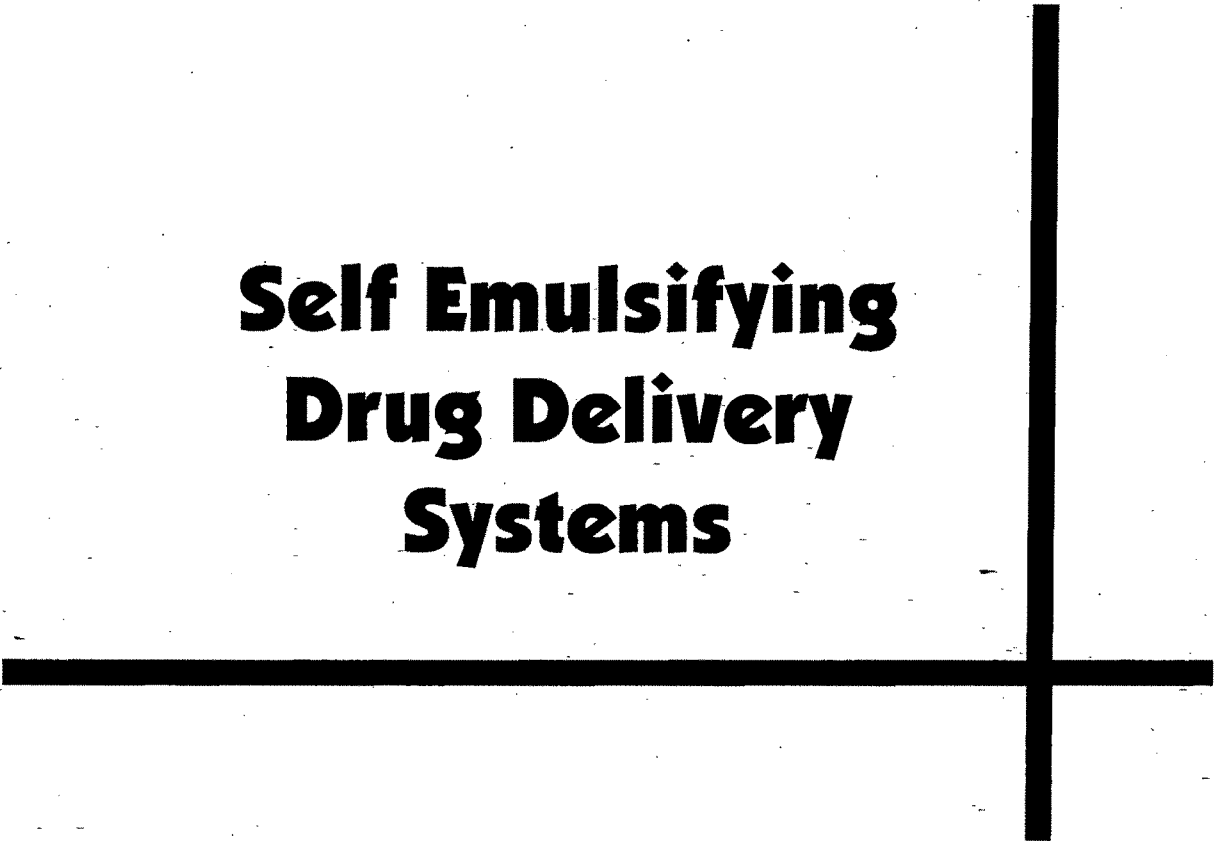


Experimental



Self Emulsifying Drug Delivery Systems



2.1. Self Emulsifying Drug Delivery Systems

2.1.1. Materials

Carbamazepine (CBZ), Oxcarbamazepine (OCBZ), Gabapentin (GPN) were received as gift samples from Relax Pharmaceuticals Limited, Vadodara, India, Torrent Research Center, Ahmedabad, India and Sun Pharmaceuticals Limited, Vadodara, India respectively. Labrasol® (Caprylocaproyl macrogolglycerides EP), Labrafac CC (Medium chain triglyceride EP), Transcutol® (Diethylene glycol monoethyl ether EP and USP – NF) and Lauroglycol FCC (Propylene glycol laureate FCC), all Gattefosse ingredients were received as generous gift sample from Colorcon Asia Pvt. Ltd., Goa, India. Hard gelatin capsule shells were obtained from Sunil Synchem Ltd (Ahmedabad, India). Propylene glycol, Polyethylene glycol 600, Glycerin, Tween 80 (polysorbate 80) and HPLC solvents were purchased from S. D. Fine-Chem Ltd., Mumbai, India. All the other chemicals and solvents were of analytical grade and were used without further purification. Deionized double-distilled water was used through out the study.

2.1.2. Methods

2.1.2.1. Construction of SEDDS

(Shah, *et al.*, 1994, Shah, 1994, Charman, *et al.*, 1992, Pouton, 1985, Nazzari, *et al.*, 2002.)

Selection of Excipients

It is believed that lipophilic surfactants with hydrophilic lipophilic balance (HLB) < 10 are capable of encouraging emulsification of the oil (lipophilic drug), but the resulting emulsions are normally too rudimentary (having erratic particle size) to be useful. However compared to lipophilic surfactants hydrophilic surfactants with HLB > 10 are much superior providing fine, consistent emulsion droplets. Also such fine droplets are supposed to get emptied rapidly from the stomach (Lacy and Embleton, **1997**). Furthermore, finer the particle larger is the surface area which facilitates faster and more complete absorption. However it is advised to derive a right blend of low and high HLB surfactants that leads to the formation of a stable microemulsion upon exposure to water (Kommuru, *et al.*, **2001**). Therefore, based on these considerations, two high value surfactants (Labrafac CC and Labrasol) and two low HLB value surfactants (transcutol and lauroglycol) were selected. All the 3 drugs were screened for maximum solubility in these surfactants. Accordingly, formulations were developed and were subjected to further characterization.

Saturation solubility was measured with the help of modified test tube shaker. Weighed amount of drug was added to 5 ml of surfactants in 7 mL screw capped test tubes. Test

tubes were shaken in 360° rotation for complete whirling motion of the contents. Contents were equilibrated for 24 hours. The supernatant was filtered through 0.42 µm syringe tip filter. First 0.5 ml of supernatant was discarded and rest was collected in glass vials. CBZ and OCBZ were analyzed by validated UV spectrophotometry method at 257 and 303 nm respectively. (Shimadzu, 1601 UV-visible Spectrophotometer, Kyoto, Japan). Whereas GPN was analyzed using validated HPLC method. Labrasol and transcitol were found to undertake highest drug load.

Preparation of SEDDS

SEDDS formulations for CBZ, OCBZ and GPN were designed using simplex centroid mixture design. A simplex is the simplest figure having $n+1$ boundary points in n -dimensional space. A simplex region for 2 components is a straight line, for 3 components a triangle, for 4 components a tetrahedron and so on. A simplex centroid design consisted of all points that are equally weighted mixtures of 1 to Q components. These include permutations of

Pure blends: (1, 0, ..., 0)

Binary blends: (1/2, 1/2, 0, ..., 0)

Tertiary blends: (1/3, 1/3, 1/3, 0, ..., 0)

and so on to the overall centroid: (1/ Q , 1/ Q , ..., 1/ Q)

(Design-Expert version 6.0.5, by Stat-Ease Inc. Minneapolis, MN).

The three ingredients, (drug, surfactant and cosurfactant) were mixed in 50 mL beaker with gentle stirring on magnetic stirrer. Each mixture was analyzed for particle size, visual inspection of self emulsification and drug dissolution studies. To discriminate Self emulsification from solution, dispersion and immiscible mixture, simple visual inspection method was used (Craig, *et al.*, **1995**). According to this method 3 ml of prepared system was diluted with 50 ml of SGF in a glass beaker at 37°C and the contents were gently mixed with a magnetic stirrer. The propensity of system to emulsify spontaneously and the progress of emulsion droplets (increase in droplet size) were observed. The tendency to form an emulsion was judged as 'good' when droplets spread easily in water and formed a fine milky emulsion, and it was judged 'bad' when there was poor or no emulsion formation with immediate coalescence of oil droplets, especially when stirring was stopped. Phase diagrams were constructed for identification of the good self-emulsifying region. All studies were performed in triplicate, with similar observations being made between repeats. Resultant system was visually inspected for droplet size, droplet uniformity and droplet stability (time taken to coalescence) (Kommuru, Gurley, Khan and Reddy, **2001**).

An attempt was made to prepare unit dosage formulation of SEDDS by filling them in hard gelatin capsules. Measured quantities of prepared SEDDS were filled in hard gelatin capsules with the help of pipette. Unfortunately due to high levels of moisture content of the ingredients used in SEDDS formulation the capsule shells were not able to retain the contents in integral condition. SEDDS formulated in this way has to be dispensed as oral

liquid dosage form. This liquid dosage form was packaged in USP type 1 glass vials for further storage.

2.1.2.2. Evaluation of SEDDS

2.1.2.2.1. Particle size evaluation

For all the batches of experimental design, prior and after self emulsification particle size analyses were carried out on Malvern Zetasizer ZS. For self emulsification, systems were subjected to dilution with 250 ml of simulated gastric fluid (SGF) USP XXVII without enzymes having pH 1.2, same that was used for *in vitro* drug dissolution studies.

2.1.2.2.2. In vitro drug dissolution

All the formulations of experimental design for CBZ, OCBZ and GPN were assessed for *in vitro* drug dissolution studies. Measured amount of sample was delivered in dissolution vessel with the help of pipette. A total volume of deaerated 250 mL Simulated gastric fluid (SGF) USP XXVII without enzymes having pH 1.2 was used as dissolution medium maintained at $37 \pm 1^\circ\text{C}$ with constant stirring speed of 50 RPM. Dissolution studies were carried out in USP XXIV type II dissolution apparatus (Veego, Mumbai, India) with a 400 mL Schott Duran beaker as a dissolution vessel. Samples (5 mL) were withdrawn at 0, 5, 10, 15, 20, 25 and 30 minutes and filtered through 0.45 μm whatmann filter paper. The first 1 mL of filtrate was discarded. The filtrate obtained was diluted suitably and analysed spectrophotometrically at 257 and 303 nm for carbamazepine and oxcarbamazepine respectively. Samples of GPN SEDDS dissolution studies were analyzed using HPLC. Sink conditions were maintained by addition of an equal volume of fresh dissolution medium maintained at the same temperature. The absorbance values were transformed to concentration by reference to a standard calibration curve obtained experimentally.

The purpose of carrying out dissolution studies in 250 mL dissolution medium was to get discriminatory results for drug dissolution pattern. Preliminary studies in 900 mL dissolution medium yielded inequitable results.

Although in routine analysis also dissolution samples are filtered the specific purpose here was due to appearance of drug in different states in the dissolution medium. Some amount of free drug, dissolved or solubilized molecules (either in the form of emulsions or micelles along with precipitated solid particles). Since the drug load is considerably higher supersaturation results which results in subsequent precipitation of the drug. These precipitated particles may grow significantly during the dissolution test. For this reason dissolution medium was filtered through 0.45 μm filter.

2.1.3. Results and Discussion

SEDDS of CBZ

2.1.4. SEDDS of CBZ using Vit. E as oil phase

The use of natural and synthetic lipids has generated much academic and commercial interest as a potential formulation strategy for improving the oral bioavailability of poorly water soluble drugs. Lipid-based formulations can reduce the inherent limitations of slow and incomplete dissolution of poorly water soluble drugs, and facilitate the formation of solubilised phases from which absorption may occur (Humberstone and Charman, **1997**). Considering this hypothesis Vitamin E, natural oil was studied for its ability to dissolve CBZ. Table 2.1.1 shows the quantitative solubility data for CBZ in various solvents. From results it was observed that transcitol showed highest solubility for CBZ. Vit. E showed less solubility compared to labrasol. It is well known fact that use of oils or lipophilic substances, bioavailability of drug is increased. Hence Vit E was used for further studies.

Table 2.1.1 Quantitative solubility data for CBZ in various solvents

Solvents	Solubility of CBZ (g/100 mL)
Water	0.0091
Vit. E	0.1306
Labrasol	0.3217
Labrafac CC	0.2954
Transcutol	0.5314
Lauroglycol	0.4121

Table 2.1.1 gives the values for experimental levels of components of mixture design along with their corresponding response values. To prevent bias, experimental runs were performed in random order. It was observed that an optimum concentration of all the three components was required for the enhancement of CBZ dissolution.

Table 2.1.3 gives the coefficient and standard error values of model analyzed for response particle size and percent drug dissolved.

Figure 2.1.1 and Figure 2.1.2 gives the contour graphs for particle size and percent drug dissolved of the analyzed model.

Figure 2.1.3 gives the particle size data measured using Malvern Zetasizer.

Table 2.1.2 Distribution of Simplex centroid mixture design experiments and results for the measured responses.

Experimental sequence	Run	Factors/Levels			Response	
		CBZ	Vitamin E	Transcutol	% CBZ dissolved	Particle size (nm)
12	1	0.00	0.00	1.00	0.00	8.24
1	2	1.00	0.00	0.00	12.39	60000.00
6	3	0.00	0.50	0.50	0.00	3.14
9	4	0.17	0.67	0.17	98.67	342.25
8	5	0.67	0.17	0.17	55.47	500.25
2	6	0.00	1.00	0.00	0.00	14.14
4	7	0.50	0.50	0.00	25.14	416.25
5	8	0.50	0.00	0.50	75.47	360.25
3	9	0.00	0.00	1.00	0.00	3.21
10	10	0.17	0.17	0.67	95.47	352.67
13	11	0.00	1.00	0.00	0.00	5.64
11	12	1.00	0.00	0.00	0.00	64000.00
7	13	0.33	0.33	0.33	80.25	400.15

Table 2.1.3 ANOVA results for model analysis of CBZ Vit E SEDDS.

Component	Coefficient for particle size	Standard Error	Coefficient for % drug dissolved	Standard Error
A-CBZ	59744.80	4445.69	0.31	20.39
B-Vit E	701.04	4445.69	4.17	20.39
C-Transcutol	701.22	4445.69	1.32	20.39
AB	-122197.50	25477.59	181.43	116.87
AC	-122387.05	25477.59	365.62	116.87
BC	17842.79	25477.59	136.50	116.87

Figure 2.1.1 Contour profile of particle size for the mixture design of CBZ Vit E SEDDS.

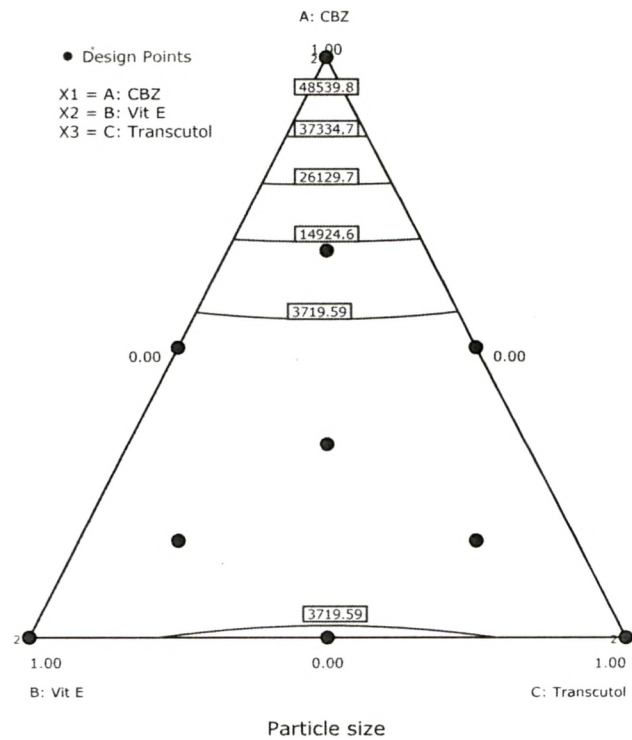


Figure 2.1.2 Contour profile of percent drug dissolved for the mixture design of CBZ Vit E SEDDS.

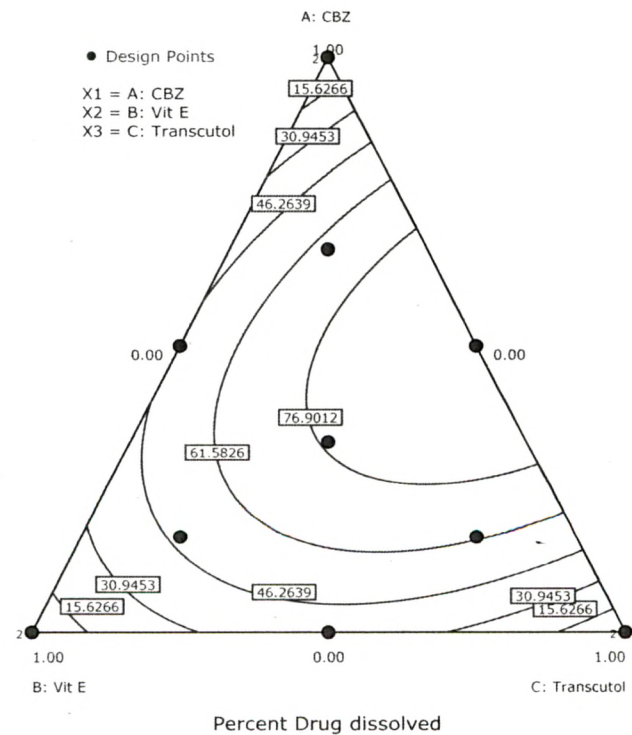
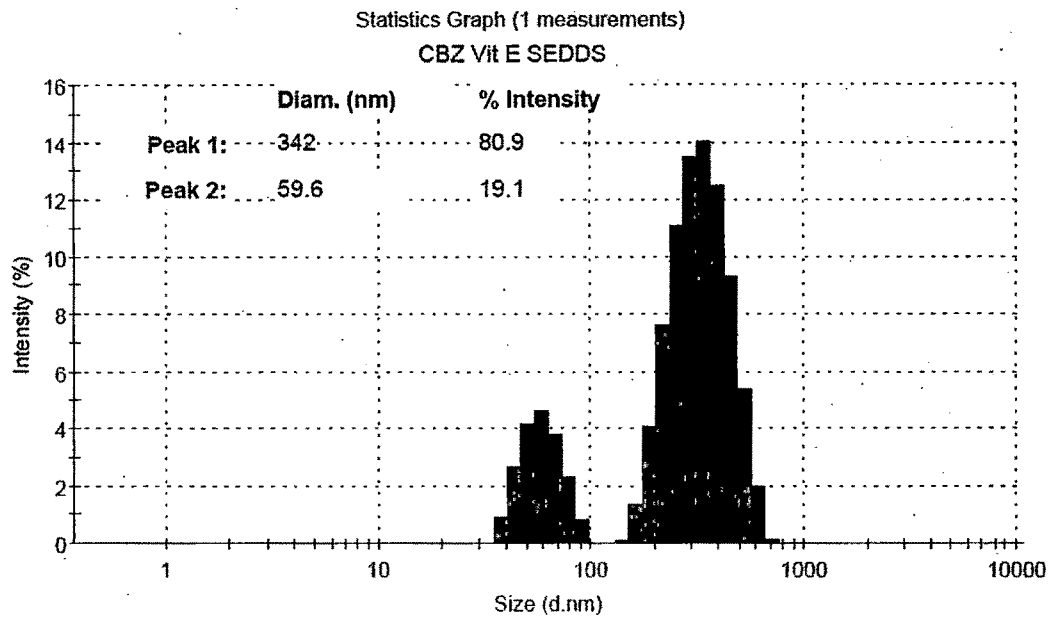


Figure 2.1.3 Particle size distribution for CBZ Vit E SEDDS.

2.1.5. SEDDS of CBZ using Labrasol

Table 2.1.4 gives the values for experimental levels of components of mixture design along with their corresponding response values. To prevent bias, experimental runs were performed in random order. It was observed that an optimum concentration of all the three components was required for the enhancement of CBZ dissolution.

Table 2.1.5 gives the coefficient and standard error values of model analyzed for response particle size and percent drug dissolved.

Figure 2.1.4 shows the contour graphs for particle size and percent drug dissolved of the analyzed model. Whereas Figure 2.1.6 gives the particle size data measured using Malvern zetasizer.

Table 2.1.4 Distribution of Simplex centroid mixture design experiments and results for the measured responses.

Experimental sequence	Run	Factors/Levels			Response	
		CBZ	Labrasol	Transcutol	% CBZ dissolved	Particle size (nm)
6	1	0.00	0.50	0.50	0.00	1.64
12	2	0.00	0.00	1.00	0.00	2.14
1	3	1.00	0.00	0.00	23.45	700000.00
8	4	0.67	0.17	0.17	75.64	341.02
2	5	0.00	1.00	0.00	0.00	12.36
3	6	0.00	0.00	1.00	0.00	14.17
4	7	0.50	0.50	0.00	65.47	400.25
5	8	0.50	0.00	0.50	55.24	200.64
10	9	0.17	0.17	0.67	97.14	102.35
9	10	0.17	0.67	0.17	92.47	110.25
7	11	0.33	0.33	0.33	88.47	105.45
11	12	1.00	0.00	0.00	25.47	670000.00
13	13	0.00	1.00	0.00	0.00	12.00

Table 2.1.5 ANOVA results for model analysis of CBZ labrasol SEDDS.

Component	Coefficient for particle size	Standard Error	Coefficient for % drug disso.	Standard Error
A-CBZ	660057.50	48795.41	19.71	18.21
B-Labrasol	7664.66	48795.41	1.45	18.21
C-Transcutol	7669.20	48795.41	2.61	18.21
AB	-1369487.04	279639.38	296.88	104.38
AC	-1370226.02	279639.38	262.89	104.38
BC	194523.48	279639.38	128.05	104.38
ABC	660057.50	48795.41	19.71	18.21

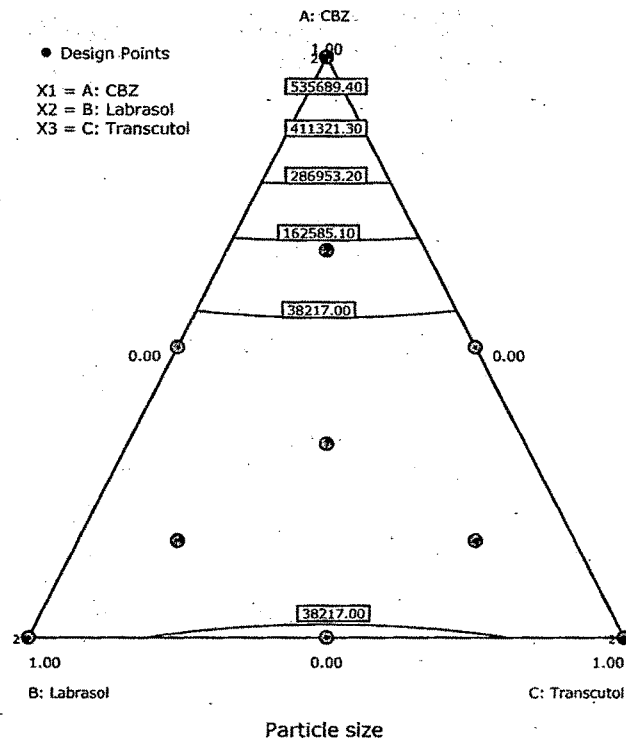
Figure 2.1.4 Contour profile of particle size for the mixture design of CBZ labrasol SEDDS.

Figure 2.1.5 Contour profile of percent drug dissolved for the mixture design of CBZ labrasol SEDDS.

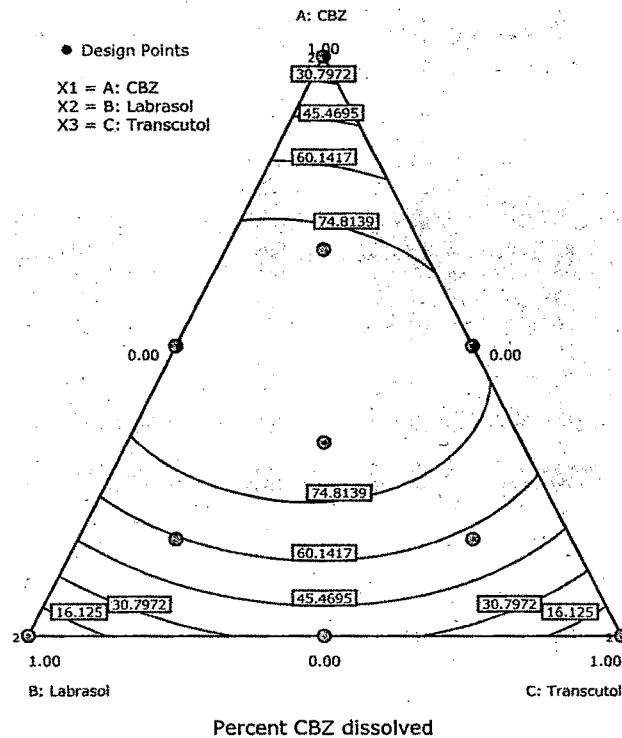
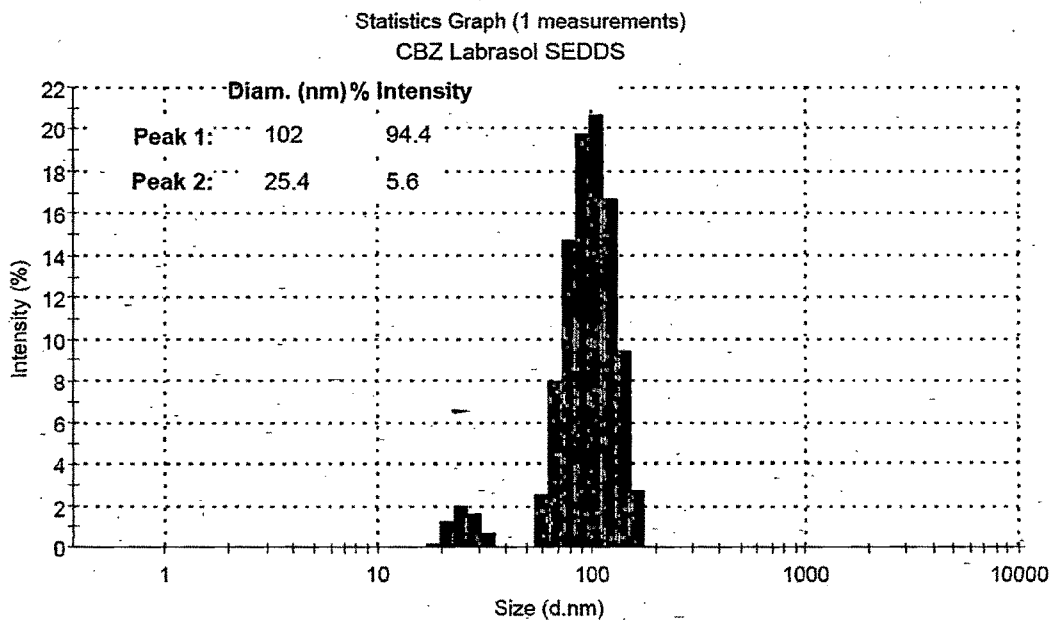


Figure 2.1.6 Particle size distribution for CBZ labrasol SEDDS.



SEDDS of OCBZ

SEDDS for OCBZ was prepared in the same manner that was followed for CBZ SEDDS. The experimental design was kept same to get comparative results of factors.

Table 2.1.6 gives the quantitative solubility data for OCBZ in solvent planned to be used for study. From solubility data it was evident that for surfactants labrasol showed more solubility of OCBZ than labrafac CC, hence it was used for SEDDS preparation. Similarly for selection of cosurfactant transcutool was selected owing to its higher solubilizing capacity for OCBZ.

Table 2.1.7 gives the detailed summary of distribution of Simplex centroid mixture design experiments and results for the measured responses for OCBZ SEDDS formulation.

Table 2.1.6 Quantitative solubility data for OCBZ in various solvents.

Solvents	Solubility of OCBZ (g/100 mL)
Water	0.0101
Labrasol	0.3612
Labrafac CC	0.3214
Transcutol	0.5941
Lauroglycol	0.4813

Table 2.1.7 Distribution of Simplex centroid mixture design experiments and results for the measured responses.

Experimental sequence	Run	Factors/Levels			Response	
		OCBZ	Labrasol	Transcutol	% OCBZ dissolved	Particle size (nm)
14	1	0.00	0.50	0.50	0.00	15.45
3	2	0.00	0.00	1.00	0.00	10.02
5	3	0.50	0.00	0.50	50.25	100.36
2	4	0.00	1.00	0.00	38.57	5.84
10	5	0.17	0.17	0.67	97.58	44.80
9	6	0.17	0.67	0.17	92.47	56.27
11	7	1.00	0.00	0.00	26.47	60000.00
1	8	1.00	0.00	0.00	30.27	65000.00
4	9	0.50	0.50	0.00	46.87	300.00
7	10	0.33	0.33	0.33	86.47	50.17
12	11	0.00	0.00	1.00	0.00	2.25
13	12	0.00	1.00	0.00	0.00	3.61
6	13	0.00	0.50	0.50	0.00	6.47

Table 2.1.8 ANOVA results for model analysis of CBZ labrasol SEDDS.

Component	Coefficient for particle size	Standard Error	Coefficient for % drug disso.	Standard Error
A-OCBZ	60103.92	4327.35	24.52	16.07
B-Labrasol	722.67	4331.63	22.43	16.07
C-Transcutol	731.88	4331.63	4.63	16.07
AB	-121898.81	24562.16	87.96	101.49
AC	-122653.39	24562.16	148.97	101.49
BC	8899.22	20492.13	-23.01	79.84
ABC			1865.76	703.18

Figure 2.1.7 Contour profile of particle size data for the OCBZ SEDDS formulation.

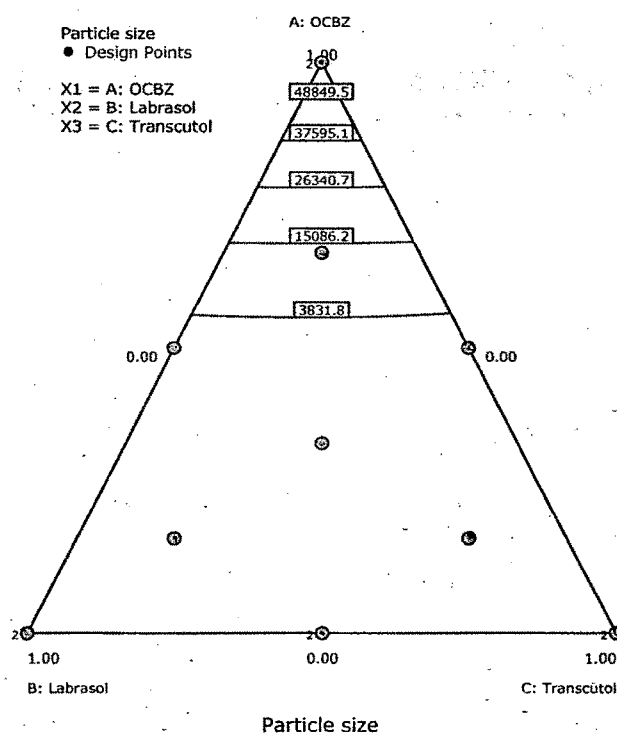


Figure 2.1.8 Contour profile of percent drug dissolved data for the OCBZ SEDDS formulation.

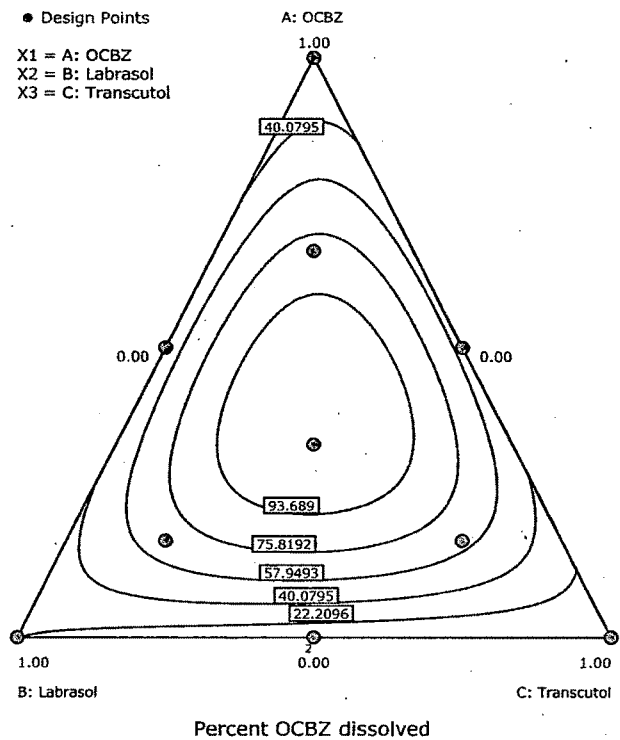
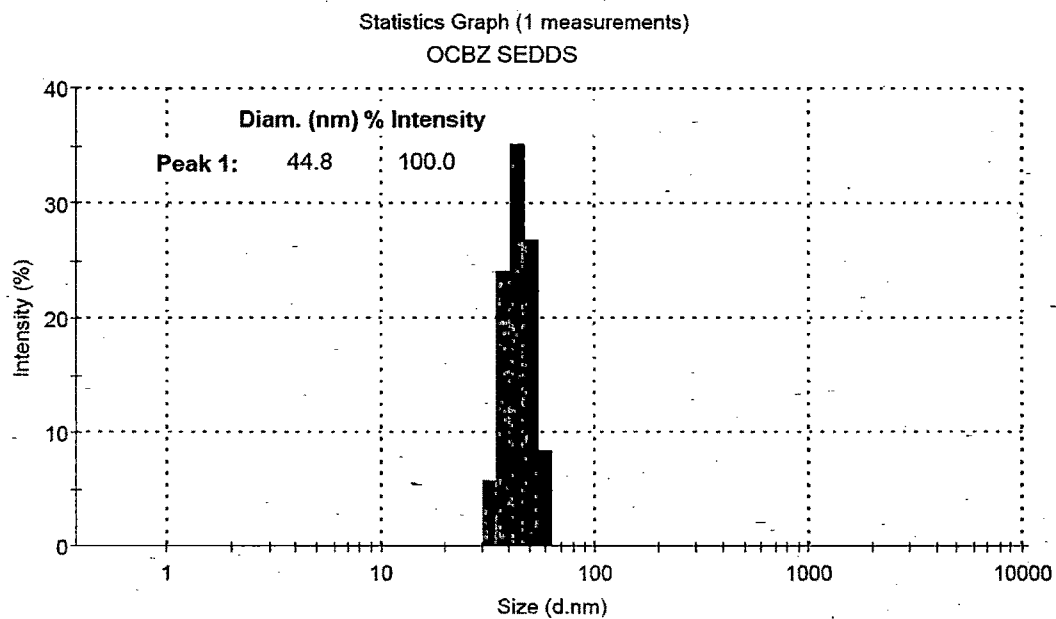


Figure 2.1.9 Particle size distribution of OCBZ SEDDS.



SEDDS of GPN

GPN SEDDS were also prepared in the same manner that was followed for preparation of OCBZ systems. The results of solubility screening of GPN in various surfactant and cosurfactants is tabulated in Table 2.1.9.

Table 2.1.10 gives the values for experimental levels of components of mixture design along with their corresponding response values. To prevent bias experimental runs were performed in random order. It was observed that an optimum concentration of all the three components was required for the enhancement of CBZ dissolution.

Table 2.1.11 gives the coefficient and standard error values of model analyzed for response particle size and percent drug dissolved.

Figure 2.1.10 and Figure 2.1.11 and gives the contour graphs for particle size and percent drug dissolved of the analyzed model respectively.

Figure 2.1.12 gives the particle size data of optimized formulation measured using Malvern zetasizer.

Table 2.1.9 Quantitative solubility data for GPN in various solvents.

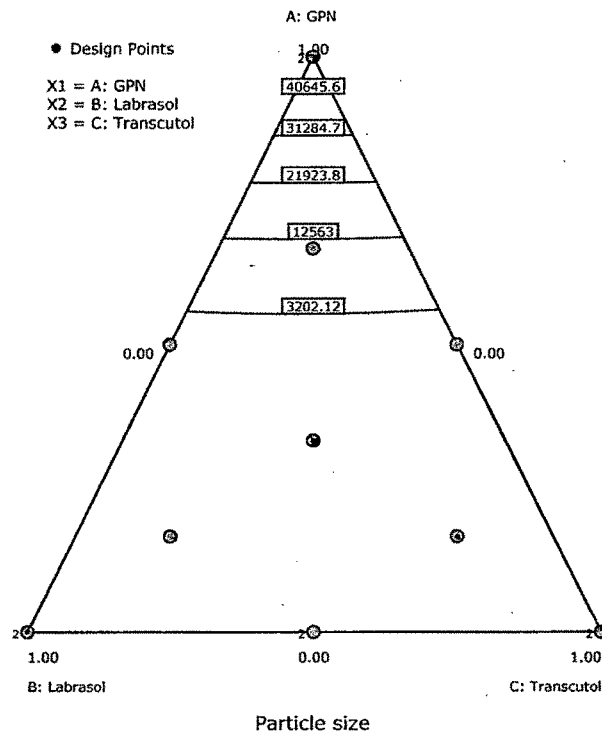
Solvents	Solubility of GPN (g/100 mL)
Water	0.2841
Labrasol	0.3689
Labrafac CC	0.3547
Transcutol	0.5631
Lauroglycol	0.5429

Table 2.1.10 Distribution of Simplex centroid mixture design experiments and results for the measured responses.

Experimental sequence	Run	Factors/Levels			Response	
		GPN	Labrasol	Transcutol	% GPN dissolved	Particle size (nm)
14	1	0.00	0.50	0.50	0.00	20.36
3	2	0.00	0.00	1.00	0.00	10.02
5	3	0.50	0.00	0.50	78.54	100.36
2	4	0.00	1.00	0.00	0.00	5.84
10	5	0.17	0.17	0.67	100.25	77.90
9	6	0.17	0.67	0.17	96.57	56.27
11	7	1.00	0.00	0.00	56.68	54000.00
1	8	1.00	0.00	0.00	62.14	50000.00
4	9	0.50	0.50	0.00	70.25	292.47
7	10	0.33	0.33	0.33	93.21	50.17
12	11	0.00	0.00	1.00	0.00	3.14
13	12	0.00	1.00	0.00	0.00	6.47
6	13	0.00	0.50	0.50	0.00	5.45

Table 2.1.11 ANOVA results for model analysis of GPN SEDDS.

Component	Coefficient for particle size	Standard Error	Coefficient for % drug disso.	Standard Error
A-GPN	50006.44	3594.97	55.47	14.61
B-Labrasol	602.00	3598.53	3.91	14.61
C-Transcutol	614.64	3598.53	4.04	14.61
AB	-101284.49	20405.19	162.01	92.29
AC	-101980.47	20405.19	195.95	92.29
BC	7406.07	17023.98	15.92	72.61
ABC			1474.83	639.43

Figure 2.1.10 Contour profile of particle size data for the GPN SEDDS formulation.**Figure 2.1.11** Contour profile of percent drug dissolved data for the GPN SEDDS formulation.

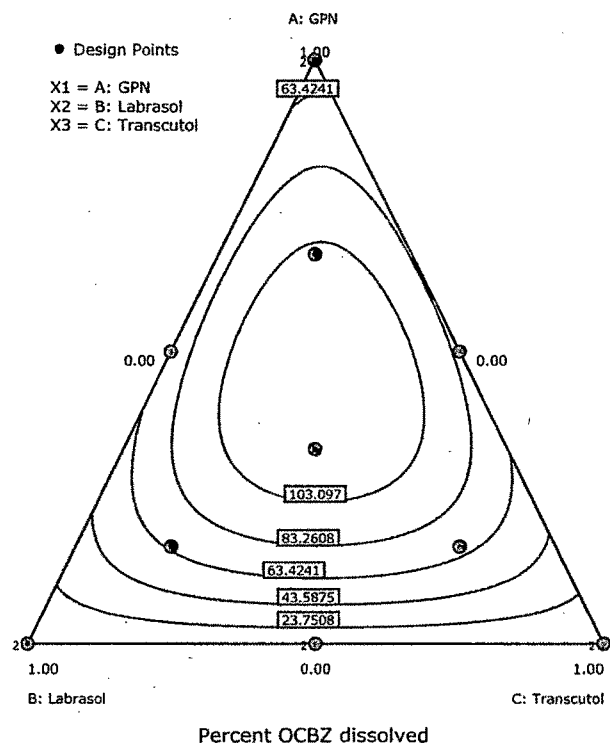
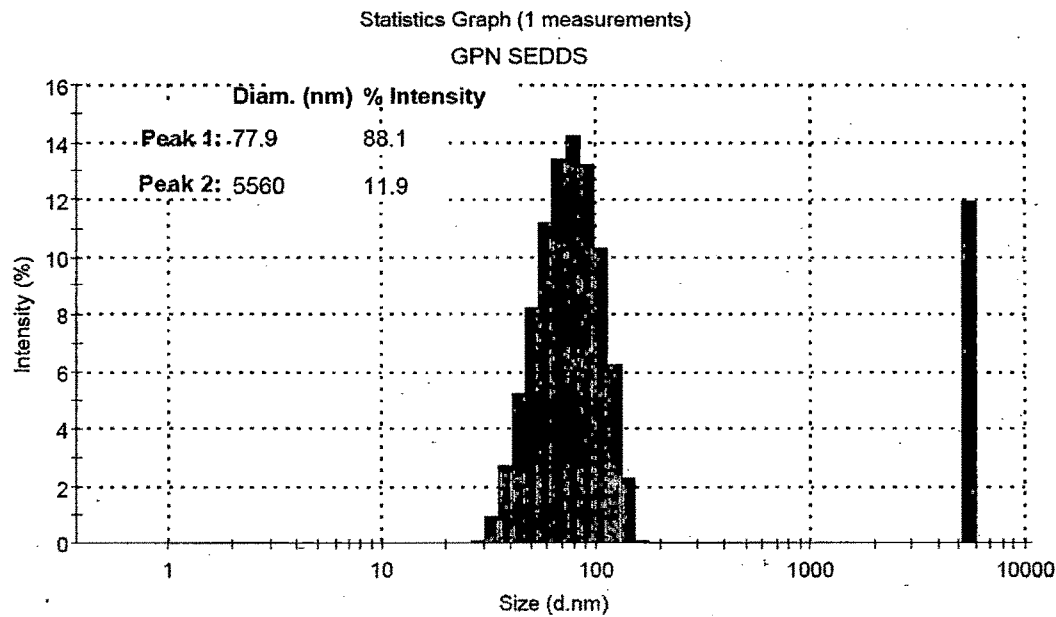


Figure 2.1.12 Particle size distribution for GPN SEDDS.

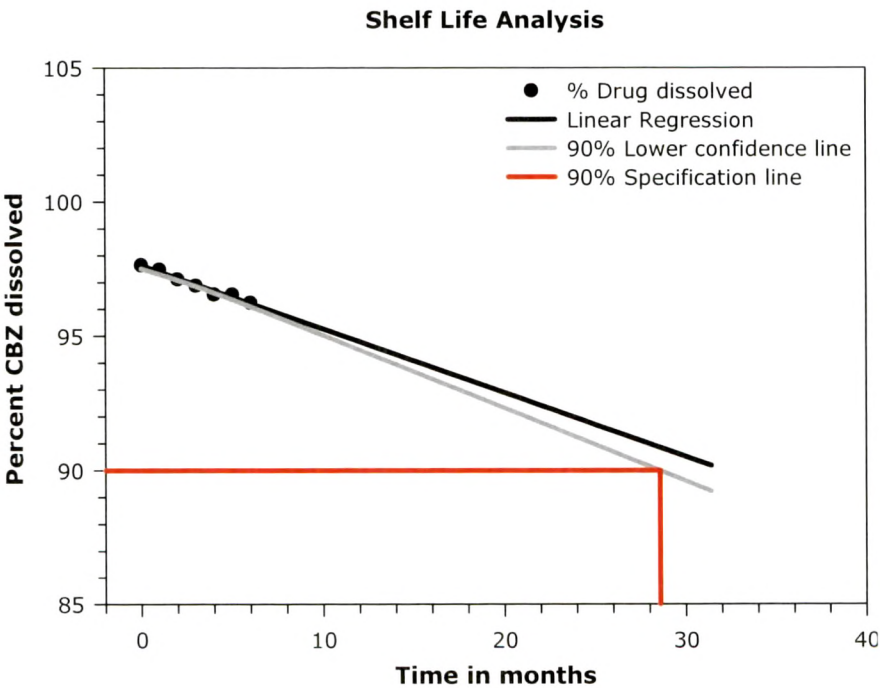


2.1.6. Stability studies for CBZ OCBZ and GPN SEDDS systems

SEDDS of CBZ, OCBZ and GPN showed promising drug dissolution results, hence they were subjected to stability studies. SEDDS of these drugs were packaged in screw capped USP type 1 glass vials. The systems were subjected to stability testing according to the International Conference on Harmonization guidelines for zone III and IV. The packed vials of all the systems were subjected for accelerated ($40^{\circ}\pm 2^{\circ}\text{C}/75\pm 5\%$ relative humidity) and long term ($30^{\circ}\pm 2^{\circ}\text{C}/65\pm 5\%$ relative humidity) stability in desiccators with saturated salt solution for up to 6 months. Long term stability samples were to be analyzed only if samples for accelerated studies ($40^{\circ}\pm 2^{\circ}\text{C}/75\pm 5\%$ RH) fail in analysis. A visual inspection (for coloration of microcrystals content), dissolution testing and pure drug content estimation was carried out every 30 days for the entire period of stability study.

Stability data of SEDDS was extrapolated using linear regression tool for the determination of shelf life of product. shows the extrapolated accelerated stability data for shelf-life calculation of CBZ Vit E SEDDS. The calculated shelf life was found to be 28.56 months (2.35 years).

Figure 2.1.13 Extrapolation of accelerated stability data of CBZ Vit E SEDDS.



For CBZ SEDDS using labrasol also the stability data was extrapolated using linear regression tool for the determination of shelf life of product. The calculated shelf life was found to be 30.2 months (2.48 years).

Figure 2.1.14 Extrapolation of accelerated stability data of CBZ labrasol SEDDS.

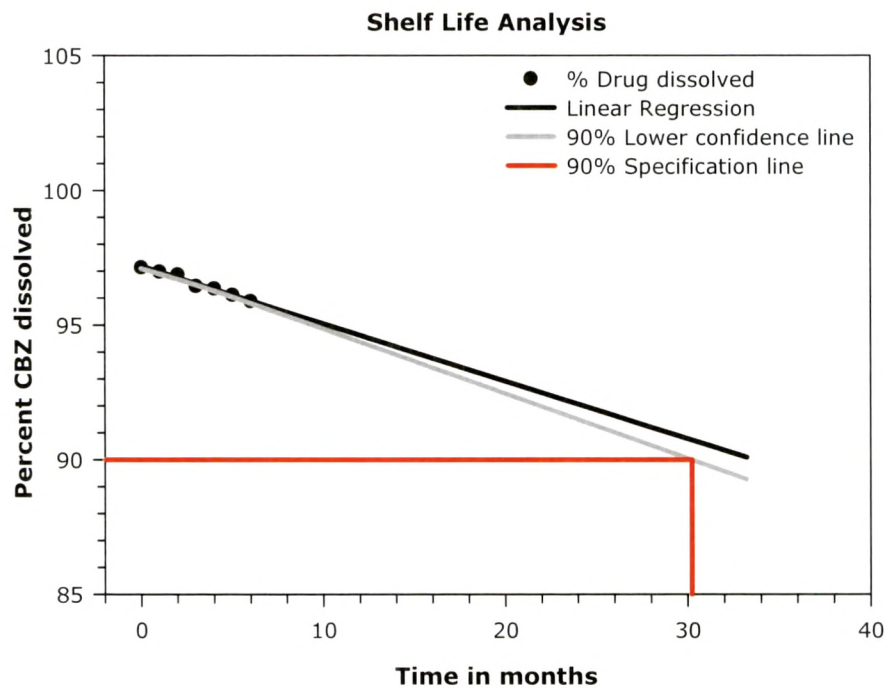


Figure 2.1.15 shows Stability data of OCBZ SEDDS was extrapolated using linear regression tool for the determination of shelf life of product. shows the extrapolated accelerated stability data for shelf-life calculation of CBZ Vit E SEDDS. The calculated shelf life was found to be 28.47 months (2.34 years).

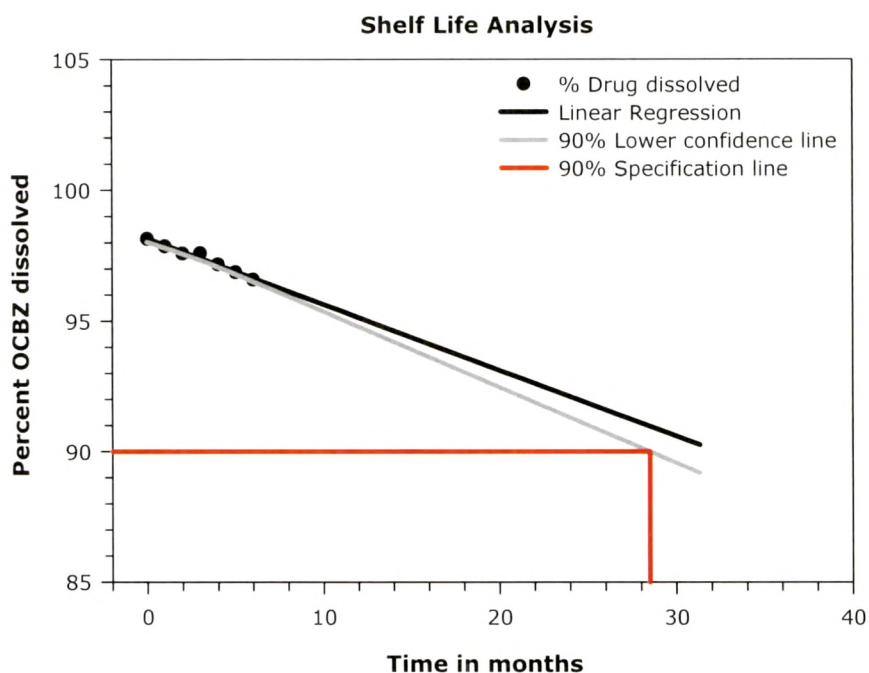
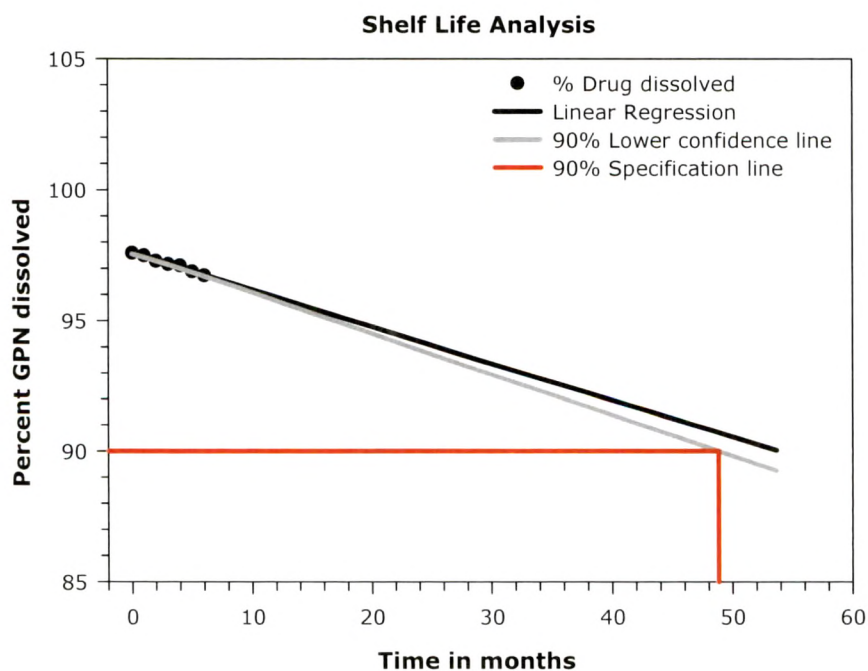
Figure 2.1.15 Extrapolation of accelerated stability data of OCBZ labrasol SEDDS.

Figure 2.1.16 shows Stability data of GPN SEDDS was extrapolated using linear regression tool for the determination of shelf life of product. shows the extrapolated accelerated stability data for shelf-life calculation of CBZ Vit E SEDDS. The calculated shelf life was found to be 48.79 months (4.01 years).

Figure 2.1.16 Extrapolation of accelerated stability data of GPN labrasol SEDDS.

2.1.7. Conclusion

Results for SEDDS of CBZ with labrasol showed incredible increase in *in vitro* dissolution of CBZ when compared with pure drug. SEDDS of CBZ with Vit E also showed dissolution enhancement but comparatively it was less than that of Vit E SEDDS. The probable reason for marked increase with labrasol than Vit E may be due to characteristic feature of surfactant – cosurfactant system combination.

OCBZ SEDDS also showed considerable increase in percent drug dissolution when compared with their pure drug counterparts.

However GPN SEDDS did not show increase in drug dissolution to the extent that previous systems of CBZ and OCBZ showed. The probable reason for this may be due to adequate aqueous solubility of GPN. Nevertheless SEDDS do have their own implications in bioavailability enhancement.

A satisfactory accelerated stability data was generated for all the systems investigated. The promising results showed an estimated life of SEDDS in the range of 2.42 to 4.01 years.

2.1.8. References

- Shah, N. H., Carvajal, M. T., Patel, C. I., Infeld, M. H. and Malick, A. W. **(1994)**. Self-emulsifying drug delivery systems (SEDDS) with polyglycolized glycerides for improving in vitro dissolution and oral absorption of lipophilic drugs. **Int J Pharm**, 106, 15-23.
- Shah, N. H. **(1994)**. SEDDS with polyglycolised glycerides for improving in vitro dissolution and oral absorption of lipophilic drugs. **Int J Pharm**, 106, 15-23.
- Charman, S. A., Charman, W. N., Rogge, M. C., Wilson, T. D., Dutko, F. J. and Pouton, C. W. **(1992)**. Self-emulsifying drug delivery systems: formulation and biopharmaceutic evaluation of an investigational lipophilic compound. **Pharm Res**, 9,1, 87-93.
- Pouton, C. W. **(1985)**. SEDDS: Assessment of the efficiency of emulsification. **Int J Pharm**, 27, 335-348.
- Nazzal, S., Nutan, M., Palamakula, A., Shah, R., Zaghloul, A. and Khan, M. A. **(2002.)**. Optimization of a self-nanoemulsified tablet dosage form of Ubiquinone using response surface methodology: effect of formulation ingredients. **Int. J. Pharm**, 240, 103-114.
- Lacy, J. E. and Embleton, J. K., No. . **(1997)**. ***Delivery systems for hydrophobic drugs.***
- Kommuru, T. R., Gurley, B., Khan, M. A. and Reddy, I. K. **(2001)**. Self-emulsifying drug delivery systems (SEDDS) of coenzyme Q10: formulation development and bioavailability assessment. **Int J Pharm**, 212,2, 233-246.
- Craig, D. Q. M., Barker, S. A., Banning, D. and Booth, S. W. **(1995)**. An investigation into the mechanisms of self-emulsification using particle size analysis and low frequency dielectric spectroscopy. **Int J Pharm**, 114, 103-110.
- Humberstone, A. J. and Charman, W. N. **(1997)**. Lipid-based vehicles for the oral delivery of poorly water soluble drugs. **Adv Drug Deliv Rev**, 25, 103-128.

Liquisolid Systems



2.2. Liquisolids

2.2.1. Materials

Carbamazepine (CBZ), Oxcarbamazepine (OCBZ), Gabapentin (GPN) were received as gift samples from Relax Pharmaceuticals Limited, Vadodara, India, Torrent Research Center, Ahmedabad, India and Sun Pharmaceuticals Limited, Vadodara, India respectively. Propylene glycol, Polyethylene glycol 600, Glycerin, Tween 80 (polysorbate 80), and Aerosil (colloidal anhydrous silica) were purchased from S. D. Fine-Chem Ltd., Mumbai, India. Avicel PH 103 (microcrystalline cellulose) was received as gift sample from Signet Chemical Corporation, Mumbai, India. Gelucire 44/14 (Lauroyl macrogolglyceride) a Gattefosse ingredient was received as generous gift sample from Colorcon Asia Pvt. Ltd., Goa, India. All the other chemicals and solvents were of analytical grade and were used without further purification. Deionized double-distilled water was used through out the study.

2.2.2. Methods

Liquisolid systems of Carbamazepine

Several liquisolid systems of CBZ (denoted as CLS-1 to CLS 12) showed in Table 2.2.2 were prepared in batches of 100 unit dosage forms. All liquisolid systems were prepared using Avicel PH 103 as carrier powder and Aerosil as coating material. CBZ was dissolved in PEG 600 (used as the liquid vehicle to prepare the liquid medication of different drug concentrations) with different drug conc. in liquid medication (15 – 25 % w/w). To further increase the dissolved solid content of vehicle 10 mg of sodium lauryl sulfate (SLS) was added in liquisolid system from CLS-1 to CLS-9 whereas 10 mg of tween 80 was added in liquisolid systems from CLS 10 to CLS 12. To this liquid medication carrier material avicel was added with constant uniform mixing. After complete addition of avicel, aerosil was added to the admixture at once. The amount of avicel and aerosil to be added to the liquid medication was decided on the basis of excipient ratio. The excipient ratio (R) was calculated using Equation 2.2.1. Where 'Q' is the amount of carrier material and 'q' is the amount of coating material. The excipient ratio was varied from 4.6 to 9.4 to get a better idea about the effect of each excipient.

Equation 2.2.1

$$R = \left(\frac{Q}{q} \right)$$

Table 2.2.2 gives key formulation aspects of prepared CBZ liquisolid systems like Excipient ratio, Liquid load factor (L_f), Fraction of molecularly dispersed drug (F_M) in the liquid

medication of liquisolid systems and Drug dissolution rate for first 10 min of dissolution studies (D_R).

Liquid load factor is the characteristic amount of liquid that is hold by carrier and coating material in duo to maintain acceptable flow properties of system. It is calculated by Equation 2.2.2, where 'W' is the amount of liquid medication and 'Q' is the amount of carrier material.

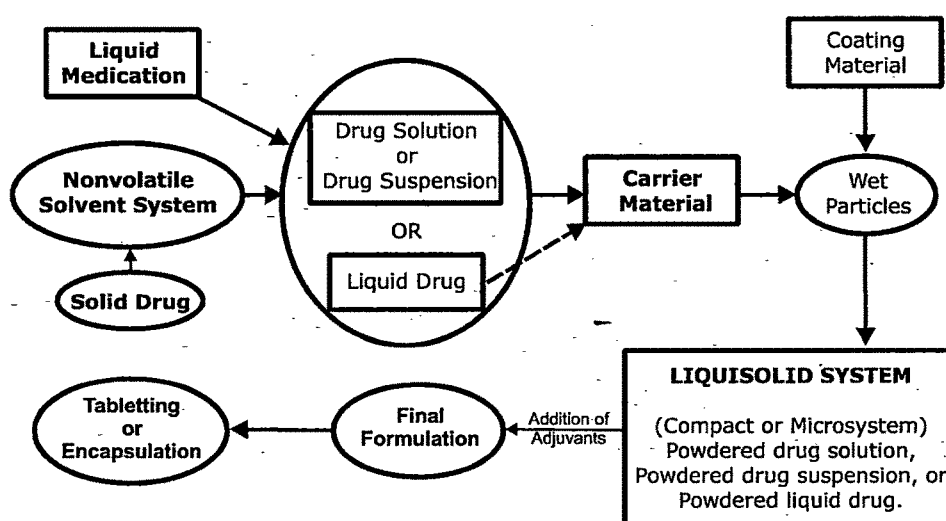
Equation 2.2.2
$$L_f = \left(\frac{W}{Q} \right)$$

The prime objective of developing the liquisolid system is to enhance dissolution properties of the drug. However the flowability of the system can not be sacrificed since it is one of the crucial factor in controlling the content uniformity of drug and weight variation of the system. Considering this, optimization of the system was dependent on the ratio of Drug : PEG 600 in formulation. So different liquid load factors ranging from 0.67 to 0.9 (w/w) were employed in liquisolid preparations. These amounts of the carrier and coating materials were found to be enough to maintain acceptable flow and capsule filling properties in initial screening experiments.

An attempt was also made to compress the liquisolid systems into directly compressible compacts. Croscarmellose Na in an amount of 6% (w/w) as the disintegrant was mixed with the system for a period of 10 min. Final mixture was dried at 50 °C for 10 min. in tray dryer. This blend was attempted to compress using single punch manual tabletting machine, but compression was not found to be feasible. Liquisolid system was scrapped out from die presenting a high degree of any "liquid squeezing out" phenomena.

Figure 2.2.1 exemplifies the graphical arrangement of the steps involved in preparation of liquisolid systems.

Figure 2.2.1 Schematic outline of steps involved in the preparation of liquisolid systems.



2.2.2.1. Solubility studies for CBZ liquisolid systems

The solubility of CBZ in water and four liquid vehicles tried to prepare the liquisolid systems, namely, propylene glycol, polyethylene glycol 600, glycerin and polysorbate 80, were studied by preparing saturated solutions of the drug in these solvents and analyzing their drug content spectrophotometrically. Specifically, CBZ was mixed in 7 ml screw capped vials with such amounts of each of the above solvents in order to produce systems containing an excess of drug. The mixtures were shaken on an automatic test tube shaking machine for 24 hrs and then settled for another 2 hrs. The screw capped vials were centrifuged at 2500 rpm for further settling of undissolved crystalline material and thereby obtaining a clear supernatant. After centrifugation, accurately measured quantities of the filtered supernatant solutions were further diluted with methanol and analyzed spectrophotometrically at 285 nm for their drug content. The results were extrapolated to determine the percent g / 100 mL of CBZ in its saturated solution with the solvents under investigation.

2.2.2.2. Evaluation of Carbamazepine Liquisolid systems

2.2.2.2.1. *In vitro* Dissolution studies

To study the effect of amount of dissolution medium on percent drug dissolution of liquisolid systems dissolution studies were conducted in 3 different dissolution medium volumes i.e. 450 mL, 600 mL and 900 mL. The dissolution study was conducted in USP XXVII simulated gastric fluid (without enzymes) having pH 1.2 ± 0.02 as dissolution media. Liquisolid systems, containing an equivalent 100 mg of drug were wrapped in cloth pouch of approximate 2 - 5 μ m mesh. This pouch was placed in basket of USP dissolution apparatus (Type I, TDT-06P, Electrolab, Mumbai, India) with 900 ml deaerated dissolution medium. Liquisolid systems were placed in cloth pouches to avert floating of them on dissolution media surface. Previously deaeration of dissolution media were done with the help of ultrasonication (Ultrasonics - 2.2, India) for 15 min. The dissolution apparatus was run at 50 RPM keeping the temperature (37 ± 1 °C) constant throughout the experiment. Samples (5 ml) were withdrawn upto 40 min of dissolution study, at an interval of 5 min and were filtered through 0.45 μ m whatmann filter membrane, diluted suitably and analysed spectrophotometrically at 285 nm (Shimadzu, UV-1601 UV, Visible spectrophotometer, Japan). An equal volume of fresh dissolution medium maintained at the same temperature was added after withdrawing sample to maintain the sink conditions.

2.2.2.2.2. Spectrophotometric analysis and standard curves

Shimadzu, UV-1601 Double beam UV, Visible spectrophotometer, Kyoto (Japan) was used for the spectrophotometric analyses of all CBZ samples in methanolic (solubility studies)

and aqueous solutions (dissolution studies) at 285 nm which was previously established as the wavelength of the drug's maximum absorbance. Standard curves were constructed by serially diluting a methanolic stock solution of the drug to obtain concentrations in the range of 2–25 µg/ml using methanol, distilled water or an aqueous 0.1 N HCl solution as the diluents ($r^2 = 0.9998$). Each concentration was analyzed in triplicate.

2.2.2.2.3. Assessment and comparison of drug dissolution rates

The dissolution rates (D_R) of CBZ, in the form of amount of drug (in mg) dissolved per min, presented by each liquisolid formulation during the first 10 min of the dissolution process, were calculated by Equation 2.2.3, where 'M' is the total amount of drug in dosage form and 'D' is the percentage of drug dissolved in 10 min.

Equation 2.2.3 $D_R \text{ (mg/mL)} = \left(\frac{M \times D}{1000} \right)$

2.2.2.2.4. Measurement of angle of repose of liquisolid systems

To get an idea about flow properties of the liquisolid systems, angle of repose for all the batches was determined. Angle of repose results were evaluated with the hypothesis that systems having angle exceeding 50°, shows poor flow properties, whereas materials having angle of repose values lesser flow easily and well. The rougher and more irregular the surface of the particles, higher is the angle of repose. (McKenna and McCafferty, 1988) The angle of repose was measured by passing liquisolids through a sintered glass funnel of internal diameter 27 mm. on the horizontal surface. The height (h) of the heap formed was measured with a cathetometer, and the radius (r) of the cone base was also determined. The angle of repose (Φ) was calculated from Equation 2.2.4. Table 2.2.1 gives an idea about the flowability behaviour of CBZ liquisolid systems in terms of the angle of repose, a well known flowability indicator.

Equation 2.2.4 $\Phi = \tan^{-1} \left(\frac{h}{r} \right)$

Table 2.2.1 Angle of repose for all the liquisolid systems prepared.

Liquisolid System	Angle of Repose
CLS-1	23.36
CLS-2	27.86
CLS-3	27.2
CLS-4	21.36
CLS-5	23.51
CLS-6	24.39
CLS-7	27.36
CLS-8	30.49
CLS-9	27.46

CLS-10	30.04
CLS-11	35.64
CLS-12	33.21

Observing the data for angle of repose of CBZ liquisolid systems it is clear that from CLS-1 to CLS-10 all the systems exhibited the values in acceptable range. Whereas liquisolid systems CLS-11 and CLS-12 showed considerable increase in angle of repose which can be attributed to the presence of tween 80.

Theoretically increase in load factor (L_f) value of system should show rise in angle of repose i.e. poor flowability characteristic.

Table 2.2.2.2 Key formulation characteristics of prepared CBZ liquid solid systems.

Liquid solid System	Vehicle	Carrier material	Coating material	Drug conc (%w/w in liquid medication)	Total wt. of liquid material (W) mg.	Wt of carrier material (Q) mg.	Wt of coating material (q) mg.	Excipient ratio (R) = Q/q	Liquid load factor (L _r) = W/Q	Unit dose wt. (mg)	Molecular fraction (F _m) = C _L /C _d	Drug dissolution rate (D _R) in mg/mL
CLS-1	PEG 600 + 10 mg SLS	Avicel PH 103	Aerosil	15	666.67	800	100	8.0	0.83	1676.67	1.47	9.31
CLS-2	PEG 600 + 10 mg SLS	Avicel PH 103	Aerosil	17	588.24	650	80	8.1	0.90	1428.24	1.29	9.31
CLS-3	PEG 600 + 10 mg SLS	Avicel PH 103 PH 103	Aerosil	19	526.32	700	80	8.8	0.75	1416.32	1.16	8.72
CLS-4	PEG 600 + 10 mg SLS	Avicel PH 103	Aerosil	19	526.32	750	100	7.5	0.70	1486.32	1.16	9.13
CLS-5	PEG 600 + 10 mg SLS	Avicel PH 103	Aerosil	21	476.19	650	100	6.5	0.73	1336.19	1.05	8.54
CLS-6	PEG 600 + 10 mg SLS	Avicel PH 103	Aerosil	23	434.78	550	100	5.5	0.79	1194.78	0.96	8.01
CLS-7	PEG 600 + 10 mg SLS	Avicel PH 103	Aerosil	23	434.78	550	120	4.6	0.79	1214.78	0.96	7.77
CLS-8	PEG 600 + 10 mg SLS	Avicel PH 103	Aerosil	25	400.00	600	120	5.0	0.67	1230.00	0.88	7.55
CLS-9	PEG 600 + 10 mg SLS	Avicel PH 103	Aerosil	27	370.37	550	120	4.6	0.67	1150.37	0.81	7.48
CLS-10	PEG 600 + 10 mg Tw 80	Avicel PH 103	Aerosil	17	588.24	750	80	9.4	0.78	1528.24	1.29	9.21
CLS-11	PEG 600 + 10 mg Tw 80	Avicel PH 103	Aerosil	20	500.00	650	100	6.5	0.77	1360.00	1.10	8.89
CLS-12	PEG 600 + 10 mg Tw 80	Avicel PH 103	Aerosil	25	400.00	600	120	5.0	0.67	1230.00	0.88	7.68

2.2.3. Results and discussion for CBZ Liquisolid systems

To choose the right solvent for preparation of liquid medication is one of the important task in designing and developing of liquisolid systems. However solubility of drug in that particular solvent is the only hunting option available for choosing right solvent. Table 2.2.3 shows the solubility profile of CBZ in purified water, polyethylene glycol (PEG) 600, polysorbate 80 (tween 80), propylene glycol and glycerin. From Table 2.2.3 it is very evident that PEG 600 has considerably hefty solubility compared to other solvents that can be used for liquid component of liquisolid system. So PEG 600 was used for liquisolid preparation of CBZ.

Table 2.2.3 Solubility of CBZ in various solvents

Solubility of CBZ in various solvents	Solubility (g/100mL)
Purified water	0.0091
PEG 600	0.4521
Tween 80	0.4237
Propylene glycol	0.3826
Glycerin	0.1533

Figure 2.2.2 shows the drug dissolution profiles of the liquisolid systems (CLS-1 to CLS-12) and the marketed conventional tablets CBZ. When 900 ml (per vessel) of SGF USP was used as the dissolution medium, liquisolid systems of CBZ displayed considerably enhanced *in-vitro* drug release characteristics than those of its conventional tabletted counterpart.

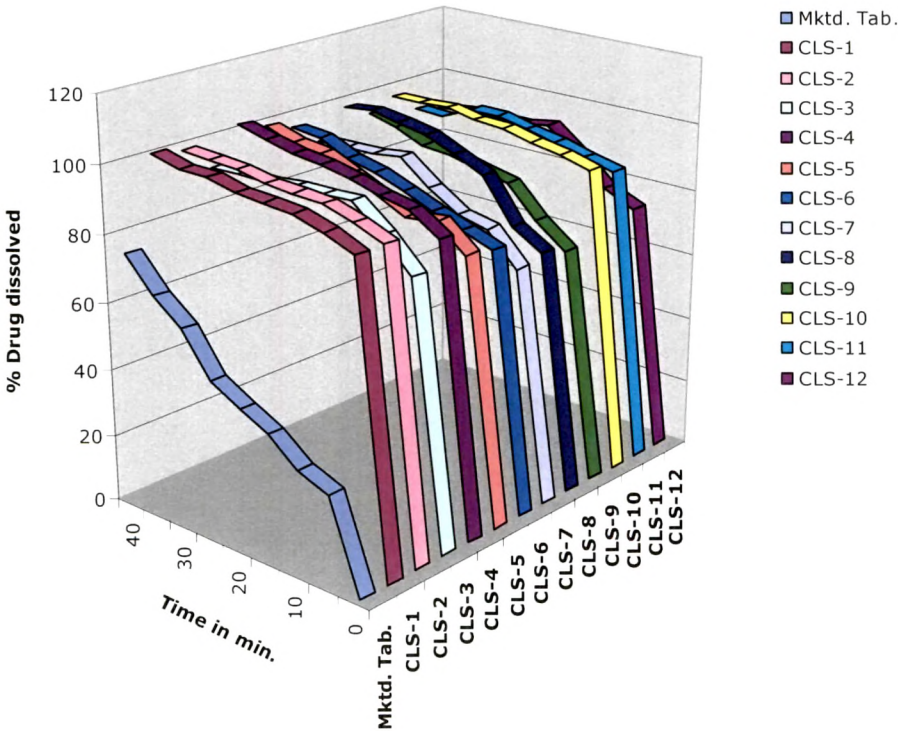


Figure 2.2.2 Percent drug dissolution profiles of liquisolid systems of CBZ

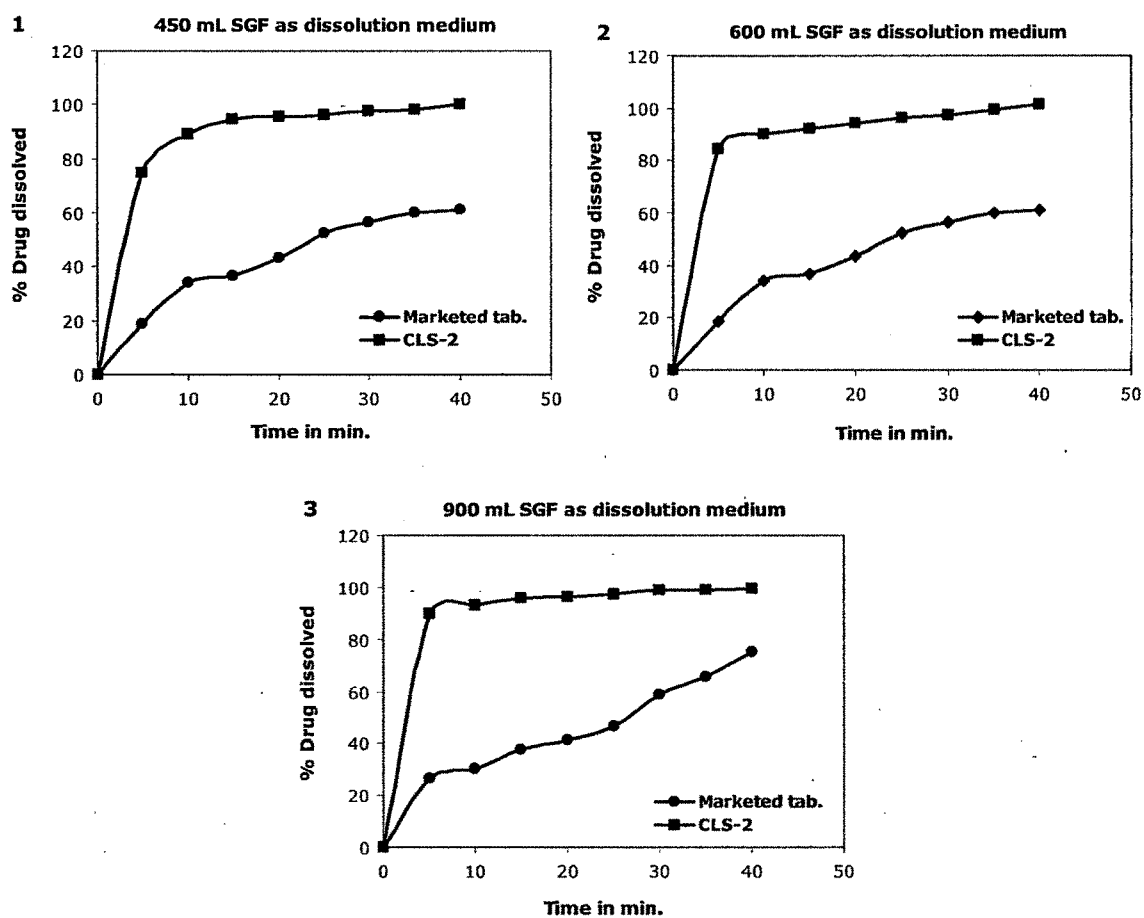


Figure 2.2.3 Comparison of CBZ *In vitro* dissolution profiles displayed by liquisolid systems and marketed tablets at different dissolution media volumes.

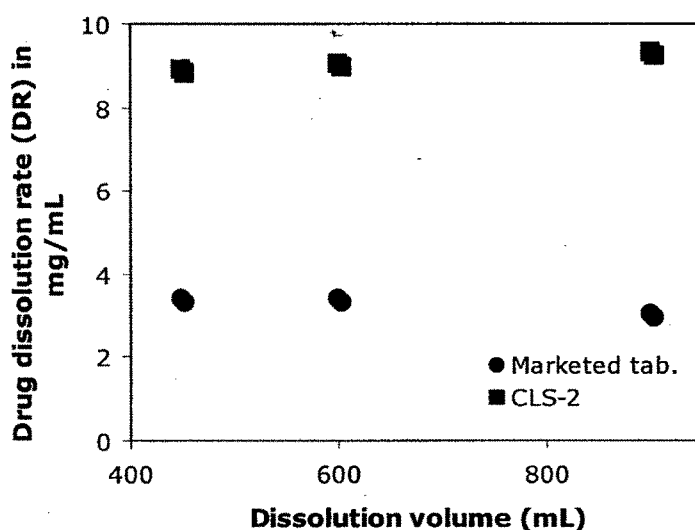


Figure 2.2.4 Effect of the dissolution volume on the initial dissolution rate of CBZ exhibited by the liquisolid systems and marketed tablets.

The higher CBZ dissolution rates displayed by the liquisolid systems compared to marketed conventional tablets are clearly observed in Figure 2.2.4 where the dissolution rate (D_R in mg of drug dissolved per min) observed during the first 10 min of the dissolution process is plotted against the volume of dissolution medium. It is clear that the drug dissolution rate of liquisolid systems is significantly faster than that of the plain tablets and it is independent of the volume of the dissolving liquid used. Furthermore, it is apparent that decreasing dissolution volumes result in a proportional decrease of the *in-vitro* drug release rates displayed by the conventional tablets. According to the 'diffusion layer model' dissolution theories (Martin, *et al.*, 1993, Hoener and Benet, 1996), the dissolution rate of a drug is directly proportional to its concentration gradient ($\Delta C = C_s - C$) in the stagnant diffusion layer formed by the dissolving liquid around the drug particles. C_s is the saturation solubility of the drug in the dissolution medium and thus, it is a constant characteristic property related to the drug and dissolving liquid involved. On the other hand, C , the drug concentration in the bulk of the dissolving medium, increases with decreasing volumes of dissolution fluid used. Therefore, the ΔC values existing in the three different dissolution volumes of dissolution tests decrease with decreasing volumes of dissolution medium. Consequently such ΔC reduction is directly related to the decreased drug dissolution rates of the conventional tablets with decreasing volumes of dissolution medium used (Figure 2.2.4). However, as demonstrated in Figure 2.2.4, decreasing dissolution volumes do not affect the drug release rate from the liquisolid systems. Since the liquisolid tablets contain a solution of the drug in PEG 600 (17% w/w), the drug surface available for dissolution is tremendously increased. Essentially after disintegration, the liquisolid primary particles suspended in the dissolving medium contain the drug in a

state of molecular dispersion, whereas the conventional tablets are merely exposing drug particles. Therefore, in the case of liquisolid systems, the surface of drug available for dissolution is related to its specific molecular surface which, by any means, is much greater than that of the CBZ particles delivered by the conventionally made tablets.

According to the classic dissolution equation (Equation 2.2.5), (Noyes and Whitney, 1897)

Equation 2.2.5
$$D_R = (D/h)S(C_s - C)$$

the drug dissolution rate (D_R) is directly proportional not only to the concentration gradient ($C_s - C$) of the drug in the stagnant diffusion layer, but also to its surface (S) available for dissolution. Moreover, since all of dissolution tests for both CBZ preparations were conducted at a constant rotational paddle speed (50 rpm) and identical dissolution media, it can be well assumed that the thickness (h) of the stagnant diffusion layer and the diffusion coefficient (D) of the drug molecules transported through it, remained almost identical under each dissolution condition. Therefore, the hypothesis that the significantly increased surface of the molecularly dispersed CBZ in the liquisolid systems may be chiefly responsible for their observed higher and consistent dissolution rates, appeared to be fundamentally valid. In addition to the preceding theory, it might be also speculated that C_s , the saturation solubility of the drug in the micro-environment, might be increased in the case of liquisolid systems. Admittedly, the relatively small amounts of liquid vehicle (PEG 600) contained per liquisolid system, are not sufficient to increase the overall saturation solubility of CBZ in the aqueous dissolution medium. At the local level, however, the solid-liquid interface between an individual liquisolid primary particle and the dissolving fluid involves minute quantities of aqueous medium adhering onto the particle surface to form the stagnant diffusion layer. In such a micro-environment, it is quite possible that the infinite amounts of propylene glycol diffusing with the drug molecules out of a single liquisolid particle, might be adequate to enhance the solubility of CBZ acting as a cosolvent with the aqueous dissolution medium of the stagnant diffusion layer. Such an increase in C_s will result, of course, in a larger drug concentration gradient (ΔC) thereby increasing the dissolution rate as defined by the Noyes-Whitney Equation 2.2.5.

The consistent and higher dissolution rates displayed by liquisolid systems may also imply enhanced oral bioavailability. From a physicochemical point of view, it is well established that the inadequate dissolution of water insoluble drugs is the major reason for their poor and erratic bioavailability, since it is the rate determining step in the absorption of non-polar molecules. As depicted in Figure 2.2.4, considering volume changes in GIT, liquisolid systems of CBZ may be expected to produce more consistent and enhanced *in vivo* dissolution and absorption characteristics. The liquid vehicle contained in the prepared liquisolid systems seems to have some effects on their drug dissolution properties (Spireas and Sadu, 1998, Javadzadeh, *et al.*, 2005, Nokhodchi, *et al.*, 2005).

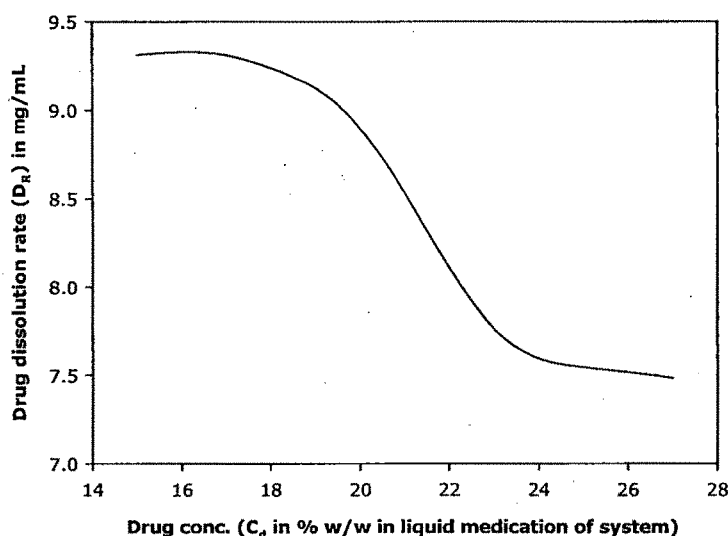


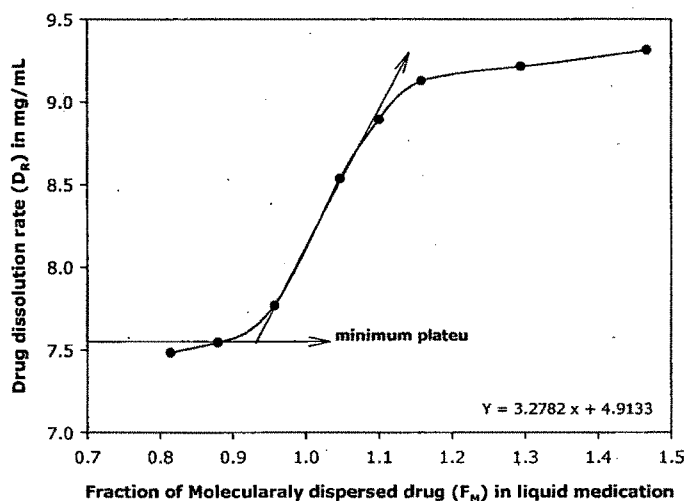
Figure 2.2.5 The effect of drug concentration in the liquid medication on the initial dissolution rate of CBZ displayed by liquisolid systems of PEG 600

Specifically, in preliminary studies conducted, CBZ release profiles from liquisolid systems containing identical drug concentrations (10 – 20 % w/w) in the liquid medications of propylene glycol and glycerin were not found to be satisfactory. These systems displayed relatively slower drug release rates for the first 10 and 20 min of dissolution. However, all liquisolid preparations exhibited significantly faster 30 min dissolution than that of the conventional tablets. The relatively poorer dissolution properties of these propylene glycol and glycerin liquisolid systems may be mainly attributed to the lower solubilities of CBZ in these liquid vehicles as compared to those in PEG 600 shown in Table 2.2.3. Since the drug is completely in solution in the liquid medications of PEG 600, it presented improved dissolution properties. However, the solubilization state of the drug in the liquid vehicle of the liquisolid systems does not entirely justify the initial drug release patterns observed. In addition to the drug solubility in the liquid vehicles, other physicochemical characteristics of the solvents used such as polarity, viscosity, molecular weight, chemical structure and hydrophilicity, may also have effect to certain extents, on the availability of the drug molecules to the dissolving medium, the disintegration and deaggregation properties of avicel included in systems, and the diffusion of the liquid medication through the primary carrying particles during the dissolution process (Spireas and Sadu, 1998).

The drug concentration in the liquid medication (C_d ranging from 15 to 25% w/w) has an apparent effect on the CBZ 10 min dissolution rates displayed by the liquisolid systems of PEG 600, as shown in Figure 2.2.5. However, at the same dissolution conditions, systems containing liquid medications with increasing C_d values exhibited declining *in vitro* release properties until reaching a minimum plateau dissolution rate displayed by the liquisolid systems containing about more than 20% w/w of drug in their liquid medications. Such differences in the drug dissolution rates of the PEG 600 liquisolid systems possessing

different C_d values, observed in Figure 2.2.5, may be justified using the previous hypothesis of the available drug surface effects on dissolution.

Figure 2.2.6 Effect of fraction (F_M) of the molecularly dispersed drug in the liquisolid systems on the 10 min dissolution rate (D_R) of CBZ containing various drug concentrations (C_d) in their liquid medications.



Apparently, the solubilization and molecular dispersion states of the drug in liquisolid systems are different. For instance, since the saturation solubility of CBZ in PEG 600 is 22% w/w Table 2.2.3, the drug is partly dissolved in the liquid medication of CLS-6, CLS-7, CLS-8, CLS-9 and CLS-12 liquisolid systems, whereas it is completely dissolved in the CLS-1, CLS-2, CLS-3, CLS-4, CLS-5, CLS-10 and CLS-11 systems containing 15, 17, 19, 19, 21, 17 and 20% w/w respectively of drug in PEG 600. In other words, the ratio of the drug's saturation solubility (C_L) in the liquid vehicle over the drug concentration (C_d) in the liquid medication carried by each system denotes the fraction (F_M) of the dissolved, or molecularly dispersed, drug in the liquid medication of the prepared liquisolid systems (Spireas and Sadu, 1998).

Equation 2.2.6

$$F_M = C_L / C_d$$

Based on the above equation, the F_M values of each liquisolid preparation have been calculated in Table 2.2.2. The dissolution rates obtained from PEG 600 liquisolid systems—possessing different C_d values, are plotted against their corresponding F_M values in Figure 2.2.6. After remaining at a minimum plateau level (about 7.5 mg/min) for F_M values ranging from 0.81 to 1.47, the 10 min dissolution rate of the drug increased in a linear manner with increasing F_M values of the liquisolid systems. Therefore, for PEG 600 liquisolid systems, one may be able to predict the dissolution rate (D_R in mg/min) of CBZ which will be obtained within the initial 10 min of the dissolution process conducted using 50 rpm as the basket speed and 450 mL of SGF without enzymes as the dissolution

medium. As shown in Figure 2.2.6 for systems with F_M values ranging from 0.81 to 1.47, the dissolution rate of CBZ may be given by $Y = 3.2782 x + 4.9133$.

Liquisolid system of Oxcarbamazepine (OCBZ)

Several liquisolid systems of OCBZ (denoted as OLS-1 to OLS 12) showed in Table 2.2.5 were prepared in batches of 100 unit dosage forms. All liquisolid systems were prepared using avicel PH 103 as carrier polymer and aerosil as coating material. OCBZ was dissolved in PEG 600 (used as the liquid vehicle to prepare the liquid medication of different drug concentrations) with different drug conc. in liquid medication (19 – 27 % w/w). To further increase the dissolved solid content of vehicle 10 mg of sodium lauryl sulfate (SLS) was added in liquisolid systems from OLS-1 to OLS-9 whereas 10 mg of tween 80 was added in liquisolid systems from OLS-10 to OLS-12. To this liquid medication carrier material avicel PH 103 was added with constant uniform mixing. After complete addition of avicel, aerosil was added to the admixture at once. The amount of avicel and aerosil to be added to the liquid medication was decided on the basis of excipient ratio.

Table 2.2.5 gives key formulation aspects of prepared CBZ liquisolid systems like Excipient ratio, Liquid load factor (L_f), Fraction of molecularly dispersed drug (F_M) in the liquid medication of liquisolid systems and Drug dissolution rate for first 10 min of dissolution studies (D_R).

Liquid load factors (L_f) of liquisolid preparations was studied in the range of 0.53 to 0.87 (w/w). These amounts of the carrier and coating materials were found to be enough to maintain acceptable flow and capsule filling properties in initial screening experiments.

2.2.3.1. Solubility studies for OCBZ liquisolid systems

The solubility of OCBZ in water and four liquid vehicles tried to prepare the liquisolid systems, namely, propylene glycol, polyethylene glycol 600, glycerin and polysorbate 80, were studied by preparing saturated solutions of the drug in these solvents and analyzing their drug content spectrophotometrically. The procedure employed was same to that of CBZ solubility determination. The diluted supernatant methanolic samples were analyzed spectrophotometrically at 303 nm for their drug content. The results were extrapolated to determine the percent w/w of OCBZ in its saturated solution with the solvents under investigation.

2.2.3.2. Evaluation of Oxcarbamazepine Liquisolid systems

2.2.3.2.1. *In vitro* Dissolution studies

To study the effect of amount of dissolution medium on percent drug dissolution of liquisolid systems dissolution studies were conducted in 3 different dissolution medium volumes i.e. 450 mL, 600 mL and 900 mL. The dissolution study was conducted in USP

XXVII simulated gastric fluid (without enzymes) having pH 1.2 ± 0.02 as dissolution media. Liquisolid systems, containing an equivalent 100 mg of drug were wrapped in cloth pouch of approximate 2 - 5 μm mesh. This pouch was placed in basket of USP dissolution apparatus (Type I, TDT-06P, Electrolab, Mumbai, India) with 900 ml deaerated dissolution medium. Liquisolid systems were placed in cloth pouches to avert floating of them on dissolution media surface. Previously deaeration of dissolution media were done with the help of ultrasonication (Ultrasonics - 2.2, India) for 15 min. The dissolution apparatus was run at 50 RPM keeping the temperature ($37 \pm 1^\circ\text{C}$) constant throughout the experiment. Samples (5 ml) were withdrawn upto 40 min of dissolution study, at an interval of 5 min and were filtered through 0.45 μm whatmann filter membrane, diluted suitably and analysed spectrophotometrically at 303 nm (Shimadzu, UV-1601 UV, Visible spectrophotometer, Japan). An equal volume of fresh dissolution medium maintained at the same temperature was added after withdrawing sample to maintain the sink conditions.

2.2.3.2.2. Spectrophotometric analysis and standard curves

Shimadzu, UV-1601 Double beam UV, Visible spectrophotometer, Kyoto (Japan) was used for the spectrophotometric analyses of all OCBZ samples in methanolic (solubility studies) and aqueous solutions (dissolution studies) at 303 nm which was previously established as the wavelength of the drug's maximum absorbance. Standard curves were constructed by serially diluting a methanolic stock solution of the drug to obtain concentrations in the range of 4-25 $\mu\text{g/ml}$ using methanol, distilled water or an aqueous 0.1 N HCl solution as the diluents ($r^2 = 0.9991$). Each concentration was analyzed in triplicate.

2.2.3.2.3. Assessment and comparison of drug dissolution rates

The dissolution rates (D_R) of OCBZ, in the form of amount of drug (in mg) dissolved per min, presented by each liquisolid formulation during the first 10 min of the dissolution process are reported in Table 2.2.5.

2.2.3.2.4. Measurement of angle of repose of liquisolid systems

To get an idea about flow properties of the liquisolid systems, angle of repose for all the batches was determined. Angle of repose results were evaluated with the hypothesis that systems having angle exceeding 50° , shows poor flow properties, whereas materials having values near the minimum flow easily and well. The rougher and more irregular the surface of the particles, higher is the angle of repose. (McKenna and McCafferty, 1988) The angle of repose was measured by employing same method used for CBZ liquisolid systems. Table 2.2.4 gives the angle of repose values for all the OCBZ liquisolid systems prepared.

Table 2.2.4 Angle of repose for all the OCBZ liquisolid systems prepared.

Liquisolid System	Angle of Repose
OLS-1	23.36
OLS-2	27.86
OLS-3	27.2
OLS-4	21.36
OLS-5	23.51
OLS-6	24.39
OLS-7	27.36
OLS-8	30.49
OLS-9	27.46
OLS-10	30.04
OLS-11	35.64
OLS-12	33.21

All the liquisolid systems prepared exhibited good flow properties. However liquisolid systems OLS-11 and OLS-12 when compared to other systems showed higher values of angle of repose 35.64 and 33.21 respectively. Increase in angle of repose values for these systems may be attributed to stickier nature of tween 80 incorporated.

Table 2.2.5 Key formulation characteristics of prepared OCBZ liquisolid systems.

Liquisolid System	Vehicle	Carrier material	Coating material	Drug conc (%w/w in liquid medication)	Total wt. of liquid material (W) mg.	Wt of carrier material (Q) mg.	Wt of coating material (q) mg.	Excipient ratio (R) = Q/q	Liquid load factor (L _l) = W/Q	Unit dose wt. mg.	Molecular fraction (F _M) = C _L /C _d	Drug dissolution rate (D _R) in mg/mL = (MxD)/1000
OLS-1	PEG 600 + 10 mg SLS	Avicel	Aerosil	19	526.32	800	100	8.0	0.66	1536.32	1.32	9.635
OLS-2	PEG 600 + 10 mg SLS	Avicel	Aerosil	21	476.19	650	80	8.1	0.73	1316.19	1.19	9.269
OLS-3	PEG 600 + 10 mg SLS	Avicel	Aerosil	23	434.78	700	80	8.8	0.62	1324.78	1.09	7.959
OLS-4	PEG 600 + 10 mg SLS	Avicel	Aerosil	25	400.00	750	100	7.5	0.53	1360.00	1.00	8.108
OLS-5	PEG 600 + 10 mg SLS	Avicel	Aerosil	25	400.00	650	100	6.5	0.62	1260.00	1.00	8.163
OLS-6	PEG 600 + 10 mg SLS	Avicel	Aerosil	21	476.19	550	100	5.5	0.87	1236.19	1.19	8.008
OLS-7	PEG 600 + 10 mg SLS	Avicel	Aerosil	23	434.78	550	120	4.6	0.79	1214.78	1.09	7.678
OLS-8	PEG 600 + 10 mg SLS	Avicel	Aerosil	23	434.78	600	120	5.0	0.72	1264.78	1.09	7.546
OLS-9	PEG 600 + 10 mg SLS	Avicel	Aerosil	27	370.37	550	120	4.6	0.67	1150.37	0.93	9.635
OLS-10	PEG 600 + 10 mg Tw 80	Avicel	Aerosil	21	476.19	750	80	9.4	0.63	1416.19	1.19	9.214
OLS-11	PEG 600 + 10 mg Tw 80	Avicel	Aerosil	23	434.78	650	100	6.5	0.67	1294.78	1.09	8.394
OLS-12	PEG 600 + 10 mg Tw 80	Avicel	Aerosil	25	400.00	600	120	5.0	0.67	1230.00	1.00	6.7775

2.2.4. Results and discussion for OCBZ liquisolid systems

Table 2.2.6 Shows the solubility profile of OCBZ in purified water, polyethylene glycol (PEG) 600, polysorbate 80 (tween 80), propylene glycol and glycerin. From Table 2.2.6 it is very evident that PEG 600 has considerably hefty solubility compared to other solvents that can be used for liquid component of liquisolid system. So PEG 600 was used for liquisolid preparation of OCBZ.

Table 2.2.6 Solubility of OCBZ in various solvents

Solubility of OCBZ in various solvents	Solubility (g/100 mL)
Purified water	0.0101
PEG 600	0.5231
Tween 80	0.4893
Propylene glycol	0.3925
Glycerin	0.3632

Figure 2.2.7 shows the drug dissolution profiles of the liquisolid systems (OLS-1 to OLS-12) and the marketed conventional tablets of OCBZ. When 900 ml (per vessel) of SGF USP was used as the dissolution medium, liquisolid systems of OCBZ displayed considerably enhanced *in-vitro* drug release characteristics than those of its conventional tabletted counterpart.

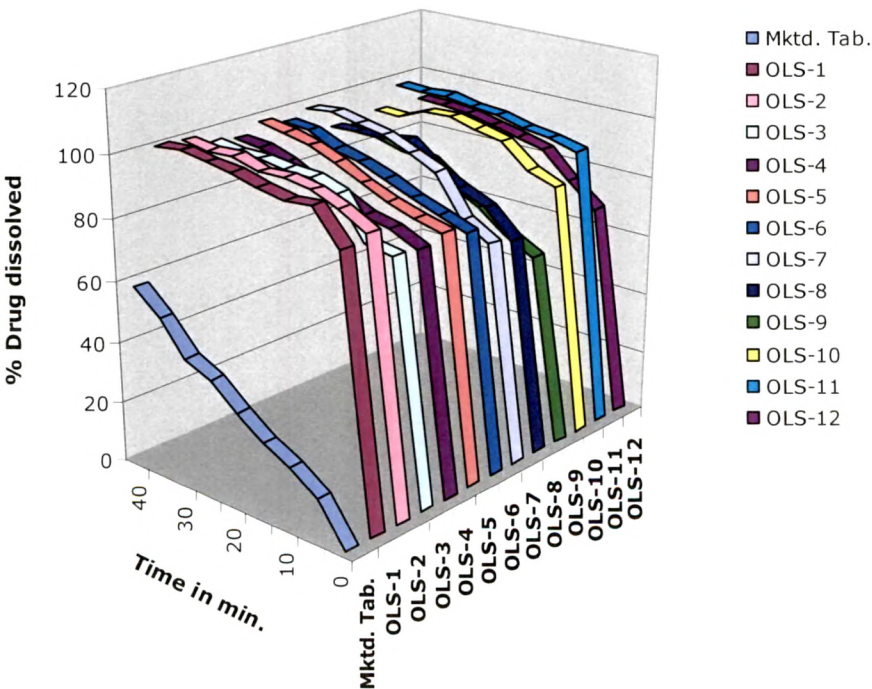


Figure 2.2.7 Percent drug dissolution profiles of liquisolid systems of OCBZ.

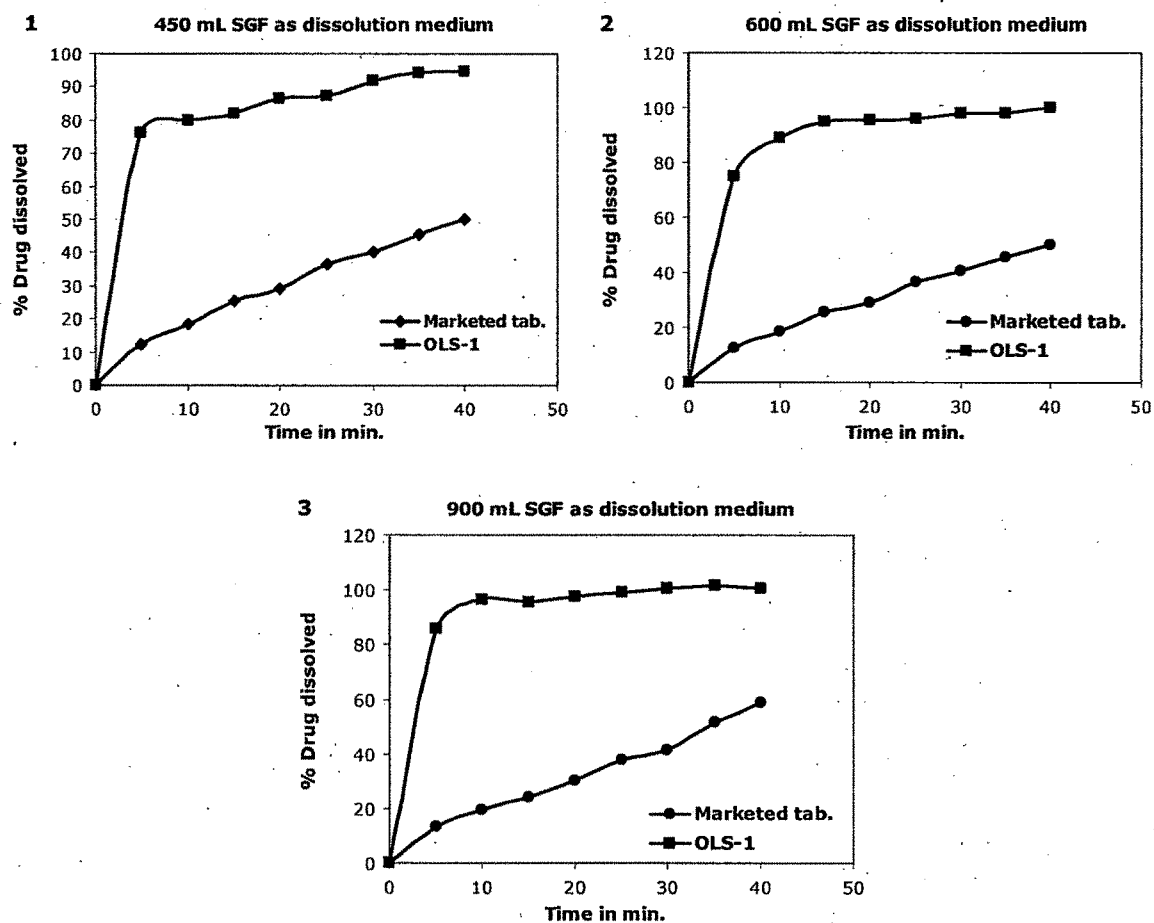


Figure 2.2.8 Comparison of OCBZ *in vitro* dissolution profiles displayed by liquisolid systems and marketed tablets in (1) 450 mL SGF, (2) 600 mL SGF and (3) 900 mL SGF as dissolution medium.

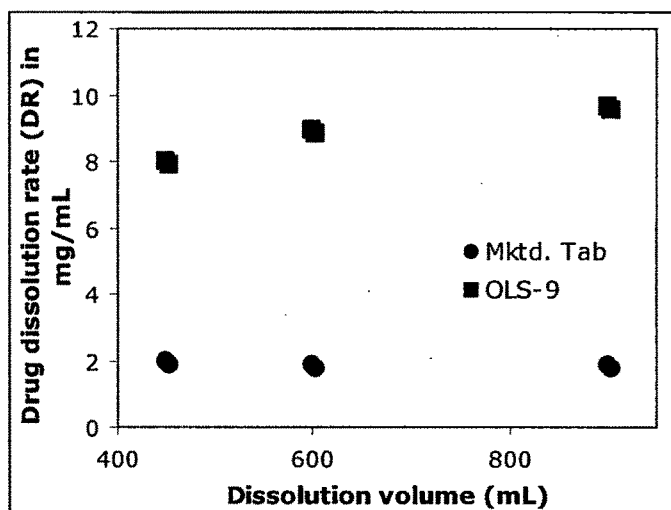


Figure 2.2.9 Effect of the dissolution volume on the initial dissolution rate of OCBZ exhibited by the liquisolid systems and marketed tablets.

The higher OCBZ dissolution rates displayed by the liquisolid systems are clearly observed in Figure 2.2.7 where the dissolution rate (D_R in mg of drug dissolved per min) observed during the first 10 min of the dissolution process is plotted against the volume of dissolution medium.

Figure 2.2.10 The effect of drug concentration in the liquid medication on the initial dissolution rate of OCBZ displayed by liquisolid systems of PEG 600.

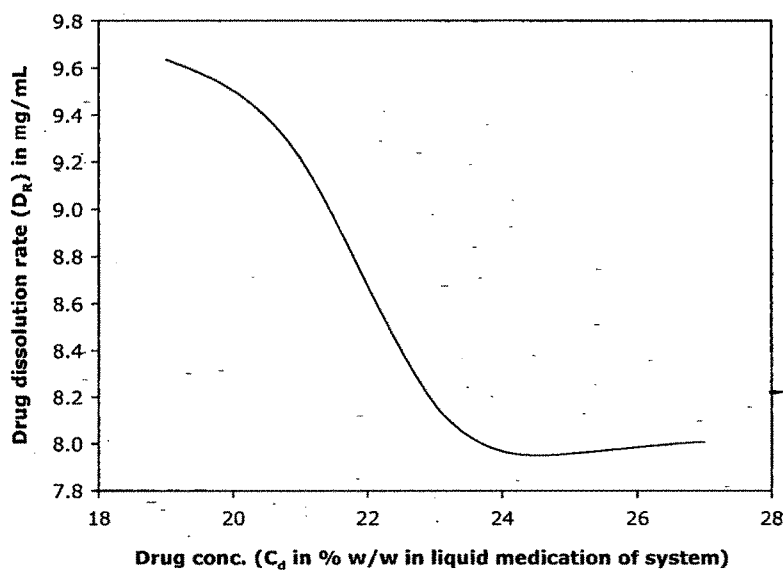
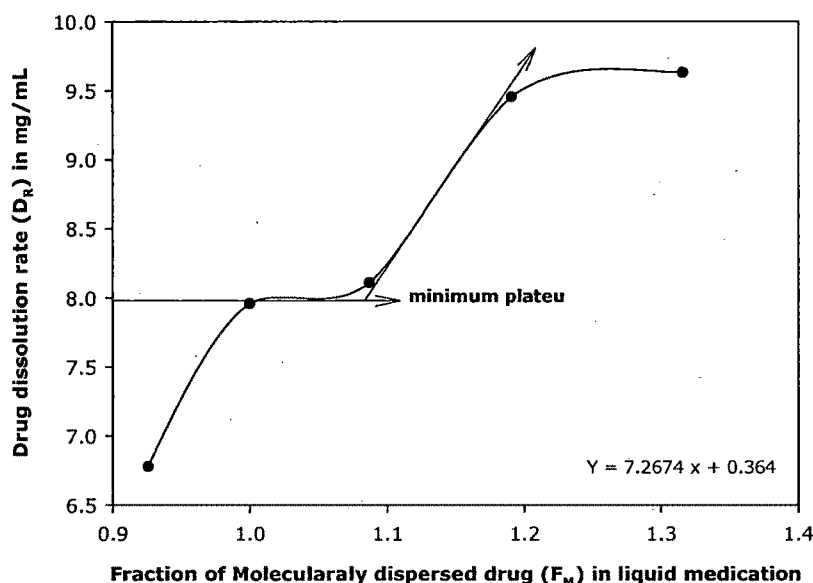


Figure 2.2.11 Effect of fraction (F_M) of the molecularly dispersed drug in the liquisolid systems on the 10 min dissolution rate (D_R) of OCBZ containing various drug concentrations (C_d) in their liquid medications.



For liquisolid systems of OCBZ, the solubilization and molecular dispersion states of the drug in liquisolid systems are different. Such as, the saturation solubility of OCBZ in PEG 600 is 26.09 % w/w (Table 2.2.6), the drug is partly dissolved in the liquid medication of OLS-9 liquisolid system, whereas it is completely dissolved in rest of the systems containing 19 to 25 % w/w of drug in PEG 600. Figure 2.2.10 shows the effect of C_d (OCBZ concentration in the liquid medication) on the 10 min drug dissolution rate (D_R). It was observed that beyond conc. of 23 % w/w of OCBZ in liquid medication there was a sharp decline in percent drug dissolved at 10 min.

Based on the Equation 2.2.6, the F_M values of each liquisolid preparation have been calculated in Table 2.2.5. The dissolution rates obtained from PEG 600 liquisolid systems possessing different C_d values are plotted against their corresponding F_M values in Figure 2.2.11. After remaining at a minimum plateau level (about 8 mg/min) for F_M values ranging from 0.93 to 1.32, the 10 min dissolution rate of the drug increased in a linear manner with increasing F_M values of the liquisolid systems. Therefore, for PEG 600 liquisolid systems, one may be able to predict the dissolution rate (D_R in mg/min) of OCBZ which will be obtained within the initial 10 min of the dissolution process conducted using 50 rpm as the basket speed and 450 mL of SGF without enzymes as the dissolution medium. As shown in Figure 2.2.11 for systems with F_M values ranging from 0.93 to 1.32, the dissolution rate of OCBZ may be given by $Y = 7.2674 x + 0.364$.

Liquisolid system of Gabapentin (GPN)

Generally Liquisolid systems are prepared for those drugs which show dissolution rate limited poor bioavailability. GPN shows good dissolution properties but erratic bioavailability. Such drugs often get dissolved quickly in GI fluid by virtue of their good solubility but remain in solution state only without being absorbed from the gut wall due to their poor lipophilic characteristics (which is important for permeation of drug through gut wall).

In present case an attempt was made to enhance the lipophilicity characteristics of GPN by virtue of addition of a lipophilic agent, Gelucire 44/14 (Lauroyl macrogolglyceride) to the normal liquisolid liquid medication.

Numerous liquisolid systems of GPN (denoted as GLS-1 to GLS 9) showed in Table 2.2.9 were prepared in batches of 100 unit dosage forms. All liquisolid systems were prepared using Avicel PH 103 as carrier powder and Aerosil as coating material. GPN was dissolved in PEG 600 (used as the liquid vehicle to prepare the liquid medication of different drug concentrations) with different drug conc. in liquid medication (19 – 30 % w/w). To this solution 10 mg of Gelucire 44/14 was added in all liquisolid systems. To this liquid medication carrier material avicel was added with constant uniform mixing. After complete addition of avicel, aerosil was added to the admixture at once. The amount of avicel and aerosil to be added to the liquid medication was decided on the basis of excipient ratio. The excipient ratio was varied from 5.5 to 12.5 to get a better idea about the effect of each excipient.

Table 2.2.9 gives key formulation aspects of prepared GPN liquisolid systems like Excipient ratio, Liquid load factor (L_f), Fraction of molecularly dispersed drug (F_M) in the liquid medication of liquisolid systems and Drug dissolution rate for first 10 min of dissolution studies (D_R).

Liquid load factor is the characteristic amount of liquid that is hold by carrier and coating material in duo to maintain acceptable flow properties of system. For GPN liquisolid systems Liquid load factor was studied in the range of 0.44 to 0.87.

2.2.4.1. Solubility studies for GPN liquisolid systems

The solubility of GPN in water and four liquid vehicles tried to prepare the liquisolid systems, namely, propylene glycol, polyethylene glycol 600, glycerin and polysorbate 80 were studied by preparing saturated solutions of the drug in these solvents and analyzing their drug content. GPN did not show absorption in entire UV – visible range. So the drug content of entire solubility and dissolution study were analyzed using validated HPLC method. GPN was mixed in 7 ml screw capped vials with such amounts of each of the above solvents in order to produce systems containing an excess of drug. The mixtures were shaken on an automatic test tube shaking machine for 24 hrs and then settled for

another 2 hrs. The screw capped vials were centrifuged at 2500 rpm for further settling of undissolved crystalline material and thereby obtaining a clear supernatant. After centrifugation, accurately weighed quantities of the filtered supernatant solutions were further diluted with methanol and analyzed with HPLC.

2.2.4.2. Evaluation of Gabapentin Liquisolid systems

2.2.4.2.1. *In vitro* Dissolution studies

To study the effect of amount of dissolution medium on percent drug dissolution of liquisolid systems dissolution studies were conducted in 3 different dissolution medium volumes i.e. 450 mL, 600 mL and 900 mL. The dissolution study was conducted in USP XXVII simulated gastric fluid (without enzymes) having pH 1.2 ± 0.02 as dissolution media. Liquisolid systems, containing an equivalent 100 mg of drug were wrapped in cloth pouch of approximate 2 - 5 μm mesh. This pouch was placed in basket of USP dissolution apparatus (Type I, TDT-06P, Electrolab, Mumbai, India) with 900 ml deaerated dissolution medium. Liquisolid systems were placed in cloth pouches to avert floating of them on dissolution media surface. Previously deaeration of dissolution media were done with the help of ultrasonication (Ultrasonics – 2.2, India) for 15 min. The dissolution apparatus was run at 50 RPM keeping the temperature (37 ± 1 °C) constant throughout the experiment. Samples (5 ml) were withdrawn upto 30 min of dissolution study, at an interval of 5 min and were filtered through 0.45 μm whatmann filter membrane, diluted suitably and analysed using validated HPLC method. An equal volume of fresh dissolution medium maintained at the same temperature was added after withdrawing sample to maintain the sink conditions.

HPLC analysis and standard curves

The parameters for HPLC analysis of GPN from solubility and dissolution studies samples are as follows.

System : Chemito LC 6600 Series,

Pump : Knauer's WellChrom isocratic HPLC K – 501.

Double piston operated with 10 mL stainless steel pump head.

Injector : Knauer's manually driven 6 port 3 channel valve with 20 μL fixed loop with 60° rotation.

Detector : Chemito LC 6600 Dual wavelength UV Visible detector.

Range of measurement – 0 – 2 AU

Integrator output – ± 1.0 V

- Autozero – Fullscale.

Software : Chemitochrom version 1.6

Column : Eurospher 100, 5 μm .-ID – 4.8 mm, Column length – 25 cm.

Mobile phase composition : 5% acetic acid in water : acetonitrile (40:60 v/v)

UV detection wavelength (λ) : 350 nm.

Flow rate: 1mL/min.

In brief, 0.5 mL of sample was mixed with internal standard (1- (aminomethyl) cycloheptaneacetic acid). After derivatization with 2,4,6-trinitrobenzenesulfonic acid at pH 8.5, samples were extracted with toluene. The organic phase was evaporated and the residue dissolved in the mobile phase. 20 μ L of sample was injected in column with fixed loop manual injector. Table 2.2.7 gives the values for precision and accuracy of the assay for the estimation of GPN.

Table 2.2.7 Precision and accuracy of the assay for the estimation of GPN.

Concentration					Deviation From nominal conc.
Nominal	Found mean	SD	RSD	CI (p=95%, n=6)	
Intra-day precision and accuracy of GPN assay					
1.03	0.93	0.04	4.0	0.05	-9.7
10.21	9.67	0.29	3.6	0.26	-5.3
20.31	19.93	0.31	2.2	0.42	-1.9
Inter-day precision and accuracy of GPN assay					
1.05	0.96	0.06	6.8	0.37	-8.6
10.19	9.85	0.31	5.4	0.34	-3.3
20.11	19.26	0.26	3.1	0.64	-4.2

Abbreviations. RSD – Relative standard deviation, CI - Confidence interval of the mean.

2.2.4.2.2. Assessment and comparison of drug dissolution rates

The dissolution rates (D_R) of GPN, in the form of amount of drug (in mg) dissolved per min, presented by each liquisolid formulation during the first 10 min of the dissolution process, were calculated by Equation 2.2.3, where 'M' is the total amount of drug in dosage form and 'D' is the percentage of drug dissolved in 10 min.

2.2.4.2.3. Measurement of angle of repose of liquisolid systems

Angle of repose for GPN liquisolid systems were determined using the same method that was used for CBZ and OCBZ systems. Table 2.2.8 gives the values for angle of repose found for GPN liquisolid systems.

Table 2.2.8 Angle of repose for all the GPN liquisolid systems prepared.

Liquisolid System	Angle of Repose
GLS-1	21.06
GLS-2	23.16
GLS-3	27.28
GLS-4	22.36
GLS-5	27.15
GLS-6	21.39
GLS-7	29.36
GLS-8	24.49
GLS-9	26.06

All the liquisolid systems of GPN prepared exhibited good flow properties. The angle of repose was found to be in range of 21.06 to 293.36⁰.

Table 2.2.9 Key formulation characteristics of prepared GPN liquisolid systems.

Liquisolid System	Vehicle	Carrier material	Coating material	Drug conc (%w/w in liquid medication)	Total wt. of liquid material (W)	Wt of carrier material (Q)	Wt of coating material (q)	Excipient ratio (R) = Q/q	Liquid load factor (L _f) = W/Q	Unit dose wt.	Molecular fraction (F _M) = C _L /C _d	Drug dissolution rate (D _R) in mg/mL = (MxD)/1000
GLS-1	PEG 600 + Gelucire 44/14	Avicel	Aerosil	25	400.00	650	80	8.1	0.62	1240.00	1.14	9.457
GLS-2	PEG 600 + Gelucire 44/14	Avicel	Aerosil	27	370.37	700	60	11.7	0.53	1240.37	1.23	8.131
GLS-3	PEG 600 + Gelucire 44/14	Avicel	Aerosil	30	333.33	750	60	12.5	0.44	1253.33	1.36	8.014
GLS-4	PEG 600 + Gelucire 44/14	Avicel	Aerosil	19	526.32	650	80	8.1	0.81	1366.32	0.86	9.327
GLS-5	PEG 600 + Gelucire 44/14	Avicel	Aerosil	21	476.19	550	80	6.9	0.87	1216.19	0.95	9.401
GLS-6	PEG 600 + Gelucire 44/14	Avicel	Aerosil	23	434.78	550	80	6.9	0.79	1174.78	1.05	8.008
GLS-7	PEG 600 + Gelucire 44/14	Avicel	Aerosil	23	434.78	600	100	6.0	0.72	1244.78	1.05	8.756
GLS-8	PEG 600 + Gelucire 44/14	Avicel	Aerosil	25	400.00	550	100	5.5	0.73	1160.00	1.14	8.836
GLS-9	PEG 600 + Gelucire 44/14	Avicel	Aerosil	27	370.37	750	100	7.5	0.49	1330.37	1.23	8.635

2.2.5. Results and discussion for GPN liquisolid systems

GPN liquisolid systems were prepared with an objective in mind to enhance and offer a consistent bioavailability pattern. The drug is reported to have sufficient solubility in aqueous medium that would provide a constant and desired dissolution profile.

To fulfill the objective of bioavailability enhancement which is not dissolution rate limited Gelucire 44/14, one of the bioavailability ingredient from Gattefosse, France., was added to each liquisolid system. The ingredient Gelucire is GRAS approved. Figure 2.2.12 shows the drug dissolution profiles of the liquisolid systems (GLS-1 to GLS-9) and the marketed conventional tablets of GPN. When 900 ml (per vessel) of SGF USP was used as the dissolution medium, liquisolid systems of GPN displayed considerably enhanced *in-vitro* drug release characteristics than those of its conventional tableted counterpart.

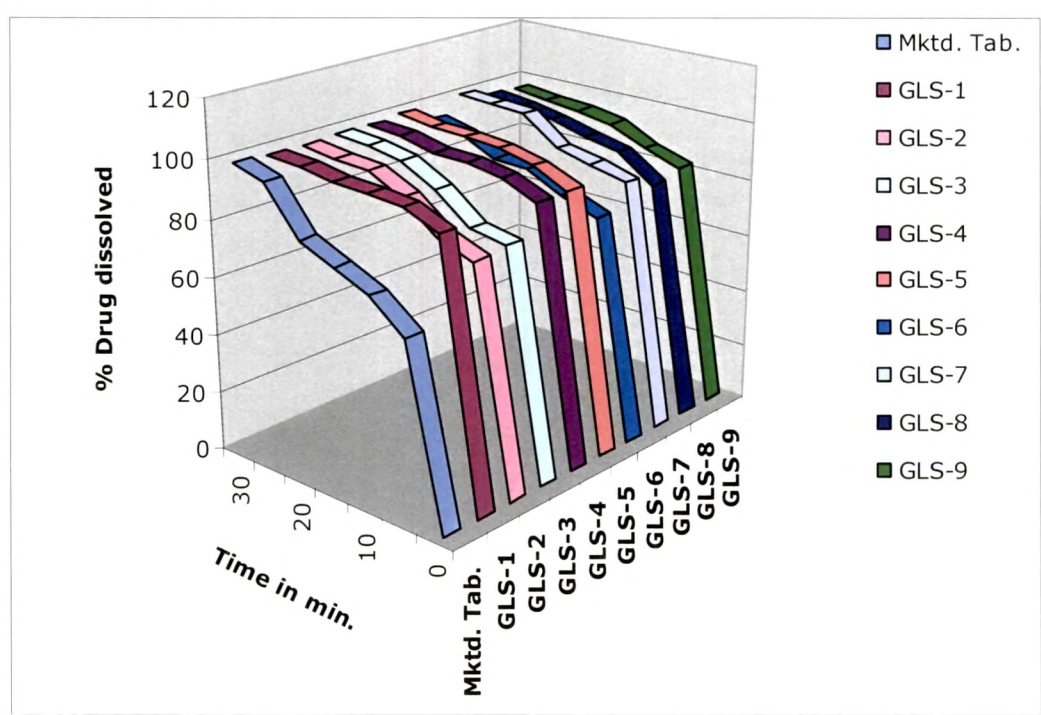


Figure 2.2.12 Percent drug dissolution profiles of liquisolid systems of CBZ

Table 2.2.10 Solubility of GPN in various solvents

Solubility of GPN in various solvents	Solubility (g/100 mL)
Purified water	0.2841
PEG 600	0.3916
Tween 80	0.3310
Propylene glycol	0.3167
Glycerin	0.3004

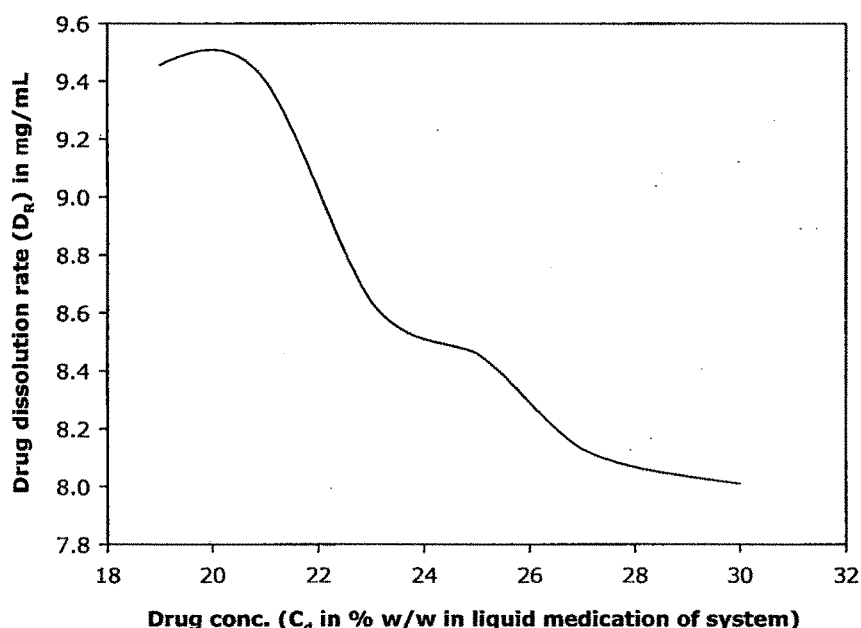
Since GPN is highly soluble in water, performing dissolution studies for GPN in 450 mL and 600 mL would not have yielded any discriminatory results. So the dissolution studies were not performed. Table 2.2.10 shows the solubility profile of CBZ in purified water, polyethylene glycol (PEG) 600, polysorbate 80 (tween 80), propylene glycol and glycerin.

Though GPN is highly soluble in water the results of dissolution studies of developed liquisolid formulations when compared with marketed tablets there was considerable difference in the dissolution rate (D_R) of GPN at 10 min. This may be attributed to lag time of disintegration required for the tablets and effect of excipients used in them.

The higher GPN dissolution rates displayed by the liquisolid systems are depicted in Figure 2.2.12 where the dissolution rate (D_R in mg of drug dissolved per min) observed during the first 10 min of the dissolution process is plotted against the volume of dissolution medium. It was observed that the drug dissolution rate of liquisolid systems is significantly faster than that of the plain tablets and it is independent of the volume of the dissolving liquid used.

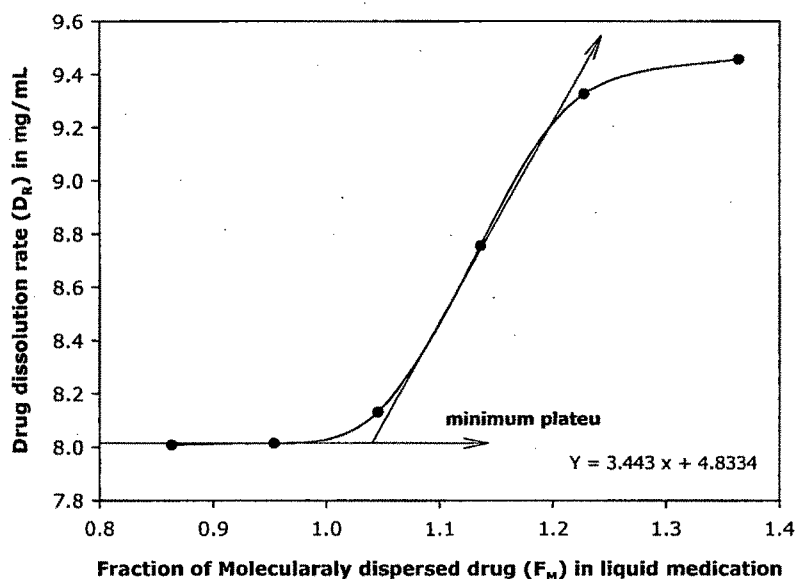
The effect of drug concentration in the liquid medication on the initial dissolution rate of GPN displayed by liquisolid systems of PEG 600.

Figure 2.2.13 The effect of drug concentration in the liquid medication on the initial dissolution rate of GPN displayed by liquisolid systems of PEG 600



The drug concentration in the liquid medication (C_d ranging from 19 to 30 % w/w) has an apparent effect on the GPN 10 min dissolution rates displayed by the liquisolid systems of PEG 600, as shown in Figure 2.2.13. However, at the same dissolution conditions, systems containing liquid medications with increasing C_d values exhibited declining *in vitro* release properties until reaching a minimum plateau dissolution rate displayed by the liquisolid systems containing about more than 28 % w/w of drug in their liquid medications. Such differences in the drug dissolution rates of the PEG 600 liquisolid systems possessing different C_d values, observed in may be justified using the previous hypothesis of the available drug surface effects on dissolution.

Figure 2.2.14 Effect of fraction (F_M) of the molecularly dispersed drug in the liquisolid systems on the 10 min dissolution rate (D_R) of GPN containing various drug concentrations (C_d) in their liquid medications.



The F_M values of each liquisolid preparation have been shown in Table 2.2.9. The dissolution rates obtained from PEG 600 liquisolid systems possessing different C_d values are plotted against their corresponding F_M values in Figure 2.2.14. After remaining at a minimum plateau level (about 8 mg/min) for F_M values ranging from 0.86 to 1.36, the 10 min dissolution rate of the drug increased in a linear manner with increasing F_M values of the liquisolid systems. Therefore, for PEG 600 liquisolid systems, one may be able to predict the dissolution rate (D_R in mg/min) of GPN which will be obtained within the initial 10 min of the dissolution process conducted using 50 rpm as the basket speed and 900 mL of SGF without enzymes as the dissolution medium. As shown in Figure 2.2.14 for systems with F_M values ranging from 0.86 to 1.36, the dissolution rate of GPN may be given by $Y = 3.443x + 4.8334$.

2.2.6. Stability studies for CBZ, OCBZ and GPN liquisolid systems

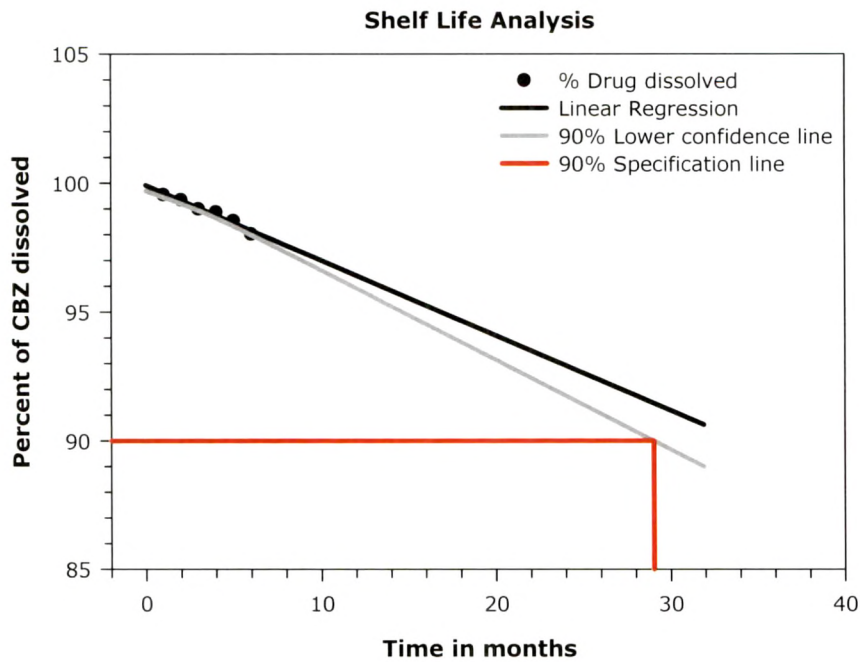
Optimized batches of Liquisolid systems of CBZ, OCBZ and GPN were packaged in high density polyethylene (HDPE) bottles with polypropylene (PP) caps (foamed polyethylene and pressure sensitive liner). The systems were subjected to stability testing according to the International Conference on Harmonization guidelines for zone III and IV. The packed containers of prepared systems along with marketed formulation and bulk pure drug CBZ, OCBZ and GPN were kept for accelerated ($40\pm 2^{\circ}\text{C}/75\pm 5\%$ relative humidity) and long term ($30\pm 2^{\circ}\text{C}/65\pm 5\%$ relative humidity) stability in desiccators with saturated salt solution for up to 6 months. A visual inspection (for discoloration of liquisolid content), dissolution testing and pure drug content estimation was carried out every 30 days for the entire period of stability study.

Samples of long term stability i.e. $30\pm 2^{\circ}\text{C}/65\pm 5\%$ RH were treated as fall back samples. They were to be analyzed only if samples for accelerated conditions fail in analysis.

Liquisolid systems of GPN were found to be dark yellow in colour with greasy appearance so they were discarded from further study.

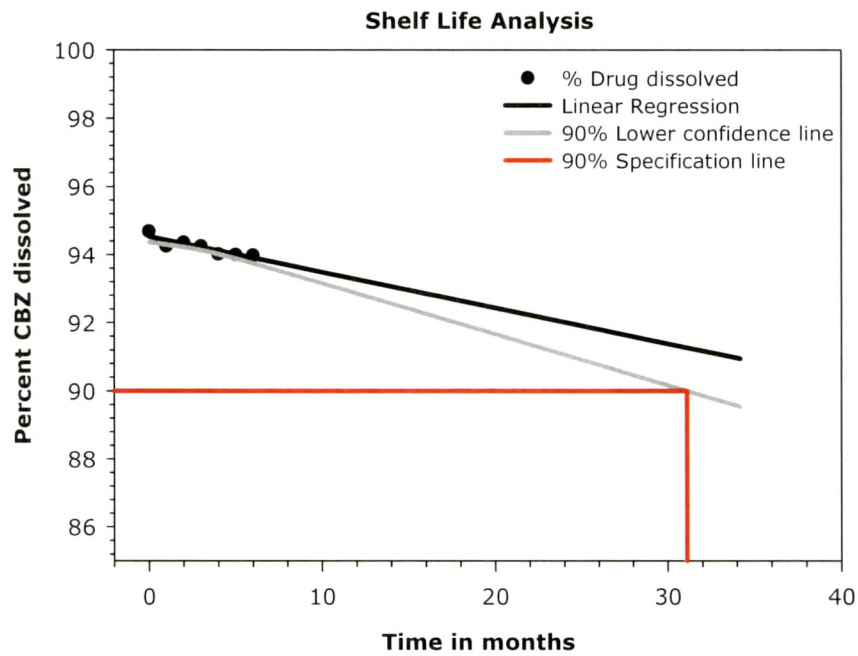
Stability data of CLS-1 liquisolid system was extrapolated using linear regression tool for the determination of shelf life of product. Figure 2.2.16 shows the extrapolated accelerated stability data for shelf-life calculation of OCBZ liquisolid. The calculated shelf life was found to be 29.028 months (2.38 years).

Figure 2.2.15 Extrapolation of accelerated stability data of CBZ liquisolid system for shelf-life calculation.



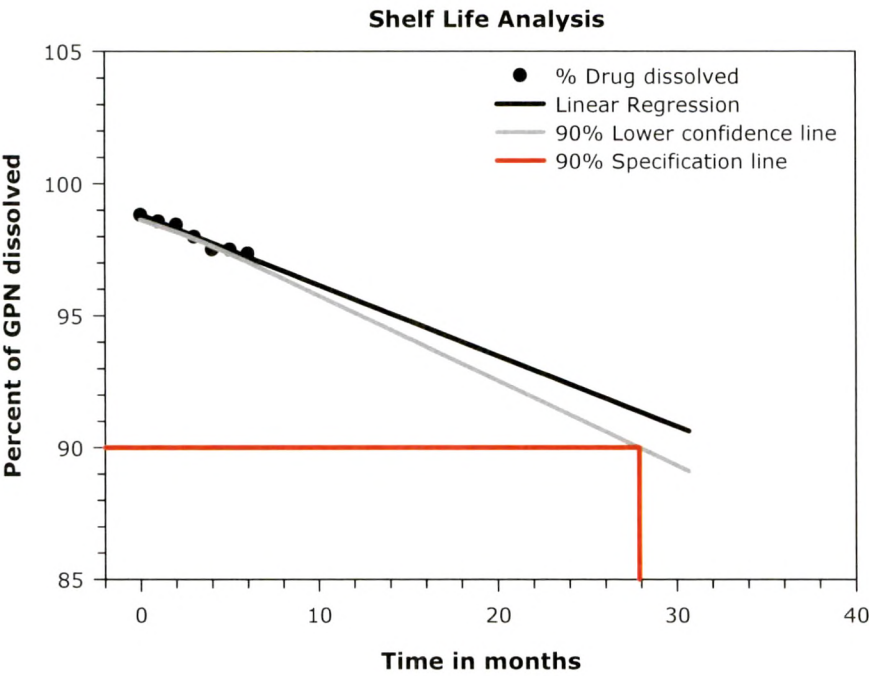
Stability data of OLS-1 liquisolid system was extrapolated using linear regression tool for the determination of shelf life of product. Figure 2.2.16 shows the extrapolated accelerated stability data for shelf-life calculation of OCBZ liquisolid. The calculated shelf life was found to be 20.92 months (1.72 years).

Figure 2.2.16 Extrapolation of accelerated stability data of CBZ Na-CMC SD for shelf-life calculation.



Stability data of GLS-1 liquisolid system was extrapolated using linear regression tool for the determination of shelf life of product. Figure 2.2.17 shows the extrapolated accelerated stability data for shelf-life calculation of GPN liquisolid. The calculated shelf life was found to be 27.88 months (2.29 years).

Figure 2.2.17 Extrapolation of accelerated stability data of CBZ Na-CMC SD for shelf-life calculation.



2.2.7. Conclusion

Liquisolid systems prepared for CBZ, OCBZ and GPN showed marked dissolution enhancement properties. Effect of additional solubilizing agent SLS and tween 80 studied on CBZ and OCBZ liquisolid formulations showed significant effect on dissolution enhancement properties of drug. Optimum liquid load factor and selection of proper solvent are the key determinants for achieving the enhanced drug dissolution.

Accelerated stability studies were performed for CBZ and OCBZ liquisolid formulations to determine the shelf life of the formulation. The results showed that the systems are stable upto 30 months.

The results from study helps in concluding that drug solution or dispersion adsorbed over carrier and coating material show significant drug dissolution compared to their powdered or conventional formulation counterpart. This shows that liquisolid systems are potential drug delivery systems for drug dissolution enhancement.

However the systems will be more fruitful if the drug dose is low. This will make adequate space for addition of more amount of carrier and coating material leading to possibility of their compression in solid dosage forms.

References

- A. McKenna and D. F. McCafferty. **(1988)**. Effect of particle size on the compaction mechanism and tensile strength of tablets. **J Pharm Pharmacol.**, 15-17, 2443-2465.
- A. Martin, J. Swarbrick and A. Commarata. **(1993)**. In: (Eds.) *Physical Pharmacy*,. 4th, pp. 331.
- B. Hoener and L. Z. Benet. **(1996)**. ***Factors influencing drug absorption and drug availability***. In: G. S. Banker and C. T. Rhodes. (Eds.) *Modern Pharmaceutics*. 3rd, pp. 129-147.
- A. A. Noyes and W. R. Whitney. **(1897)**. The rate of solution of solid substances in their own solutions. **J. Am. Chem. Soc.**, 930-934.
- S. Spireas and S. Sadu. **(1998)**. Enhancement of prednisolone dissolution properties using liquisolid compacts. **Int J Pharm**, 177-188.
- Y. Javazadeh, M. R. Siahi-Shadbad, M. Barzegar-Jalali and A. Nokhodchi. **(2005)**. Enhancement of dissolution rate of piroxicam using liquisolid compacts. **Farmaco**, 4, 361-365.
- A. Nokhodchi, Y. Javazadeh, M. R. Siahi-Shadbad and M. Barzegar-Jalali. **(2005)**. The effect of type and concentration of vehicles on the dissolution rate of a poorly soluble drug (indomethacin) from liquisolid compacts. **J Pharm Pharm Sci**, 1, 18-25.

Solid Dispersions



2.3. Solid Dispersions (SDs)

2.3.1. Materials

Carbamazepine (CBZ) and Oxcarbamazepine (OCBZ) were received as gift samples from Relax Pharmaceuticals Limited, Vadodara, India., and Torrent Research Center, Ahmedabad, India respectively. Sodium carboxy methyl cellulose and Hydroxyl propyl methyl cellulose were purchased from S. D. Fine-Chem Ltd., Mumbai, India. Chito Clear® chitosan were received as a generous gift sample from Primax Biopolymers, Ireland. All the other chemicals and solvents were of analytical grade and were used without further purification. Deionized double-distilled water was used through out the study.

2.3.2. Methods

2.3.2.1. Preparation of Solid dispersion.

Solid dispersions for carbamazepine and oxcarbamazepine using three different polymers Na-CMC, HPMC and Chitosan individually, were prepared by the method illustrated below.

Solid dispersions of all the three polymers were prepared by modified solvent evaporation method (Rasenack, *et al.*, **2003**) wherein drug was dissolved in acetone at its saturation solubility with continued stirring upto 30 minutes. Polymer was suspended in sufficient amount of water (upto wet mass of polymer). The drug solution was poured at once in polymer suspension. The entire solvent was evaporated under reduced pressure at 60 – 70°C with Rotavapor (Heidolph, Germany) with solvent recovery. The recovered solvent was used for next batch. The solid dispersion was obtained in flask which was dried at 70 – 80°C and stored in desiccator for 24 hours.

Solid dispersions for CBZ and OCBZ with Na-CMC, HPMC and Chitosan, individually were prepared in following pattern.

- ☒ Solid Dispersions of CBZ with Na CMC
- Solid Dispersions of CBZ with HPMC
- Solid Dispersions of CBZ with Chitosan
- ☒ Solid Dispersions of OCBZ with Na CMC
- Solid Dispersions of OCBZ with HPMC
- Solid Dispersions of OCBZ with Chitosan

2.3.2.2. Experimental Design

To study all the possible combinations of individual polymer and drug, solid dispersions of CBZ and OCBZ were prepared according to three levels full factorial design (3^2). The experiments were constructed and conducted in a fully randomized order. (Derringer and Suich, 1980) For experimental design the dependent variables measured were percent drug dissolved at various time points and particle size of solid dispersion.

Independent variables of the 3^2 full factorial design with their coded and actual values are shown in Table 2.3.1. The range of a factor was chosen in order to adequately measure its effect on the response variables. This design was selected as it provides sufficient degrees of freedom to resolve the main effects as well as the factor interactions. MLR analysis was used to find out the control factors that affects significantly on response variables.

2.3.2.3. Solubility Determination

For the solubility determination of each solid dispersion of factorial design, excess of material was placed in contact with 7 mL of solvent in sealed glass tubes. The tubes were shaken on a vortex mixer and were maintained at 25°C for 24 hours. The saturated solution was centrifuged and the supernatant was filtered through 0.45 μ m whatmann filter paper, diluted suitably with water and analysed UV spectrophotometrically at 285 nm for CBZ, at 303 nm for OCBZ and (Model UV-1601 UV, Visible spectrophotometer, Shimadzu, Japan).

2.3.2.4. Differential Scanning Calorimetry (DSC)

Differential scanning calorimetric analysis was used to characterize the thermal behaviour of the solid dispersions and pure drugs. DSC thermograms were obtained using an automatic thermal analyzer system (DSC-60, Shimadzu, Japan). Temperature calibration was performed using indium as a standard. About 2 – 3 mg accurately weighed samples were crimped in a standard aluminium pan and heated from 40^o – 300^oC at a heating rate of 10°C/min under constant purging of dry nitrogen at 30 ml/min. An empty pan, sealed in the same way as the sample, was used as a reference. The characteristic endothermic peaks and specific heat of the melting endotherm were recorded.

2.3.2.5. Scanning Electron Microscopy (SEM)

The purpose of SEM study was to obtain a topographical characterization of solid dispersions. SEM photographs for pure drugs and their SDs with Na-CMC, HPMC and chitosan were taken with scanning electron microscope (JSM-5610LV, Jeol Corporation., Japan). Samples were individually glued on the brass stubs with the help of double sided adhesive tape. The images were captured at an excitation voltage of 15 KV at varying

magnification from 50X to 650X with a working distance of 39 mm at room temperature with the secondary electron image (SEI) as a detector.

2.3.2.6. In Vitro Dissolution Study for Solid Dispersions

The dissolution study for all the solid dispersions of experimental design for CBZ and OCBZ with Na-CMC, HPMC and chitosan were performed using USP XXVII simulated gastric fluid (SGF) without enzymes having pH 1.2. Accurately weighed amount of solid dispersion, containing equivalent to 100 mg of pure drug was wrapped in cloth pouch of approximate 2 - 5 μ m mesh. This pouch was placed in basket of USP dissolution apparatus (Type I, TDT-06P, Electrolab, Mumbai, India) with 900 ml deaerated dissolution medium.

SD systems were placed in cloth pouches to avert floating of them on dissolution media surface. Previously deaeration of dissolution media were done with the help of ultrasonication (Ultrasonics – 2.2, India) for 15 min. The dissolution apparatus was run at 50 RPM keeping the temperature ($37^{\circ} \pm 1^{\circ}\text{C}$) constant throughout the experiment. Samples (5 ml) were withdrawn upto 40 min of dissolution study, at an interval of 5 min and were filtered through 0.45 μ m whatmann filter paper, diluted suitably and analysed spectrophotometrically at 285 nm for CBZ and 303 nm for OCBZ (Shimadzu, UV-1601 UV, Visible spectrophotometer, Japan). An equal volume of fresh dissolution medium maintained at the same temperature was added after withdrawing sample to maintain the sink conditions.

2.3.2.7. Wettability Studies

To get an idea about wettability properties of the SDs prepared wettability studies were performed. Study was performed with hypothesis in mind that faster the wetting of system faster would be the dissolution. Sample weighed about 1 gm was placed in sintered glass funnel of 27 mm. internal diameter. Bridge was formed at the neck of funnel with the help of cotton plug. The funnel was held in upright position in a beaker filled with water such that water level in beaker just touches the cotton plug. Methylene blue powder was layered over surface of pure drug in funnel. Time required to raise the water through drug till wetting of methylene blue powder occurs was recorded (Gohel and Patel, **2003**). The procedure was followed for all the SDs.

2.3.2.8. Angle of repose

To get an idea about flowability properties of the solid dispersions, angle of repose for all the batches of experimental design was determined. If the angle exceeds 50° , the material will not flow satisfactorily, whereas materials having values lesser flow easily and well. The rougher and more irregular the surface of the particles, higher is the angle of repose. (McKenna and McCafferty, **1988**) The angle of repose was measured by passing SD through a sintered glass funnel of internal diameter 27 mm. on the horizontal surface. The

height (h) of the heap formed was measured with a cathetometer, and the radius (r) of the cone base was also determined. The angle of repose (Φ) was calculated from Equation 2.3.1.

Equation 2.3.1
$$\Phi = \tan^{-1} \left(\frac{h}{r} \right)$$

2.3.3. Results and Discussion

The rate of oral absorption of poorly soluble drugs is often controlled by their dissolution rate in gastrointestinal tract (Lobenberg and Amidon, **2000**). Thus solubility and dissolution rate are the key determinants of oral bioavailability which is the concluding point drawn for fate of oral bioavailability (Desai, *et al.*, **2003**, Rawat and Jain, **2003**). Carbamazepine (CBZ) and oxcarbamazepine (OCBZ) are widely prescribed antiepileptic drugs having poor water solubility (about 170 and 180 mg/L at 25°C respectively) (Moneghini, *et al.*, **2002**). Due to this its absorption is dissolution rate limited which often results in irregular and delayed absorption (Bertilsson, **1978**).

Solid dispersion is one of the most promising drug dissolution enhancement method for formulators due to its ease of preparation, ease of optimization and reproducibility (Chiou and Reigelman, **1971**, Ford, **1986**, Goldberg, *et al.*, **1966**, Leuner and Dressman, **2000**). In case of SDs poorly soluble drug are dispersed in an inert hydrophilic polymer or matrix by melting, solution formation or solvent melting to yield solid dispersion. (Chiou and Reigelman, **1971**, Ford, **1986**)

Usually SDs are prepared with water soluble low melting point synthetic polymers like polyvinyl pyrrolidone (PVP), mannitol or high molecular weight polyethylene glycols (PEGs) (El-Zein, *et al.*, **1998**). These polymers show superior results in drug dissolution enhancement, but the amount of these polymers required was relatively large, around 1:2 to 1:8 (drug/polymer) ratio (Narang and Srivastava, **2002**). In certain similar experiments it has been observed that, PVP and PEG gets dissolved first in dissolution media (owing to their high water solubility) leaving the drug back in undissolved state. In such case though the drug is in controlled crystallization state or amorphous state the polymers are unable to provide wetting ability to the drug particles. In such cases there may be possibility of rapid reversion of amorphous drug to the more stable crystalline state in presence of small amount of plasticizers like water (Hancock and Parks, **2000**).

Literature survey revealed that certain hydrophilic swellable polymers like Na-CMC, HPMC and chitosan have still been unexplored for their potential to form solid dispersion in order to improve dissolution properties of poorly soluble drugs. For this reason, in the present work, water swellable polymers or normal excipients of solid dosage forms were used. These polymers were supposed to hold the drug in intimate contact with water (owing to

their water retention potential) and increase its wettability. Solid dispersions were prepared with modified solvent evaporation technique.

Full factorial experimental design is one of the best tools to study effect of different variables on the quality determinant parameters of any formulation. In the present study independent variables were assigned to amount of polymer and amount of solvent at three different levels whereas responses or dependant variables for them was assigned to percent drug dissolved at various time points in USP simulated gastric fluid without enzymes. Q_{30} i.e. percent drug dissolved at 30 minutes was determined for SGF without enzymes (USP XXVII). The MLR analysis of results led to equations that adequately described the influence of the independent variables on the selected responses. Polynomial regression equations and contour plots were used to relate the dependent variables. As part of the optimization process, the main effects, interaction effects and quadratic effects of amount of polymer and amount of solvent on percent drug dissolved of solid dispersion were investigated.

2.3.4. Solid Dispersions of Carbamazepine

Quantitative solubility data for CBZ in water, polyethylene glycol 600 and SDs of CBZ with Na-CMC, HPMC and Chitosan with highest polymer content is given in Table 2.3.1. Solubility of carbamazepine in Na-CMC solid dispersion increased to 0.1903 mg/mL from its 0.0091 mg/mL aqueous solubility.

Table 2.3.1 Quantitative solubility data for pure CBZ, in different solid dispersion systems and polyethylene glycol 600.

	Solvents		Solid dispersion system		
	Water	PEG 600	Na-CMC	HPMC	Chitosan
Solubility of CBZ (g/100mL)	0.0091	0.1782	0.1903	0.1411	0.1168

Stepwise multivariate linear regression was performed to evaluate the relationship obtained between response and independent variables. For each polymer 3^2 full factorial design was applied. The independent and dependent factors, their levels and the matrix of variables and responses for 3^2 factorial design of each polymer are shown in Table 2.3.2.

The statistical evaluation of dependent variables was carried out by analysis of variance (ANOVA) using Microsoft Excel Version – 2003. The ANOVA results (p values and coefficients of percent drug dissolved for the equations representing the quantitative effect of the independent variables) on percent drug dissolved in SGF without enzymes for each polymer are shown Table 2.3.3. The significant parameters in the equations can be selected using a stepwise forward and backward elimination for the calculation of regression analysis. However in present study full model having both significant and nonsignificant 'p' values were used in obtaining dependent variables (Gohel and Panchal, 2002). in table 3. The equations for each polymer can be generated by putting values of coefficients in Equation 2.3.2.

Equation 2.3.2
$$y = b_0 + b_1X_1 + b_2X_2 + b_{11}X_1^2 + b_{22}X_2^2 + b_{12}X_1X_2$$

Table 2.3.2 Matrix of independent variables and responses for 3² factorial design for each polymer.

Batch	Variables with levels *		Response Values			
	X ₁	X ₂	Q ₃₀ for % Drug Disso. in SGF	Particle Size of Optimized Batch (μm)	Angle of repose for Optimized Batch (°)	Wettability time for Optimized Batch (minutes)
Polymer : Na-CMC						
SCSD-1	-1	-1	64.25	15 -17	29.43	03.15
SCSD-2	-1	0	68.45			
SCSD-3	-1	1	67.21			
SCSD-4	0	-1	76.85			
SCSD-5	0	0	83.54			
SCSD-6	0	1	85.65			
SCSD-7	1	-1	91.14			
SCSD-8	1	0	93.47			
SCSD-9	1	1	94.69			
Polymer : HPMC						
HCSD-1	-1	-1	62.46	2 - 79	33.25	03.56
HCSD-2	-1	0	64.23			
HCSD-3	-1	1	65.28			
HCSD-4	0	-1	66.47			
HCSD-5	0	0	70.25			
HCSD-6	0	1	72.19			
HCSD-7	1	-1	71.25			
HCSD-8	1	0	69.69			
HCSD-9	1	1	70.58			
Polymer : Chitosan						
CCSD-1	-1	-1	61.26	138 -158	34.56	4.49
CCSD-2	-1	0	65.24			
CCSD-3	-1	1	65.36			
CCSD-4	0	-1	74.21			
CCSD-5	0	0	75.29			
CCSD-6	0	1	76.91			
CCSD-7	1	-1	80.24			
CCSD-8	1	0	82.91			
CCSD-9	1	1	83.16			

*

Independent variables		Levels		
		Low	Medium	High
X1	Amount of Polymer (gm)	1	2	3
X2	Amount of Solvent (mL)	150	200	250

Table 2.3.3 ANOVA results ('p' value) effect of the variables on percent drug dissolved of solid dispersions.

Polymer	Factor	For Dissolution in SGF	
		Coefficient	'p' Value
Na CMC	X_1	13.2317	0.0005
	X_2	2.5517	0.0523
	X_1^2	-2.1450	0.2266
	X_2^2	-1.8550	0.2810
	X_1X_2	0.1475	0.8921
Chitosan	X_1	9.075	0.0001
	X_2	1.6183	0.0155
	X_1^2	-2.4383	0.0226
	X_2^2	-0.9583	0.1866
	X_1X_2	-0.2950	0.5116
HPMC	X_1	3.2583	0.0188
	X_2	1.3117	0.1580
	X_1^2	-2.3883	0.1438
	X_2^2	-0.0183	0.9889
	X_1X_2	-0.8725	0.3843

Coefficients with one factor indicates the effect of that particular factor while the coefficients with more than one factor and those with second order terms represent the interaction between those factors and the quadratic nature of the phenomena, respectively. Positive sign of the term indicates positive (additive) effect while negative sign indicates negative (antagonistic) effect of the factor on the response. (Hancock and Parks, 2000)

It can be concluded from equations (that can be generated from anova results) that x_1 (amount of polymer) showed the largest positive effect whereas the term x_2 (amount of solvent) showed statistically insignificant positive effect on percent drug dissolved. The quadratic terms of x_1 and x_2 also had significant positive effect on percent drug dissolved.

Figure 2.3.1, Figure 2.3.2 and Figure 2.3.3 shows the response surface plots for percent CBZ dissolved from SDs in SGF of Na-CMC, HPMC and chitosan at 30 minutes (Q_{30}) respectively. Response surface shows that higher the amount of polymer, significant is the dissolution enhancement. However, for HPMC this was not observed which may be attributed to controlled release matrix forming ability of HPMC (Cao, *et al.*, 2004).

Figure 2.3.1 Response surface plot for effect of Na-CMC and amount of solvent on % CBZ dissolved.

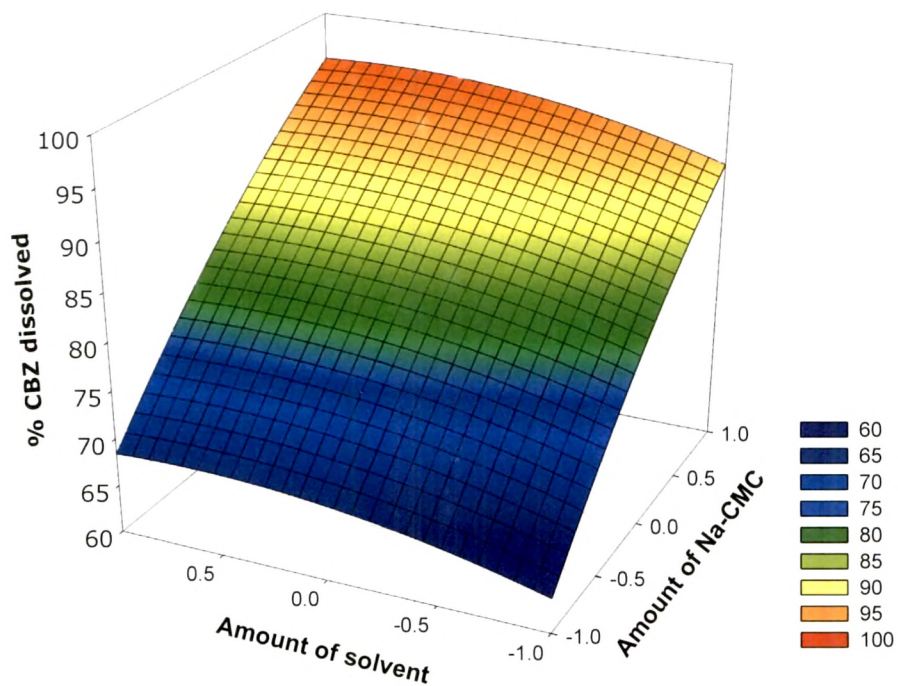


Figure 2.3.2 Response surface plot for effect of HPMC and amount of solvent on % CBZ dissolved.

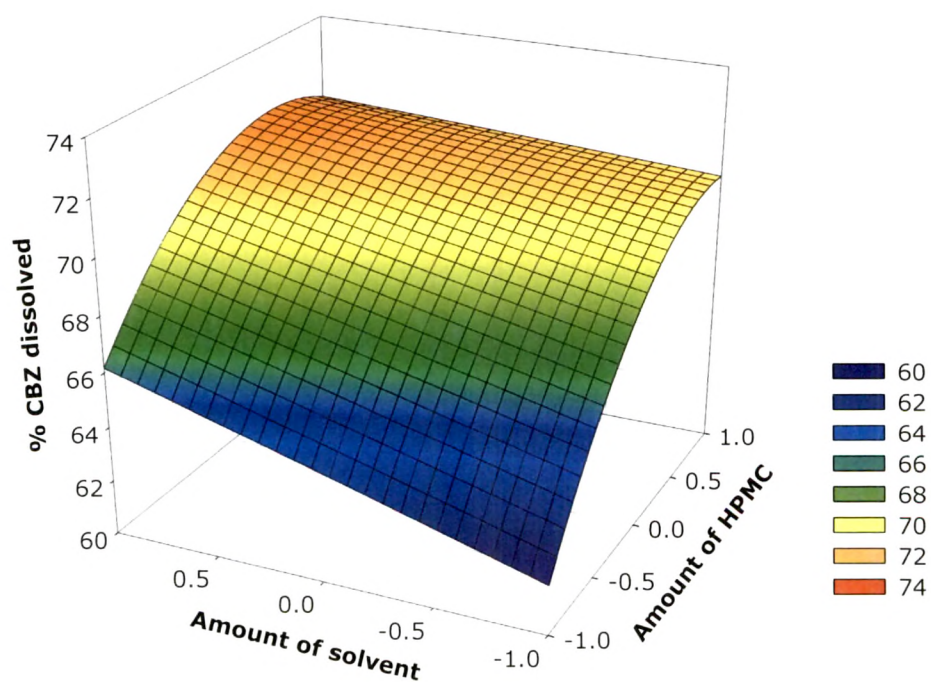
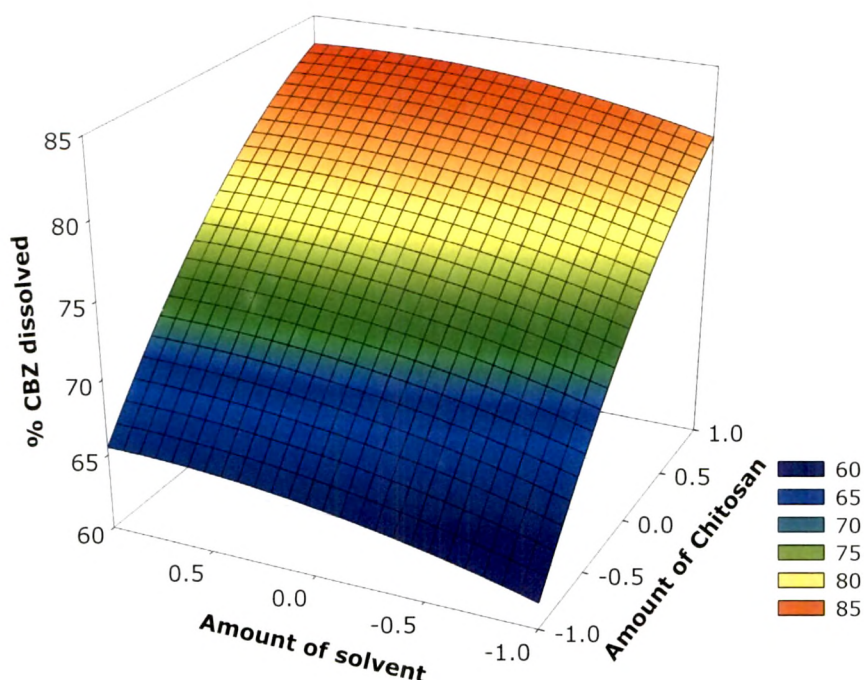


Figure 2.3.3 Response surface plot for effect of Chitosan and amount of solvent on % CBZ dissolved.



The reliability of the equations that described the influence of factors on percent drug dissolved was assessed by preparing three additional check points SDs using the amount of x_1 and x_2 as -0.5, 0.25 and 0.75. (Mashru, *et al.*, **2005**) The experimental values and predicted values of each response are shown in Table 2.3.4. Equation 2.3.3 was used to compute the % relative error between predicted values and experimental values of each response.

Equation 2.3.3 % Relative error = $\left(\frac{|\text{Predicted value} - \text{Experimental value}|}{\text{Predicted value}} \right) \times 100$

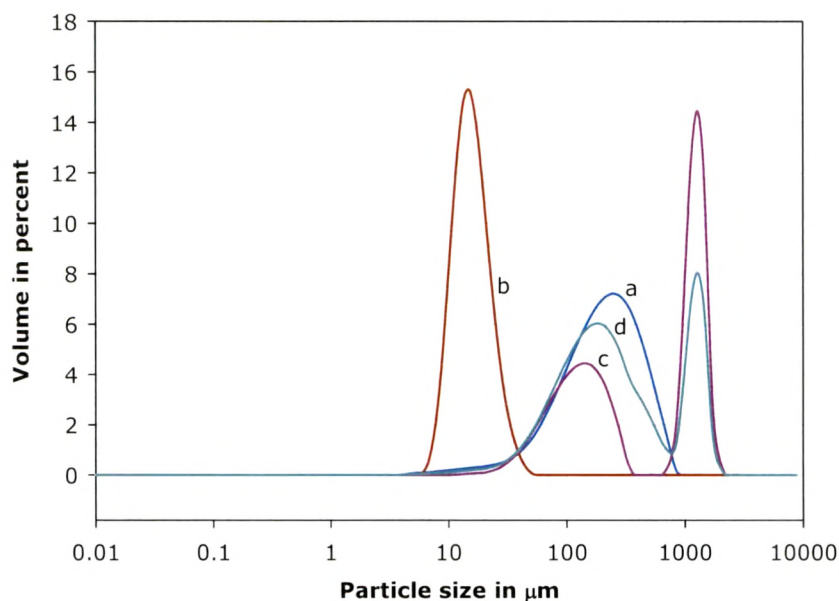
The percent relative error obtained from checkpoint batches was in range of 1.62 to 6.70. These low values of the relative error showed that for all the polymers there was a reasonable agreement of predicted values and experimental values. This proved the validity of model and ascertained the effects of Na-CMC, HPMC, chitosan and amount of solvent on percent drug dissolved.

Table 2.3.4 Cross validation of model obtained using observed and predicted results of checkpoint batches.

Polymer	X1	X2	Predicted values	Experimental values	% Relative Error
Na CMC	-0.5	0.75	76.91	80.25	4.34
	0.25	0.5	87.25	88.67	1.62
	0.75	-0.5	90.17	87.65	2.80
HPMC	-0.5	0.75	68.72	64.12	6.70
	0.25	0.5	70.86	66.29	6.44
	0.75	-0.5	70.42	72.67	3.20
Chitosan	-0.5	0.75	71.74	76.36	6.43
	0.25	0.5	78.75	82.37	4.59
	0.75	-0.5	80.60	78.21	2.97

Particle sizes of pure drug and SDs were determined using Malvern Mastersizer (Malvern Mastersizer, UK) with petroleum ether as dispersion medium for sample. Results of particle size analyses are shown in Figure 2.3.4. Particle size of pure drug was found to be in a broad range of 150 – 600 μm . SDs with Na-CMC were observed with most uniformity in particle size which ranged from 15 – 17 μm . SDs of CBZ with HPMC also showed considerable decrease in the particle size of CBZ, however a major fraction of HPMC SD particles was found in the range of 1000 to 1200 μm . In case of SDs with chitosan there were two particle size distributions almost of equal quantity, first in the range of 138 – 158 μm and the other in 1000 – 2500 μm . The latter can be very well attributed to particle size of plain chitosan whereas first can be credited to decreased particle size of drug. This shows that SDs of CBZ with Na – CMC, HPMC and chitosan showed considerable decrease in the particle size of CBZ.

Figure 2.3.4 Particle size analyses. (a) Pure CBZ, (b) SD of CBZ with Na CMC, (c) SD of CBZ with HPMC and (d) SD of CBZ with Chitosan.



The release of drug from SDs was analyzed in SGF without enzymes. In order to assess comparative extent of dissolution rate enhancement from its SDs mean dissolution time (MDT) was calculated. The dissolution data obtained of marketed conventional CBZ tablets and SDs of all polymers was treated according to Equation 2.3.4 (Barzegar-Jalali, *et al.*, 2002).

Equation 2.3.4

$$\text{MDT}_{\text{in vitro}} = \frac{\sum_{i=1}^n t_{\text{mid}} \Delta M}{\sum_{i=1}^n \Delta M}$$

where i is dissolution sample number, n is number of dissolution sample times, t_{mid} is time at the midpoint between times t_i and t_{i-1} , and ΔM is the amount of CBZ dissolved (μg) between times t_i and t_{i-1} . The results for MDT calculated are shown in Table 2.3.5. The MDT value of marketed CBZ tablets SGF without enzymes was found to be 16.07 min. which was decreased to 7.14 in case of SD of drug with Na-CMC. This depicts the fulfillment of objective of dissolution enhancement of CBZ.

Table 2.3.5 Mean Dissolution Time (MDT) calculated for all the batches of CBZ SD of experimental design for Na-CMC, HPMC and Chitosan.

Batches		MDT for dissolution in SGF		
X1	X2	Na-CMC	HPMC	Chitosan
-1	-1	8.50	9.29	9.29
-1	0	9.46	9.22	10.20
-1	1	8.79	9.19	9.91
0	-1	9.70	8.75	10.65
0	0	9.03	8.69	8.76
0	1	8.20	8.32	7.85
1	-1	8.44	7.55	7.71
1	0	8.80	7.95	8.23
1	1	7.14	9.81	7.15

The amount of percent drug dissolved in 30 minutes (Q_{30}) in SGF without enzymes for all the SDs prepared according to experimental design is reported in Table 2.3.2.

SDs of polymers Na-CMC and chitosan showed increase in dissolution rate on increase in amount of polymer. Whereas in case of HPMC solid dispersions increase in amount of polymer upto certain level led to enhanced drug dissolution but further addition of polymer resulted in decrease of dissolution of CBZ. This may be correlated to matrix forming ability of HPMC.

The SEM images for pure CBZ and its SDs with Na-CMC, HPMC and chitosan are shown in Figure 2.3.5, Figure 2.3.6, Figure 2.3.7 and Figure 2.3.8 respectively. Pure CBZ image showed crystalline drug of irregular shapes and sizes ranging from 50 to 600 μm . whereas images of SD of drug with Na-CMC upto 100X magnification did not show any crystalline material. In case of SDs with HPMC and chitosan although a significant decrease in size of drug crystals was observed, agglomeration of crystals was also observed.

Figure 2.3.5 SEM image of Pure crystalline CBZ.



Figure 2.3.6 SEM image of optimized batch of SD of CBZ with Na CMC.

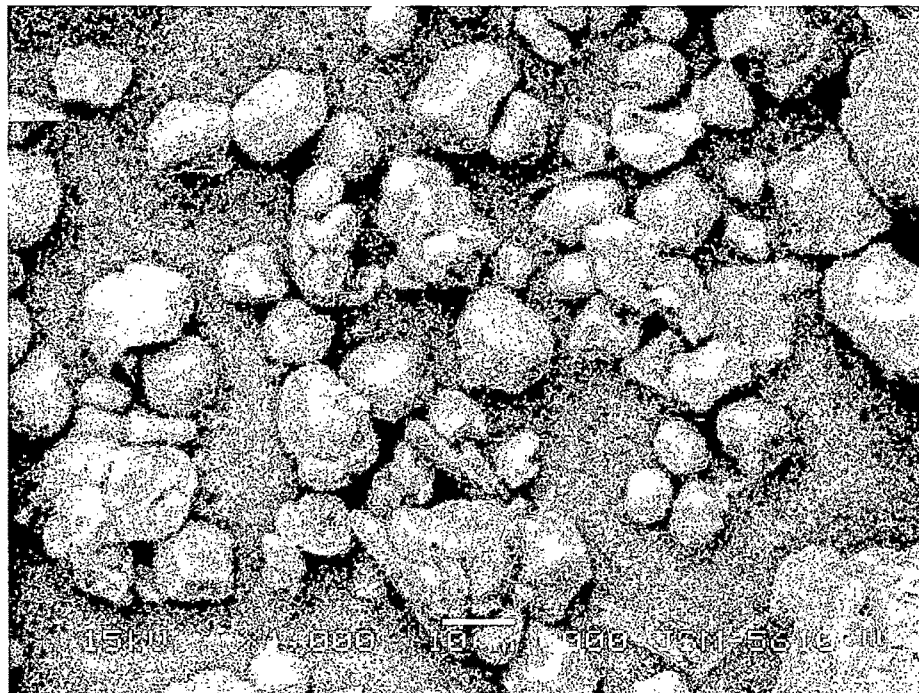


Figure 2.3.7 SEM image of optimized batch of SD of CBZ with HPMC.

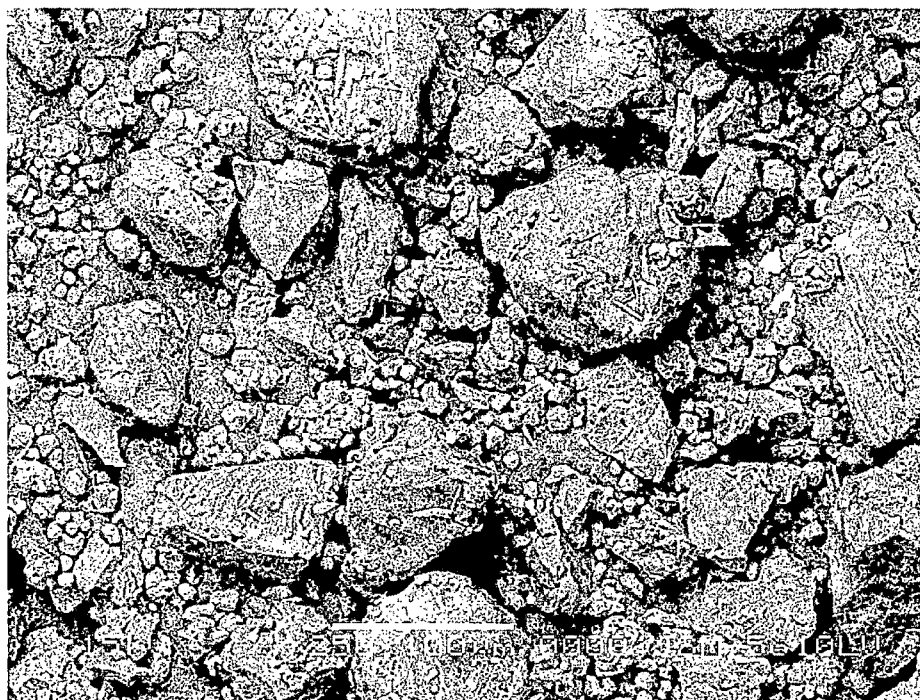


Figure 2.3.8 SEM image of optimized batch of SD of CBZ with Chitosan.

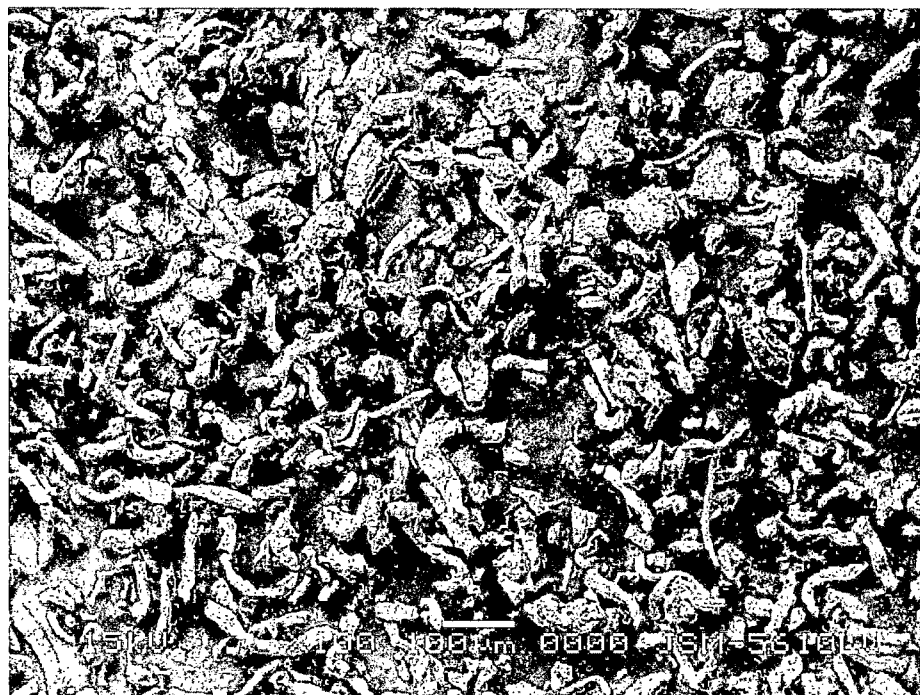


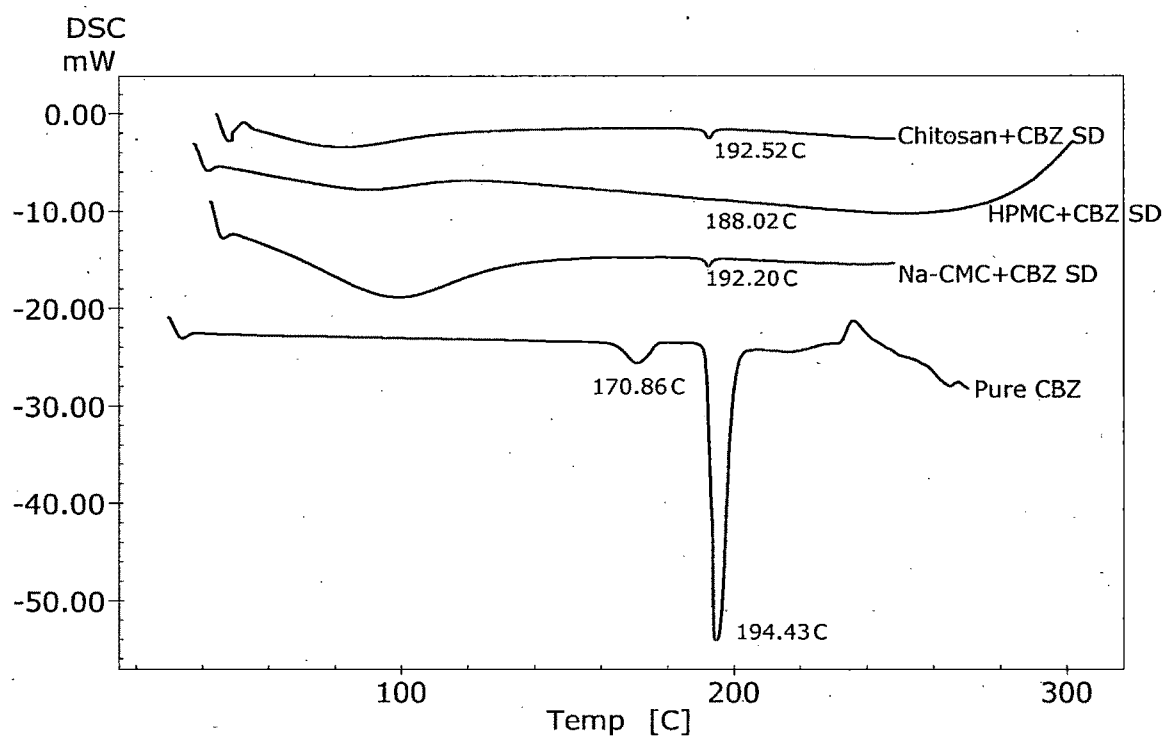
Figure 2.3.9 shows the thermograms for pure CBZ, SDs of CBZ with Na – CMC, HPMC and Chitosan. Pure CBZ showed a sharp melting endotherm at 194.43 °C. A small endothermic

peak at 170.86°C was also observed which can be attributed to presence of small amount of polymorphic form of carbamazepine. CBZ Na-CMC and CBZ chitosan SDs showed considerable decrease in the energy change of the melting endotherm, attributable to a great extent of reduction in crystallinity of drug. In case of thermogram for SD of CBZ with HPMC the melting endotherm for crystalline CBZ has disappeared which ascertained complete amorphization of CBZ.

Time required for rising water through capillary action to wet the methylene blue powder was found to be in the range of 3 – 5 minutes for all the solid dispersions which was significantly less when compared to 10 – 15 minutes for pure drug.

For all the SDs prepared angle of repose was determined. It was found to be in the range of 29° – 35°. This illustrated the free flowability of SDs and their ability to be used for formulation into solid dosage forms.

Figure 2.3.9 DSC thermograms of Pure crystalline CBZ, Na-CMC + CBZ SD, HPMC + CBZ SD and Chitosan + CBZ SD.



2.3.5. Solid dispersions of Oxcarbamazepine

Quantitative solubility data for OCBZ in water, polyethylene glycol 600 and SDs of OCBZ with Na-CMC, HPMC and Chitosan with highest polymer content is given in Table 2.3.6. Solubility of OCBZ in Na-CMC solid dispersion increased to 0.2095 mg/mL from its 0.0101 mg/mL aqueous solubility.

Table 2.3.6 Quantitative solubility data for pure OCBZ, in different solid dispersion systems and polyethylene glycol 600.

	Solvents		Solid dispersion system		
	Water	PEG 600	Na-CMC	HPMC	Chitosan
Solubility of OCBZ (g/100mL)	0.0101	0.1964	0.2095	0.1921	0.1845

Stepwise multivariate linear regression was performed to evaluate the relationship obtained between response and independent variables. For each polymer 3^2 full factorial design was applied. The independent and dependent factors, their levels and the matrix of variables and responses for 3^2 factorial design of each polymer are shown in Table 2.3.7.

The statistical evaluation of dependent variables was carried out by analysis of variance (ANOVA) using Microsoft Excel Version – 2003. The ANOVA results (p value) of the variables on percent drug dissolved of solid dispersion are shown in Table 2.3.8. The significant parameters in the equations can be selected using a stepwise forward and backward elimination for the calculation of regression analysis. However in present study full model having both significant and nonsignificant 'p' values were used in obtaining dependent variables (Gohel and Panchal, 2002). The equations for each polymer can be generated by putting values of coefficients given in Table 2.3.8 in Equation 2.3.5.

Equation 2.3.5 $y = b_0 + b_1x_1 + b_2x_2 + b_{11}x_1^2 + b_{22}x_2^2 + b_{12}x_1x_2$

Table 2.3.7 Matrix of independent variables and responses for 3² factorial design for each polymer.

Batch	Variables with levels *		Response Values			
	X ₁	X ₂	Q ₃₀ for % OCBZ Disso. in SGF	Particle Size of Optimized Batch (µm)	Angle of repose for Optimized Batch (°)	Wettability time for Optimized Batch (minutes)
Polymer : Na-CMC						
SOSD-1	-1	-1	66.58	10 – 100	24.01	03.15
SOSD-2	-1	0	70.21			
SOSD-3	-1	1	71.35			
SOSD-4	0	-1	82.64			
SOSD-5	0	0	87.63			
SOSD-6	0	1	88.54			
SOSD-7	1	-1	93.58			
SOSD-8	1	0	95.21			
SOSD-9	1	1	95.64			
Polymer : HPMC						
HOSD-1	-1	-1	65.68	100 – 120	32.25	03.56
HOSD-2	-1	0	66.54			
HOSD-3	-1	1	66.25			
HOSD-4	0	-1	68.35			
HOSD-5	0	0	73.5			
HOSD-6	0	1	74.56			
HOSD-7	1	-1	70.21			
HOSD-8	1	0	69.25			
HOSD-9	1	1	69.58			
Polymer : Chitosan						
COSD-1	-1	-1	64.25	180 – 220	30.56	4.49
COSD-2	-1	0	67.51			
COSD-3	-1	1	67.85			
COSD-4	0	-1	76.36			
COSD-5	0	0	78.21			
COSD-6	0	1	78.62			
COSD-7	1	-1	83.64			
COSD-8	1	0	84.25			
COSD-9	1	1	85.65			

*

Independent variables		Levels		
		Low	Medium	High
X1	Amount of Polymer (gm)	1	2	3
X2	Amount of Solvent (mL)	150	200	250

Table 2.3.8 ANOVA results ('p' value) effect of the variables on percent drug dissolved of solid dispersions.

Polymer	Factor	For Dissolution in SGF	
		Coefficient	'p' Value
Na CMC	X_1	12.72	0.00
	X_2	2.12	0.01
	X_1^2	-4.18	0.01
	X_2^2	-1.30	0.15
	X_1X_2	-0.68	0.25
Chitosan	X_1	8.99	0.00
	X_2	1.31	0.02
	X_1^2	-2.21	0.02
	X_2^2	-0.60	0.29
	X_1X_2	-0.40	0.31
HPMC	X_1	1.76	0.15
	X_2	1.03	0.35
	X_1^2	-4.22	0.08
	X_2^2	-0.66	0.71
	X_1X_2	-0.30	0.81

Coefficients with one factor indicates the effect of that particular factor while the coefficients with more than one factor and those with second order terms represent the interaction between those factors and the quadratic nature of the phenomena, respectively. Positive sign of the term indicates positive (additive) effect while negative sign indicates negative (antagonistic) effect of the factor on the response. (Hancock and Parks, 2000)

It can be concluded from equations (that can be generated from anova results) that x_1 (amount of polymer) showed the largest positive effect whereas the term x_2 (amount of solvent) showed statistically insignificant positive effect on percent drug dissolved. The quadratic terms of x_1 and x_2 also had significant positive effect on percent drug dissolved.

Figure 2.3.10, Figure 2.3.11 and Figure 2.3.12 shows the response surface plots for percent OCBZ dissolved from SDs in SGF of Na-CMC, HPMC and chitosan at 30 minutes (Q_{30}) respectively. Response surface shows that higher the amount of polymer, significant is the dissolution enhancement. However, for HPMC this was not observed which may be attributed to controlled release matrix forming ability of HPMC (Cao, *et al.*, 2004).

Figure 2.3.10 Response surface plot for effect of Na-CMC and amount of solvent on % OCBZ dissolved.

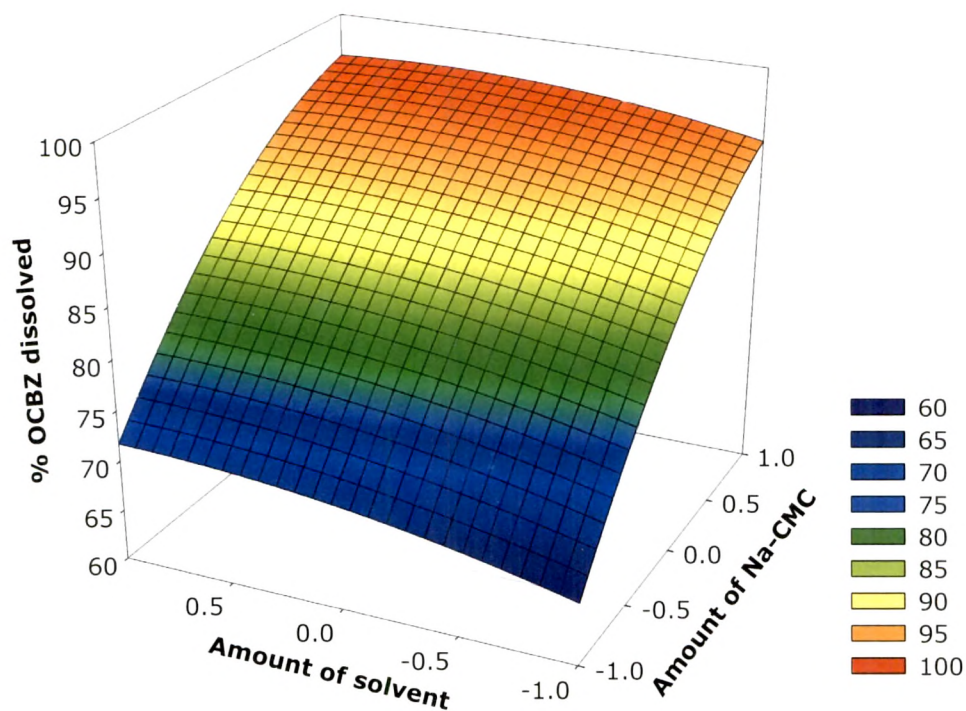


Figure 2.3.11 Response surface plot for effect of HPMC and amount of solvent on % OCBZ dissolved.

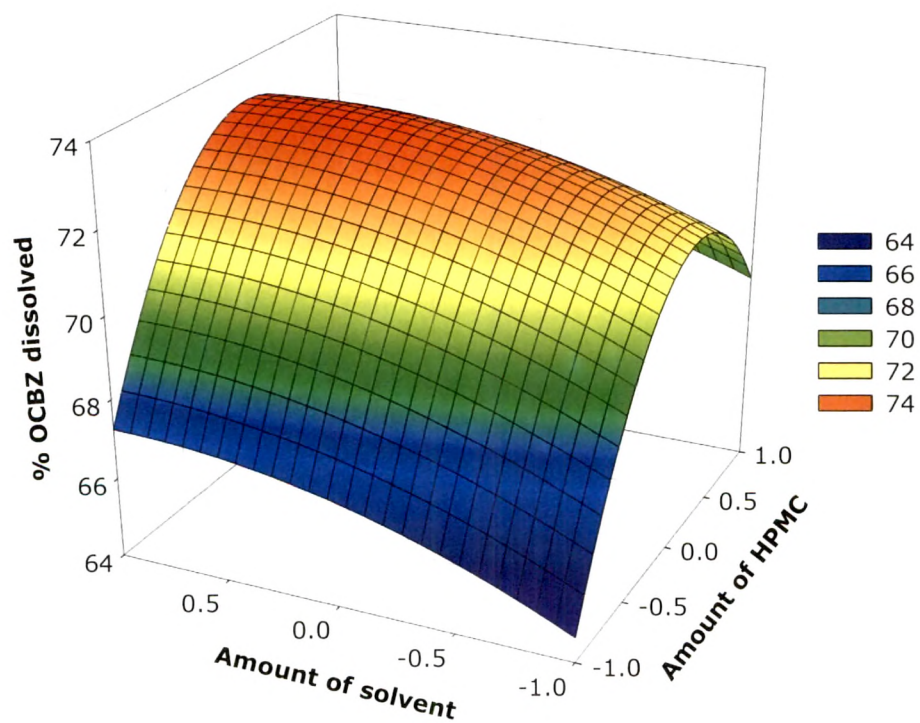
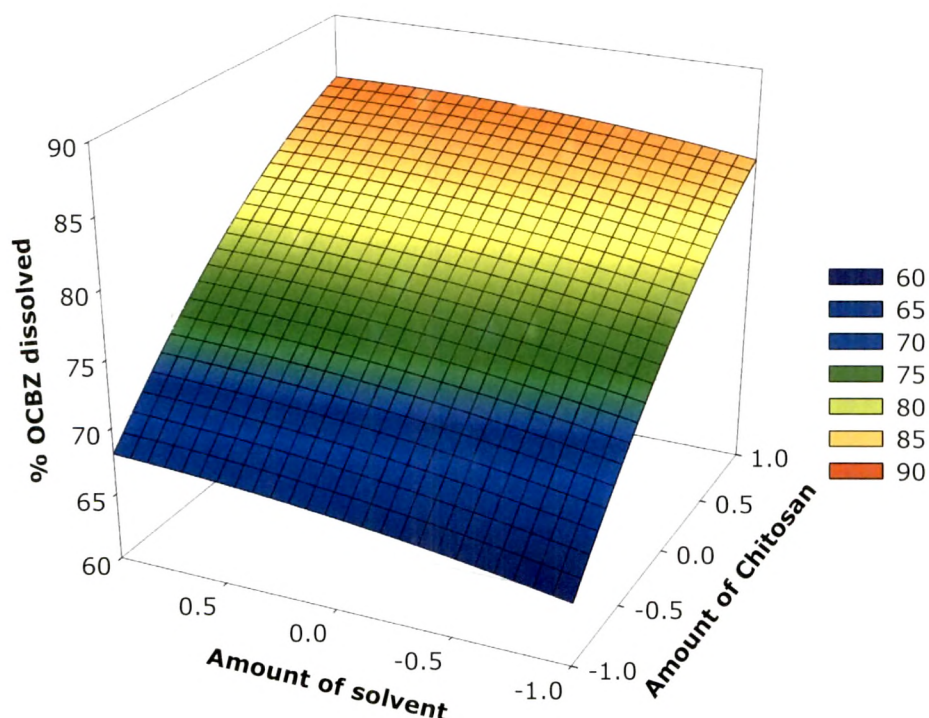


Figure 2.3.12 Response surface plot for effect of Chitosan and amount of solvent on % OCBZ dissolved.



The reliability of the equations that described the influence of factors on percent drug dissolved was assessed by preparing three additional check points SDs using the amount of x_1 and x_2 as -0.5, 0.25 and 0.75. (Mashru, *et al.*, **2005**) The experimental values and predicted values of each response are shown in Table 2.3.4. Equation 2.3.3 was used to compute the % relative error between predicted values and experimental values of each response.

Equation 2.3.6 % Relative error = $\left(\frac{|\text{Predicted value} - \text{Experimental value}|}{\text{Predicted value}} \right) \times 100$

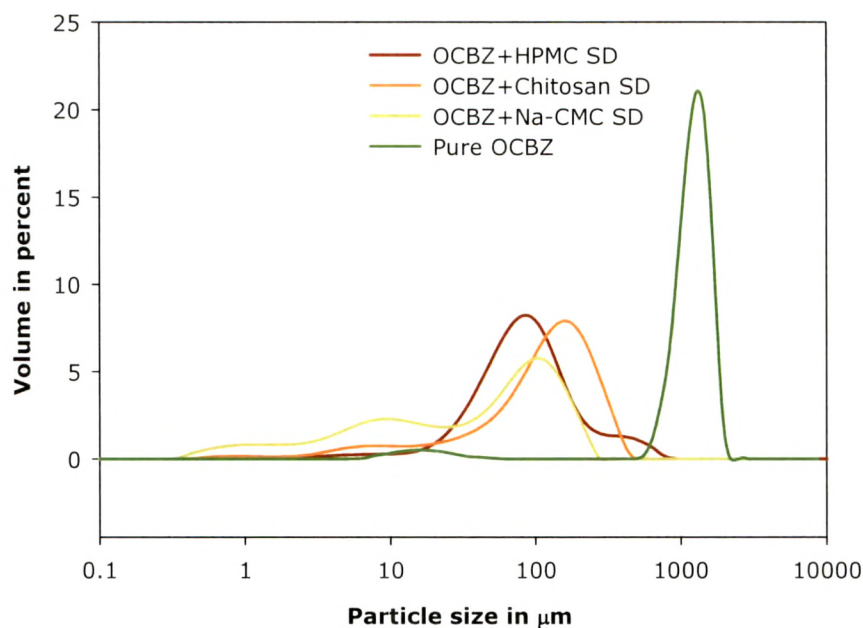
The percent relative error obtained from checkpoint batches was in range of 1.62 to 6.70. These low values of the relative error showed that for all the polymers there was a reasonable agreement of predicted values and experimental values. This proved the validity of model and ascertained the effects of Na-CMC, HPMC, chitosan and amount of solvent on percent drug dissolved.

Table 2.3.9 Cross validation of model obtained using observed and predicted results of checkpoint batches.

Polymer	X1	X2	Predicted values	Experimental values	% Relative Error
Na CMC	-0.5	0.75	80.85	85.25	5.44
	0.25	0.5	90.70	84.67	6.65
	0.75	-0.5	93.19	93.25	0.06
HPMC	-0.5	0.75	71.15	68.15	4.22
	0.25	0.5	73.06	70.36	3.70
	0.75	-0.5	70.96	75.28	6.09
Chitosan	-0.5	0.75	73.88	75.57	2.29
	0.25	0.5	80.69	82.64	2.41
	0.75	-0.5	82.97	78.15	5.81

Particle sizes of pure drug and SDs were determined using Malvern Mastersizer (Malvern Mastersizer, UK) with petroleum ether as dispersion medium for sample. Results of particle size analyses are shown in Figure 2.3.4. Particle size of pure drug was found to be in a broad range of 150 – 600 μm . SDs with Na-CMC were observed with most uniformity in particle size which ranged from 15 – 17 μm . SDs of OCBZ with HPMC also showed considerable decrease in the particle size of OCBZ, however a major fraction of HPMC SD particles was found in the range of 1000 to 1200 μm . In case of SDs with chitosan there were two particle size distributions almost of equal quantity, first in the range of 138 – 158 μm and the other in 1000 – 2500 μm . The latter can be very well attributed to particle size of plain chitosan whereas first can be credited to decreased particle size of drug. This shows that SDs of OCBZ with Na – CMC, HPMC and chitosan showed considerable decrease in the particle size of OCBZ.

Figure 2.3.13 Particle size analyses. (a) Pure OCBZ, (b) SD of OCBZ with Na CMC, (c) SD of OCBZ with HPMC and (d) SD of OCBZ with Chitosan.



The release of drug from SDs was analyzed in SGF without enzymes. In order to assess comparative extent of dissolution rate enhancement from its SDs mean dissolution time (MDT) was calculated. The dissolution data obtained of marketed conventional OCBZ tablets and SDs of all polymers was treated according to Equation 2.3.4 (Barzegar-Jalali, *et al.*, **2002**).

Equation 2.3.7

$$\text{MDT}_{\text{in vitro}} = \frac{\sum_{i=1}^n t_{\text{mid}} \Delta M}{\sum_{i=1}^n \Delta M}$$

where i is dissolution sample number, n is number of dissolution sample times, t_{mid} is time at the midpoint between times t_i and t_{i-1} , and ΔM is the amount of OCBZ dissolved (μg) between times t_i and t_{i-1} . The results for MDT calculated are shown in Table 2.3.5. The MDT value of marketed OCBZ tablets SGF without enzymes was found to be 16.07 min. which was decreased to 7.14 in case of SD of drug with Na-CMC. This depicts the fulfillment of objective of dissolution enhancement of OCBZ.

Table 2.3.10 Mean Dissolution Time (MDT) calculated for all the batches of OCBZ SD of experimental design for Na-CMC, HPMC and Chitosan.

Batches		MDT for dissolution in SGF		
X1	X2	Na-CMC	HPMC	Chitosan
-1	-1	8.29	9.46	8.41
-1	0	7.79	9.35	7.92
-1	1	8.06	10.39	8.14
0	-1	8.49	8.71	7.98
0	0	8.03	8.53	7.07
0	1	7.78	8.36	6.54
1	-1	7.90	7.30	7.37
1	0	7.40	7.07	6.51
1	1	6.83	10.06	6.34

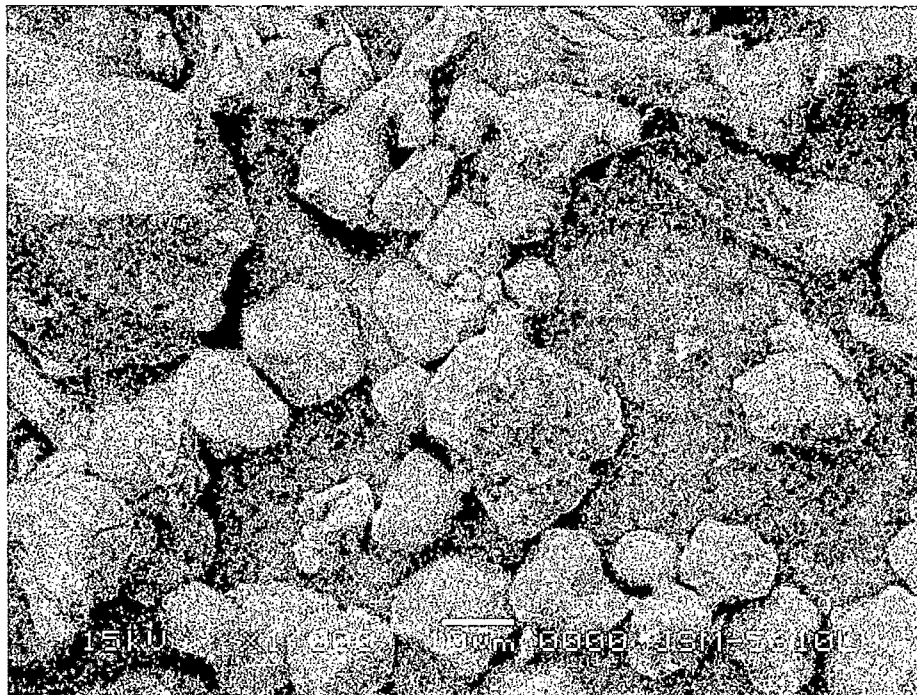
The amount of percent drug dissolved in 30 minutes (Q_{30}) in SGF without enzymes for all the SDs prepared according to experimental design is reported Table 2.3.7. SDs of polymers Na-CMC and chitosan showed increase in dissolution rate on increase in amount of polymer. Whereas in case of HPMC solid dispersions increase in amount of polymer upto certain level led to enhanced drug dissolution but further addition of polymer resulted in decrease of dissolution of OCBZ. This may be correlated to matrix forming ability of HPMC.

The SEM images for pure OCBZ and its SDs with Na-CMC, HPMC and chitosan are shown in Figure 2.3.14, Figure 2.3.15, Figure 2.3.16 and Figure 2.3.17 respectively. Pure OCBZ image showed crystalline drug of pencil or rod shapes and sizes ranging from 60 to 700 μm . whereas images of SD of drug with Na-CMC upto 1000X magnification did not show any crystalline material. In case of SDs with HPMC and chitosan although a significant decrease in size of drug crystals was observed, agglomeration of crystals was also observed.

Figure 2.3.14 **SEM image of Pure crystalline OCBZ.**



Figure 2.3.15 SEM image of optimized batch of SD of OCBZ with Na CMC.

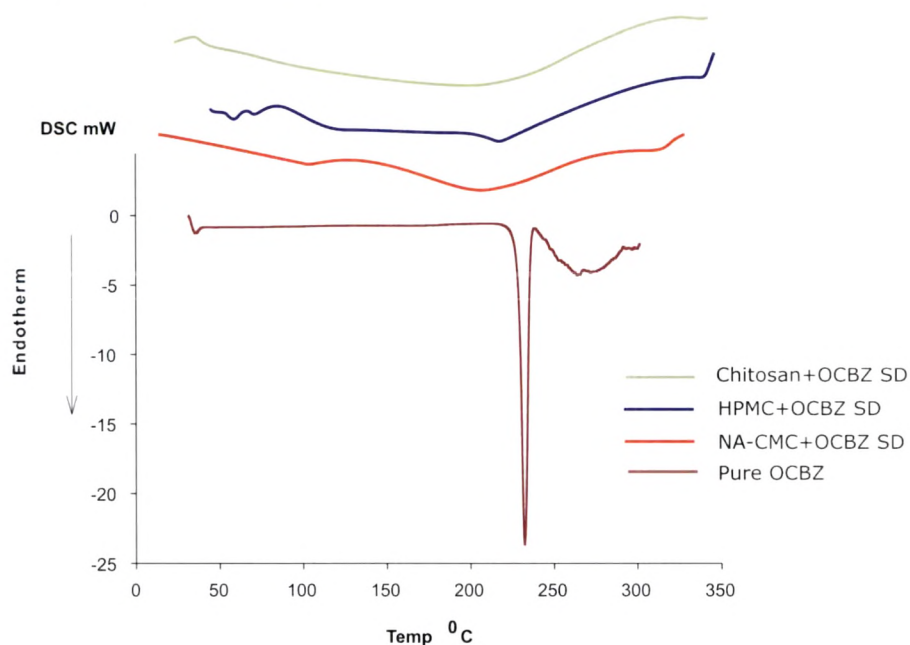


for OCBZ Na-CMC SD showed disappearance of melting endotherm of OCBZ. This may be attributed to loss of crystallinity or conversion into amorphous state of the drug. SDs of HPMC and chitosan showed considerable decrease in the energy change of melting endotherm which also confirms a considerable extent of reduction in crystallinity of drug.

Time required for rising water through capillary action to wet the methylene blue powder was found to be in the range of 3.6 – 5.8 minutes for all the solid dispersions which was significantly less when compared to 12 – 15 minutes for pure drug.

For all the SDs prepared angle of repose was determined. It was found to be in the range of 24° – 33° . This was comparatively lesser than observed for CBZ SDs. The angle of repose values illustrate the free flowability of SDs and their ability to be used for formulation into solid dosage forms.

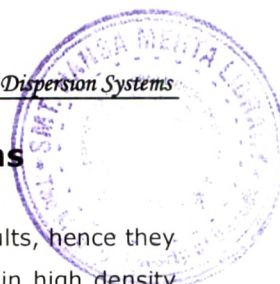
Figure 2.3.18 DSC thermograms of Pure crystalline OCBZ, Na-CMC + OCBZ SD, HPMC + OCBZ SD and Chitosan + OCBZ SD.



Hydrophilic polymer – drug solid dispersions increase drug dissolution due to the possible reasons as,

1. usually in solid dispersions, the drug is partially dissolved in melted or dissolved polymer. After drying of these solid dispersions, the drug will not nucleate to form firm crystals resulting in formation of microcrystals. Drug microcrystals are embedded in the water soluble matrix where hydrophilic polymers present the ability of rapid wetting and thereby dissolution of drug (Arias, *et al.*, **1996**). Generally polyethylene glycols and polyvinyl pyrrolidone (PVP) solid dispersions follow this principle.
2. for solid dispersions of SSG higher dissolution rates observed when compared to other excipients may be due to their easy and rapid dispersibility in the aqueous dissolution fluids (Chowdary and Rao, **2000**).
3. solid dispersions of hydrophilic swellable polymers like CMC and HPMC get gelatinized in the dissolution medium. This gelatinized solid dispersion gets constantly crushed by the attrition during stirring and these finely gelatinized SD diffuse to bulk solution through diffusion layer (Okimoto, *et al.*, **1997**). Being water retentive gelatinized dispersions also increase wetting of the drug which attributes to increase in dissolution. However the gelatinized dispersion formed should not be a barrier for the drug diffusion owing to its viscosity. In present work HPMC showed less drug dissolution compared to Na CMC may be due to formation of highly viscous barrier layer at the interface of drug and dissolution medium.

P/Th
11/4/65

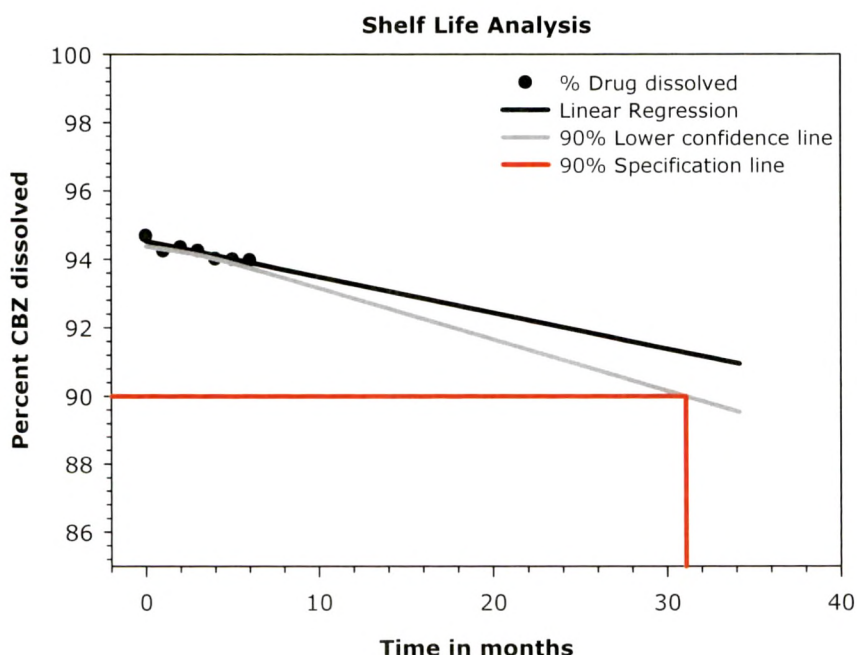


2.3.6. Stability studies for CBZ and OCBZ SD systems

SDs of CBZ and OCBZ with Na-CMC showed promising drug dissolution results, hence they were subjected to stability studies. Powders of these SDs were packaged in high density polyethylene (HDPE) bottles with polypropylene (PP) caps (foamed polyethylene and pressure sensitive liner). The systems were subjected to stability testing according to the International Conference on Harmonization guidelines for zone III and IV. The packed containers of prepared systems along with marketed formulation and bulk pure drug CBZ, and OCBZ were kept for accelerated ($40\pm 2^\circ\text{C}/75\pm 5\%$ relative humidity) and long term ($30\pm 2^\circ\text{C}/65\pm 5\%$ relative humidity) stability in desiccators with saturated salt solution for up to 6 months. Long term stability samples were to be analyzed only if samples for accelerated studies ($40\pm 2^\circ\text{C}/75\pm 5\%$ RH) fail in analysis. A visual inspection (for coloration of SD content), dissolution testing and pure drug content estimation was carried out every 30 days for the entire period of stability study.

Stability data of SDs was extrapolated using linear regression tool for the determination of shelf life of product. Figure 2.3.19 shows the extrapolated accelerated stability data for shelf-life calculation of CBZ Na-CMC SD. The calculated shelf life was found to be 31.08 months (2.55 years).

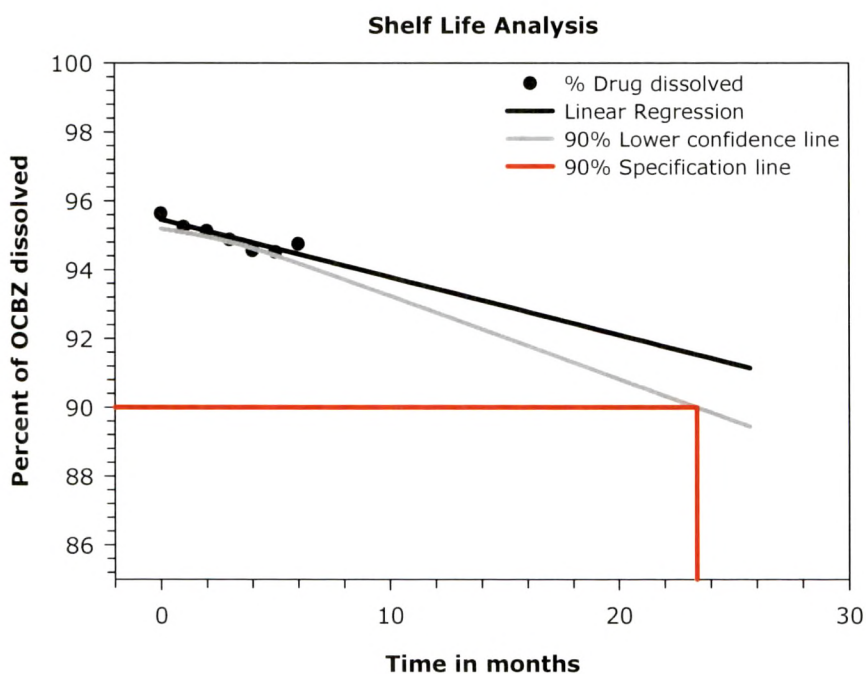
Figure 2.3.19 Extrapolation of accelerated stability data of CBZ Na-CMC SD for shelf-life calculation.



Similarly for OCBZ Na-CMC SDs stability data of was extrapolated using linear regression tool for the determination of shelf life of product.

Figure 2.3.20 shows the extrapolated accelerated stability data for shelf-life calculation of OCBZ Na-CMC SD. The calculated shelf life was found to be 23.38 months (1.92 years).

Figure 2.3.20 Extrapolation of accelerated stability data of OCBZ Na-CMC SD for shelf-life calculation.



2.3.7. CONCLUSION

MLR analysis of results of experimental design illustrated that SD of CBZ and OCBZ when prepared with hydrophilic swellable polymers showed marked increase in percent drug dissolution in SGF without enzymes which was illustrated with the help of mean dissolution time. SDs prepared with Na-CMC showed the highest drug dissolution compared to HPMC and chitosan owing to its optimum wetting properties by gelatinization and control over particle size of drug. Na-CMC is a popular excipient of tablets and its SD showed good free flowing properties which further may not need extra excipients for compression or filling in hard gelatin capsules. Extrapolated accelerated stability results for the SDs prepared showed a good shelf life of developed systems. This helps in understanding the stability of the systems in view of recrystallization of drug from amorphous state (reverting back).

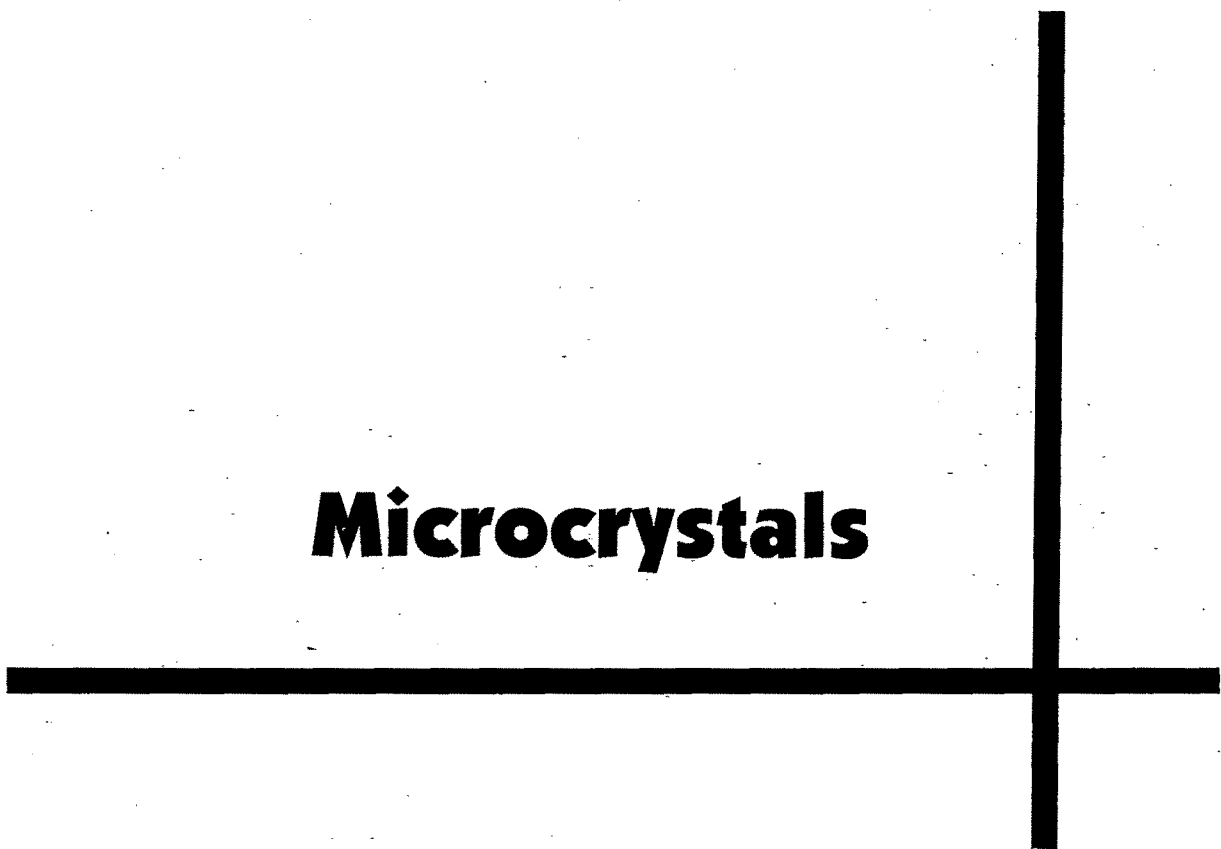
Similar studies can be used to screen other polymers for more efficiency and compatibility of the drug material.

2.3.8. References

- Arias, M. J., Gines, J. M., Moyano, J. R. and Rabasco, A. M. (1996). Dissolution properties and in vivo behaviour of triamterene in solid dispersions with polyethylene glycols. **Pharm Acta Helv**, 71,(4), 229-235.
- Barzegar-Jalali, M., Maleki, N., Garjani, A., Khandar, A. A., Haji- Hosseinloo, M., Jabbari, R. C. and Dastmalchi, S. (2002). Enhancement of dissolution rate and anti-inflammatory effects of piroxicam using solvent deposition technique. **Drug Dev. Ind. Pharm.**, 28, 681- 686.
- Bertilsson, L. (1978). Clinical pharmacokinetics of carbamazepine. **Clin Pharmacokinet.**, (3), 128-143.
- Cao, Q. R., Choi, H. G., Kim, D. C. and Lee, B. J. (2004). Release behavior and photo-image of nifedipine tablet coated with high viscosity grade hydroxypropylmethylcellulose: effect of coating conditions. **Int J Pharm**, 274,(1-2), 107-117.
- Chiou, W. L. and Reigelman, S. (1971). Pharmaceutical applications of solid dispersion systems. **J Pharm Sci.**, 60, 1281-1302.
- Chowdary, K. P. and Rao, S. S. (2000). Investigation of dissolution enhancement of itraconazole by solid dispersion in superdisintegrants. **Drug Dev Ind Pharm**, 26,(11), 1207-1211.
- Derringer, G. and Suich, R. (1980). Simultaneous optimization of several responses variables. **J Qual Tech.**, 12,(4), 214-219.
- Desai, K. G. H., Kulakarni, A. R. and Aminbhavi, T. M. (2003). Solubility of Rofecoxib in presence of methanol, ethanol and sodium lauryl sulphate at (298.15, 303.15 and 308.15) K. **J Chem Engg Data.**, 48, 942-945.
- El-Zein, H., Riad, L. and El-Bary, A. A. (1998). Enhancement of carbamazepine dissolution : in vitro and in vivo evaluation. **Int J Pharm.**, 168, 209-220.
- Ford, J. L. (1986). The current status of solid dispersions. **Pharm Acta Helv.**, 61, 69-88.
- Gohel, M. C. and Panchal, M. K. (2002). Novel use of similarity factor f2 and Sd for the development of Diltiazem HCl Modified-release tablets using a 32 factorial design. **Drug Dev Ind Pharm.**, 28,(1), 77-87.
- Gohel, M. C. and Patel, L. D. (2003). Processing of nimesulide - PEG 400 - PG - PVP solid dispersions : Preparation, characterization and in vitro dissolution. **Drug Dev Ind Pharm.**, 29,(3), 299-310.
- Goldberg, A. H., Gibaldi, M. and Kanig, J. L. (1966). Increasing dissolution rates and gastrointestinal absorption of drugs via solid solutions and eutectic mixtures II - experimental evaluation of a eutectic mixture: urea-acetaminophen system. **J Pharm Sci.**, 55,(482-487),
- Hancock, B. C. and Parks, M. (2000). What is true solubility advantage for amorphous pharmaceuticals? **Pharm Res.**, 17, 397-404.
- Leuner, C. and Dressman, J. (2000). Improving drug solubility for oral delivery using solid dispersions. **Eur J Pharm Biopharm.**, 50, 47-60.
- Lobenberg, R. and Amidon, G. L. (2000). Modern bioavailability, bioequivalence and and biopharmaceutics classification system: new scientific approaches to international regulatory standards. **Eur J Pharm Biopharm.**, 50, 3-12.
- Mashru, R. C., Sutariya, V. B., Sankalia, M. G., Sankalia, J. M. and Parikh, P. P. (2005). Development and evaluation of fast dissolving film of salbutamol sulphate. **Drug Dev. Ind. Pharm.**, 1, 25-34.
- McKenna, A. and McCafferty, D. F. (1988). Effect of particle size on the compaction mechanism and tensile strength of tablets. **J Pharm Pharmacol.**, 14,(15-17), 2443-2465.

- Moneghini, M., Voinovich, D., Perissutti, B. and Princivalle, F. **(2002)**. Action of carriers on Carbamazepine dissolution. **Pharm Dev Technol.**, 7,(3), 289-296.
- Narang, A. S. and Srivastava, A. K. **(2002)**. Evaluation of solid dispersions of clofazimine. **Drug Dev Ind Pharm.**, 28,(8), 1001-1013.
- Okimoto, K., Miyake, M., Ibuki, R., Yasumura, M., Ohnishi, N. and Nakai, T. **(1997)**. Dissolution mechanism and rate of solid dispersion particles of nilvadipine with hydroxypropylmethylcellulose. **Int J Pharm**, 159, 85-93.
- Rasenack, N., Hartenhauer, H. and Müller, B. **(2003)**. Microcrystals for dissolution rate enhancement of poorly water-soluble drugs. **Int J Pharm.**, 254, 137-145.
- Rawat, S. and Jain, S. K. **(2003)**. Rofecoxib- -cyclodextrin inclusion complex for solubility enhancement. **Pharmazie.**, 58, 639-641.

Microcrystals



2.4. Microcrystals

In the present work effect of Na CMC, HPMC and chitosan on microcrystal formulation for dissolution enhancement of carbamazepine (CBZ) and oxcarbazepine (OCBZ) using controlled crystallization technique coupled with spray drying was explored. The work was extended for exploration of simplified approach for stable particle size reduction. The study was performed with an experimental design approach i. e. a fractional factorial design of resolution 5 (with all 2 factor interaction) for the screening of predefined independent variables drug concentration, chitosan concentration, feed rate, inlet temperature and percent aspiration for spray drying. Whereas percent drug dissolved, wettability time, flowability in terms of angle of repose and particle size were designated as response variables.

Conversion of a crystalline form of drug to an amorphous form is nothing but the alteration of molecular architecture of drug which helps in rapid solubilization with high energy advantage (Kaushal, *et al.*, **2004**). To take the solubility and rapid dissolution advantage of amorphous drugs from their crystalline counterparts there are several techniques available for reducing the particle size of drugs which utilize high energy processes such as micronisation by jet milling, cutting, freeze drying, spray drying, melt extrusion etc. But the systems resulting from use of such techniques are often referred to incomplete or partially amorphous products (Hancock and Zografi, **1997**). It is because the high internal energy and specific volume of the amorphous state compared to original crystalline state eventually have enhanced dissolution and bioavailability but there is always danger of getting converted back of the amorphous systems to a more stable crystalline state during processing or storage (Ambike, *et al.*, **2005**). They are also susceptible for agglomerations resulting decrease in drug dissolution. In milling there is fracture of crystalline drug due to which electrostatic effects can occur. The products obtained with these techniques have their disadvantages posing serious questions for stability of amorphous systems. It is reported that changes in surface energy influences processing properties such as the powder flow of the system which is undesirable for compression or hard gelatin capsule fill. Micronized powders which have a higher energy on surface (measured by inverse gas chromatography) showed poorer flow properties (Feeley, *et al.*, **1998**). High specific surface of micronized particles always make them. A further disadvantage of jet milling processes is a broad size distribution (Müller *et al.*, 1996). It has been reported that amorphous systems are more unstable and highly susceptible for drug degradation than crystalline systems (Byrn, *et al.*, **2001**).

In the present work an attempt was made to reduce the crystalline particle size of CBZ, and OCBZ using controlled crystallization technique which was coupled with hydrophilic polymeric coprecipitation and spray drying. Till the date several hydrophilic polymers like hydroxypropylmethyl cellulose (Yamada, *et al.*, **2000**, Kapsi and Ayres, **2001**, Mitchell, *et al.*, **2003**), hydroxypropylmethylcellulose phthalate (Ishikawa, *et al.*, **2000**, Qi and Ping,

2004, Sertsou, *et al.*, 2002), lactose (Abberger, *et al.*, 2002, Chidavaenzi, *et al.*, 2001, Christensen, *et al.*, 2001, Corrigan, *et al.*, 2002, Cilurzo, *et al.*, 2002), polyvinyl alcohol (Wiedmann, *et al.*, 1997), polyvinyl pyrrolidone (Ambike, Mahadik and Paradkar, 2005, Corrigan, Healy and Corrigan, 2002, Doherty and York, 1989) have been utilized for the controlled crystallization of drugs. Chitosan also have been found to be with more promising results (Bodek, 2002).

Na CMC, HPMC and chitosan were selected as suitable polymers for preparation of microcrystals.

If there are several variables (multivariable) in a system design of experiments (DOE) a powerful statistical tool should be used for optimization of such systems. In past several years, it is observed that pharmaceutical industry has used experimental designs more for the optimization of pharmaceutical agents; but, only a few are reported in the literature for the development of dosage forms (Rotthäuser, *et al.*, 1998, Nazzal, *et al.*, 2002.). The present study was performed with fractional factorial design of resolution 5 (with all 2 factor interaction) for the screening of drug concentration, chitosan concentration, feed rate, inlet temperature and percent aspiration for spray drying. Whereas percent drug dissolved, wettability time, flowability in terms of angle of repose and particle size were designated as response variables.

2.4.1. Materials

Carbamazepine (CBZ) and Oxcarbamazepine (OCBZ) were received as gift samples from Relax Pharmaceuticals Limited, Vadodara, India., and Torrent Research Center, Ahmedabad, India respectively. Sodium carboxy methyl cellulose and Hydroxyl propyl methyl cellulose were purchased from S. D. Fine-Chem Ltd., Mumbai, India. Chito Clear® chitosan were received as a generous gift sample from Primax Biopolymers, Irland. All the other chemicals and solvents were of analytical grade and were used without further purification. Deionized double-distilled water was used through out the study.

2.4.2. Methods

2.4.2.1. Experimental design

For the experiments performed as per design coded and actual values of independent variables are depicted in table 1. Two levels -1 and 1 were used for study and for centre points a third level was set at '0' for all the independent variables (drug concentration, chitosan concentration, feed rate, inlet temperature and percent aspiration). Table 2 shows the experiments performed as per the fractional factorial design.

2.4.2.2. Microcrystal preparation (for both CBZ and OCBZ)

Microcrystals of CBZ and OCBZ were prepared using solvent change method. In this method two liquids were rapidly mixed into each other and the mixing was accompanied by presence of a stabilizing agent. The formed microcrystals were grown naturally in medium and spray dried to completely dry the microcrystal product and not for formation of the particles or microcrystals. Weighed amount of drug was dissolved in 250 ml of acetone. The drug was dissolved in solvent with constant stirring for 15 min. on magnetic stirrer. In a separate beaker weighed amount of chitosan was dissolved in 5% glacial acetic acid. The chitosan solution was kept for 4 - 6 hrs to allow complete hydration and obtain a clear solution. To this solution drug solution was added with vigorous stirring over magnetic stirrer for 5 to 10 min. The resultant mixture was allowed to stand for further 10 min. to allow association of chitosan molecules with naturally growing microcrystals dispersion. This microcrystals' dispersion was then spray dried (JISL Lab Mini Spray Dryer, Mumbai, India). Spray drying parameters like feed rate, inlet temperature and percent aspiration decide the quality of final product like particle size, flow properties as well drug loading capacity of the system. In the present work these parameters were termed as independent variables.

2.4.2.3. Characterization and evaluation of microcrystals

2.4.2.3.1. Particle size measurements

The volume Particle size of microcrystals was determined with the laser diffraction particle size analyzer (MAN 0244/ HYDRO 2000 SM, Malvern Instruments Ltd., UK). Petroleum ether was used as dispersion medium for carrying out measurements.

2.4.2.3.2. *In vitro* Dissolution studies

The dissolution study was conducted in USP XXVII simulated gastric fluid (without enzymes) having pH 1.2 ± 0.02 . Accurately weighed amount of microcrystals, containing equivalent 100 mg of drug were wrapped in cloth pouch of approximate 2 - 5 μm mesh. This pouch was placed in basket of USP dissolution apparatus (Type I, TDT-06P, Electrolab, Mumbai, India) with 900 ml deaerated dissolution medium. Microcrystals were placed in cloth pouches to avert floating of them on dissolution media surface. Deaeration of dissolution media were done with the help of ultrasonication (Ultrasonics - 2.2, India) for 15 min. The dissolution apparatus was run at 50 RPM keeping the temperature ($37 \pm 1^\circ\text{C}$) constant throughout the experiment. Samples (5 ml) were withdrawn at 0, 5, 10, 15, 20, 25 and 30 minutes and were filtered through 0.45 μm whatmann filter paper, diluted suitably and analysed spectrophotometrically at 303 nm (Shimadzu, UV-1601 UV, Visible spectrophotometer, Japan). An equal volume of fresh dissolution medium maintained at the same temperature was added after withdrawing sample to maintain the sink

conditions. The absorbance values were transformed to concentration by reference to a standard calibration curve obtained experimentally ($r^2 = 0.9998$). The dissolution test was performed in triplicate for each batch.

2.4.2.3.3. Angle of repose measurements (Flowability indicator)

For measurement of angle of repose of microcrystals, they were passed through a funnel on the horizontal surface. The height (h) of the heap formed was measured with a cathetometer and the radius (r) of the cone base was also determined. The angle of repose (Φ) was calculated from Equation 2.4.1.

Equation 2.4.1
$$\Phi = \tan^{-1} \left(\frac{h}{r} \right)$$

2.4.2.3.4. Wettability Studies

For determination of powder wettability two approaches were used. All the experimental batches were evaluated for wettability time whereas the contact angle, well reported measure of powder wettability; of optimized batch of microcrystals and pure drug was determined using tensiometer (GBX Tensiometer, France equipped with Mettler Toledo balance and 3S software). For wettability time determination sample powder weighed about 1 gm was placed in sintered glass funnel of 27 mm. internal diameter. Bridge was formed at the neck of funnel with the help of cotton plug. The funnel was held in upright position in a beaker filled with water such that water level in beaker just touches the cotton plug. Methylene blue powder was layered over surface of pure drug in funnel. Time required to rise the water through drug till wetting of methylene blue powder occurs was recorded (Gohel and Patel, 2003).

2.4.2.3.5. Scanning electron microscopy (SEM)

To get a topographical image analysis of microcrystals SEM study was performed. The beads were mounted on brass stubs using double-sided adhesive tape. SEM photographs were taken with scanning electron microscope (JSM-5610LV, Jeol Ltd., Japan) at the required magnification at room temperature. The working distance of 39 mm was maintained and acceleration voltage used was 15 kV, with the secondary electron image (SEI) as a detector.

2.4.2.3.6. X – Ray powder diffraction Studies (XRPD)

XRPD studies were used for getting a defining idea about the crystallinity of the drug in the dosage form or formulation. In present work also XRPD studies were performed (Philips PW 1830) to get the crystalline morphology of the drug in microcrystals formed. The samples were scanned from a starting angle of 5° to an end angle of 60° with a step size of 0.0160° .

2.4.2.3.7. Differential scanning calorimetry (DSC)

To have an idea about the amount of presence of free crystalline drug along with change in energy of the system DSC thermograms for different formulations were obtained using an automatic thermal analyzer system (DSC-60, Shimadzu, Kyoto, Japan). Temperature calibration was performed using indium as a standard. About 2 – 3 mg accurately weighed samples were crimped in a standard aluminium pan and heated from 40^o – 300^oC at a heating rate of 10^oC/min under constant purging of dry nitrogen at 30 ml/min. An empty pan, sealed in the same way as the sample, was used as a reference. The characteristic endothermic peaks and specific heat of the melting endotherm were recorded.

The study was performed with a fractional factorial design of resolution 5 i.e. with all 2 factor interaction. The independent variables selected for predefined screening were drug concentration, polymer concentration, feed rate, inlet temperature and percent aspiration for spray drying. Whereas percent drug dissolved, wettability time, flowability in terms of angle of repose and particle size were designated as response variables. For determination of the experimental error, the experiment at the centre point was replicated three times at different intervals. The results for these centre points showed comparable results which is an indication of reproducibility of the experiment.

The results were statistically evaluated with the help of analysis of variance (ANOVA) using statistical software package (JMP 5.1, The Statistical Discovery Software, USA.). The quadratic model was selected for this analysis.

2.4.2.4. Microcrystals of carbamazepine

The crystallization process involves creation of hydrophobic surfaces with a tendency to achieve a low energy stable condition. However in this process due to the surface energy of the seeds energy of the system increased. In such condition hydrophilic polymers, being in physical immediacy have an attachment with new born particles which prevents further crystal growth of the particles which were also sterically stabilized (Schott, 1985). Thereby small particles failed to aggregate for lowering the surface energy. Thus surface energy and consequently the enthalpy of the system were reduced.

Table 2.4.1 gives quantitative solubility data for CBZ microcrystals. CBZ Na-CMC microcrystals were found to have maximum solubility for CBZ.

Figure 2.4.1, Figure 2.4.2 and Figure 2.4.3 shows the leverage plots of predicted and actual values for the experimental design with percent drug dissolved, particle size, wettability time and angle of repose as responses for microcrystals of CBZ with Na-CMC, HPMC and Chitosan respectively. The points on a leverage plot for simple regression are actual data coordinates, and the horizontal line for the constrained model is the sample mean of the response. But when the leverage plot is for one of multiple effects, the points are no longer actual data values. The horizontal line then represents a partially constrained model instead of a model fully constrained to one mean value. The response values of all the experiments (except for 2 of 3 centre points) lie between the confidence intervals of the leverage plot. Also the confidence region for the line of fit does contain the horizontal line of the mean; this predicts that effects (dependent variables) are significant.

Table 2.4.1 Quantitative solubility data for pure CBZ, in different microcrystals and polyethylene glycol 600.

	Solvents		Microcrystals		
	Water	PEG 600	Na-CMC	HPMC	Chitosan
Solubility of CBZ (g/100mL)	0.0091	0.1782	0.2331	0.2114	0.2248

Figure 2.4.1 Actual vs. Predicted values for (A) percent drug dissolved, (B) particle size, (C) wettability time, (D) angle of repose for CBZ Na-CMC microcrystals.

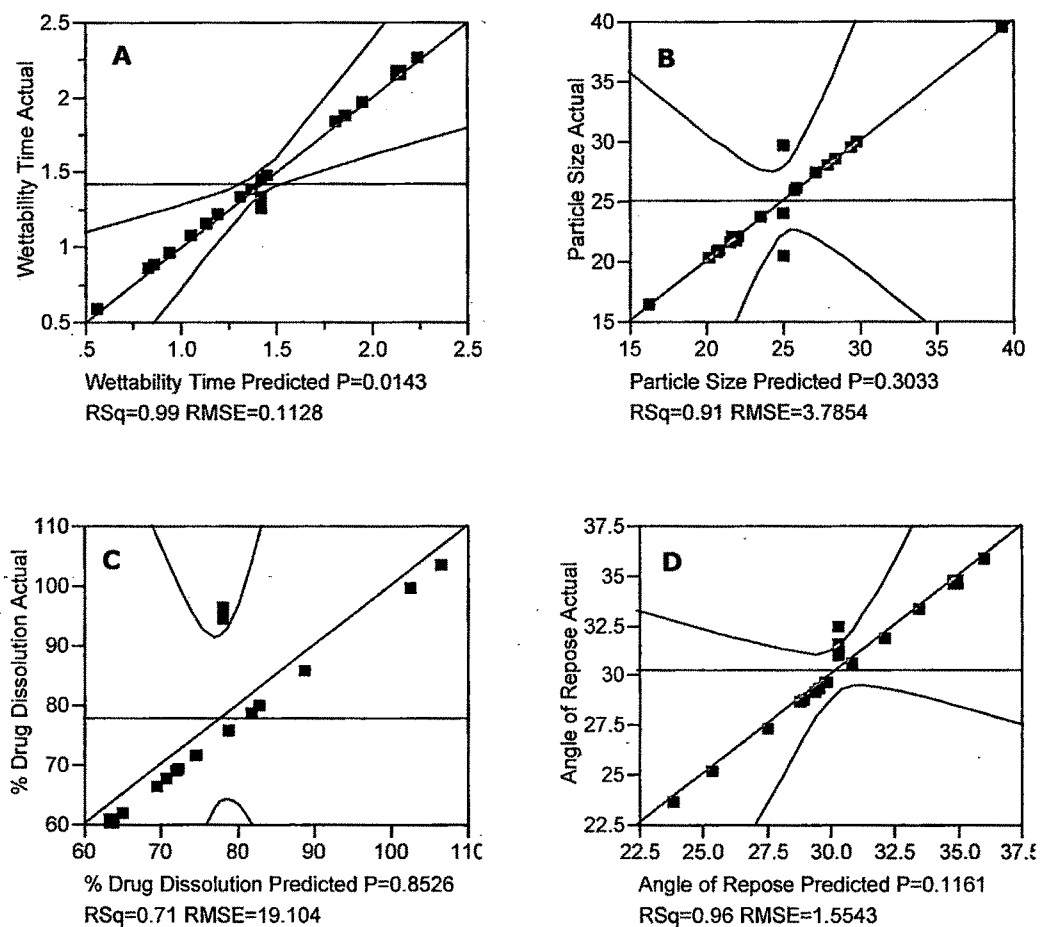


Figure 2.4.2 Actual vs. Predicted values for (A) percent drug dissolved, (B) particle size, (C) wettability time, (D) angle of repose for CBZ HPMC microcrystals.

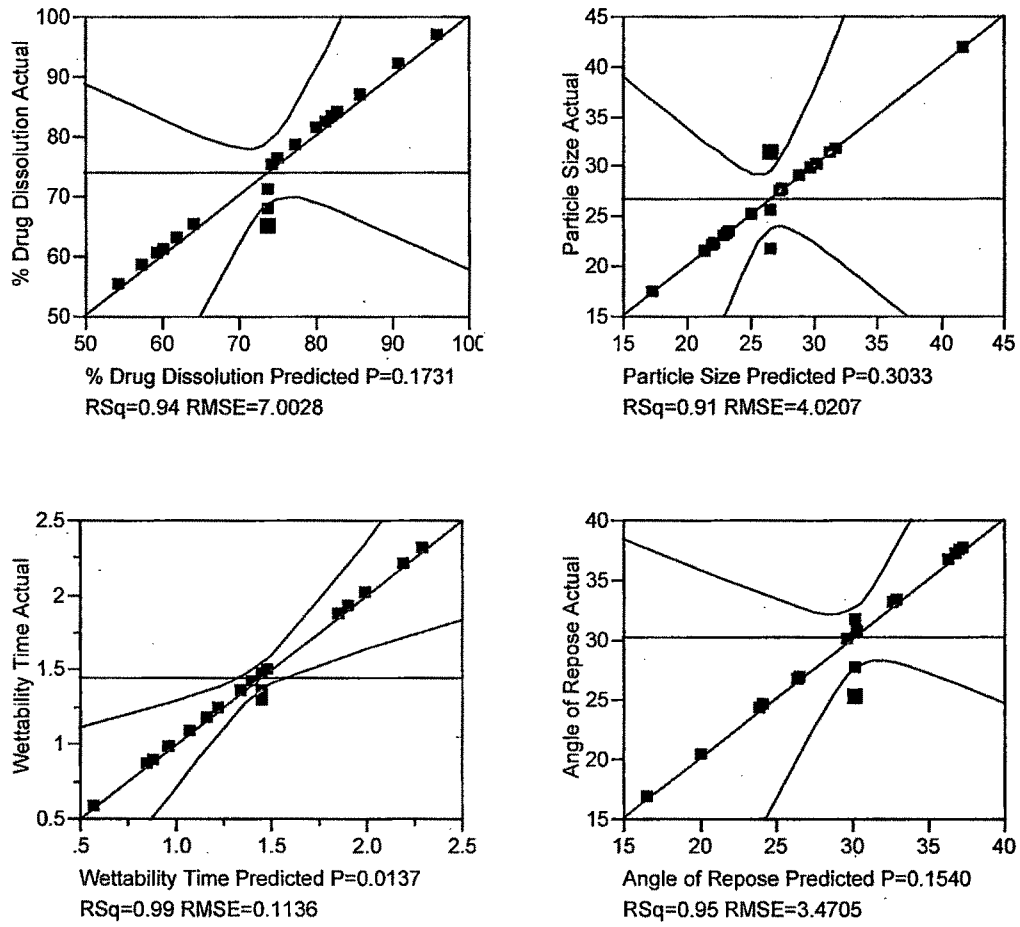
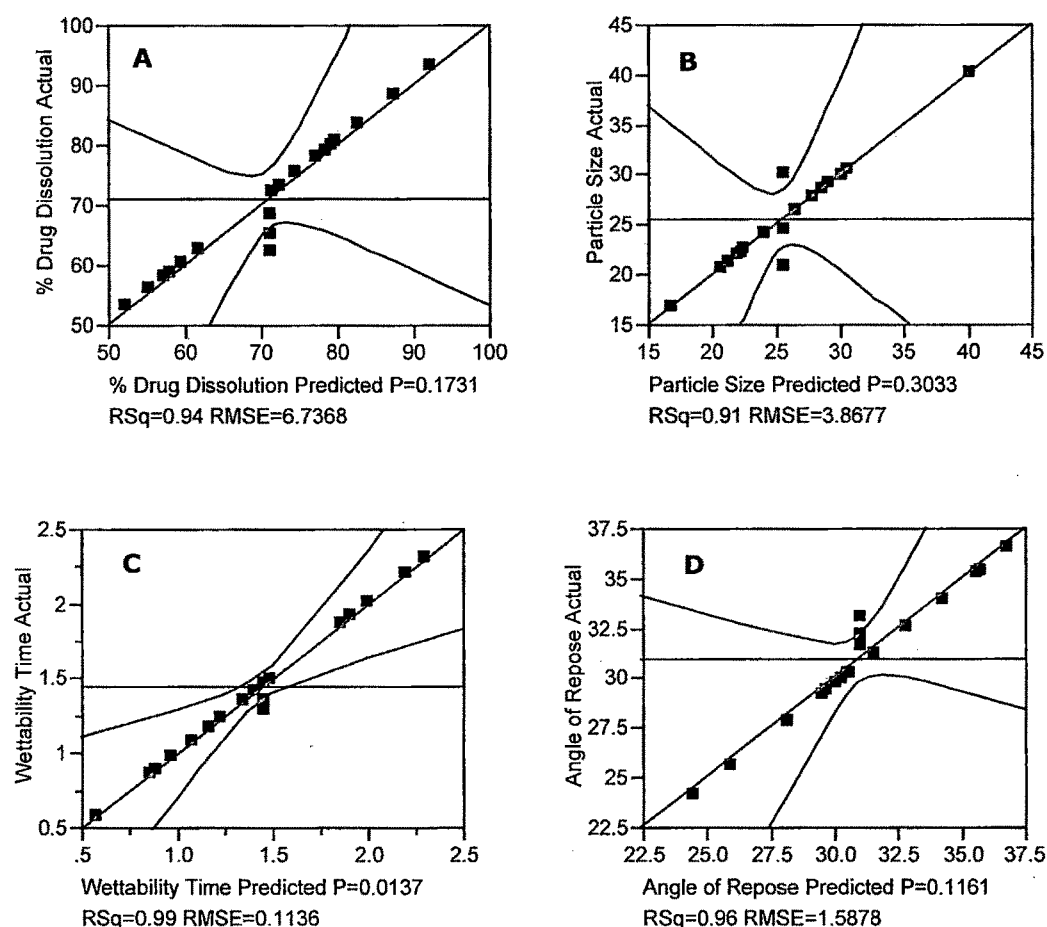


Figure 2.4.3 Actual vs. Predicted values for (A) percent drug dissolved, (B) particle size, (C) wettability time, (D) angle of repose for CBZ Chitosan microcrystals.



The computed profiles of the effect of all independent variables over dependent variables of the microcrystals are shown in Figure 2.4.4, Figure 2.4.5 and Figure 2.4.6. These profiles when analyzed suggest that all the profiles have significant effect on percent drug dissolution wettability time and angle of repose in more or less prototype. The optimization parameters for spray drying process also have significant effect on product quality, such as increasing in feed rate increases particle size of product considerably. However it did not show any statistically significant effect on percent drug dissolution. Increase in inlet temperature of the system showed decrease in the angle of repose of product which is a flowability indicator. The probable reason for it can be traced to complete drying of the product (i.e. lesser moisture or water content of product). However increase in inlet temperature also showed decrease in percent drug dissolution. It may be hypothesized due to immediate or rapid drying of drug and polymer which leads to incomplete interaction among them. Aspiration did not show any significant effect on the designated dependent variables but it showed momentous effect on morphological characteristics of the product.

Figure 2.4.4 Computed profile for all the dependant variables for CBZ Na-CMC microcrystals.

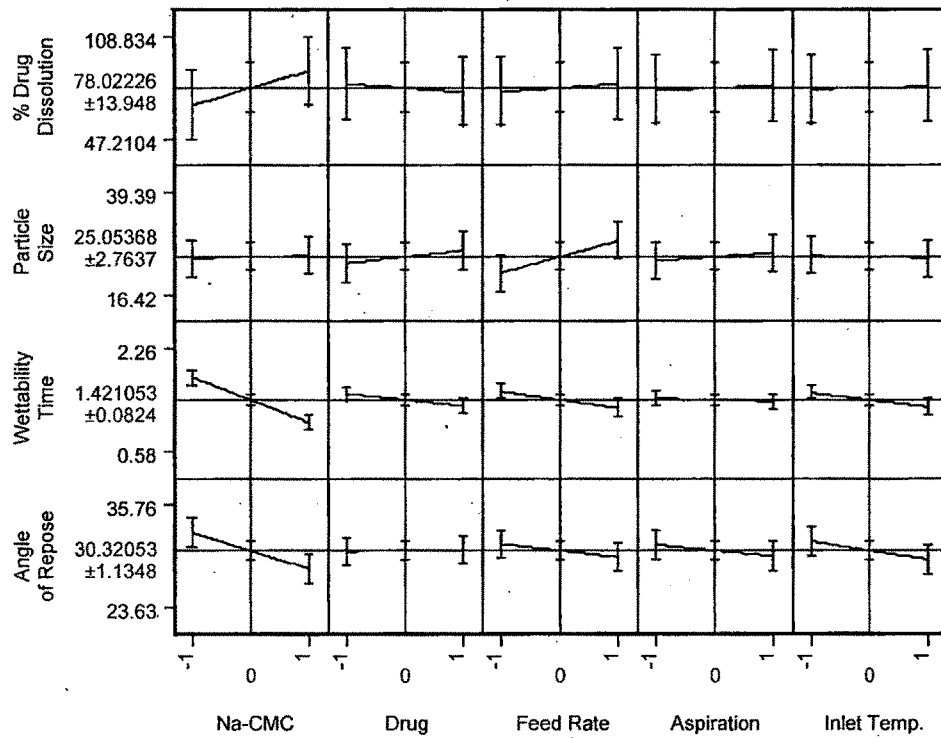


Figure 2.4.5 Computed profile for all the dependant variables for CBZ HPMC microcrystals.

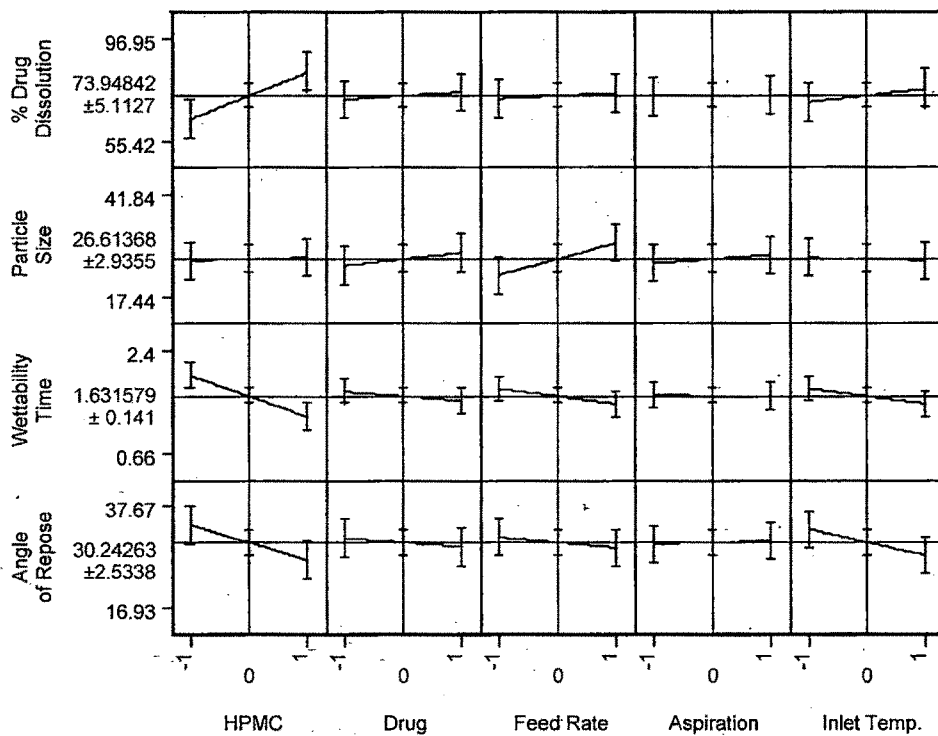


Figure 2.4.6 Computed profile for all the dependant variables for CBZ Chitosan microcrystals.

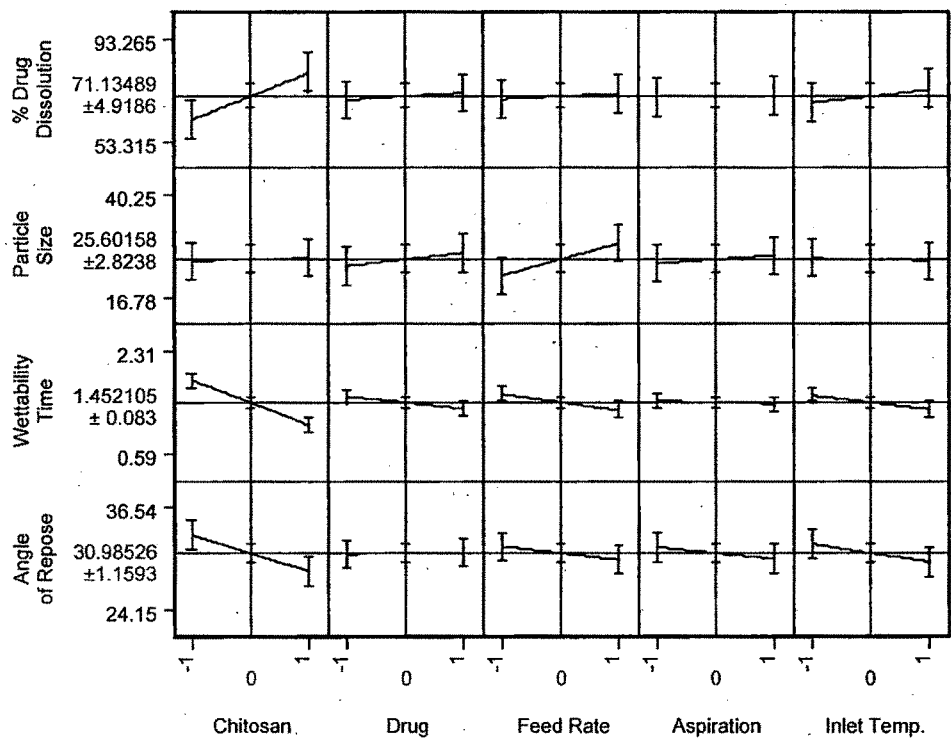


Table 2.4.2 Matrix of the experiments and results for the measured responses of fractional factorial design for CBZ Na-CMC microcrystals.

Experi- ment No.	Pattern	Chitosan (A)	Drug (B)	Feed Rate (C)	Aspiration (D)	Inlet Temp. (E)	Percent drug dissolved	Particle Size (µm)	Wettability Time (min.)	Angle of Repose (°)	Predicted Percent drug dissolved
1	-----+	-1	-1	-1	-1	1	61.84	20.22	2.26	29.36	65.12
2	-----+	-1	-1	-1	1	-1	61.75	23.69	1.97	35.76	65.03
3	--++--	-1	-1	1	-1	-1	60.49	29.45	1.83	34.60	63.77
4	--+++	-1	-1	1	1	1	69.16	28.04	1.88	29.63	72.44
5	-+----	-1	1	-1	-1	-1	60.34	21.86	2.16	34.69	63.62
6	-+---+	-1	1	-1	1	1	67.52	22.08	1.97	33.27	70.80
7	-++---	-1	1	1	-1	1	66.39	25.97	0.85	30.58	69.67
8	-+++-	-1	1	1	1	-1	68.96	27.26	1.47	29.60	72.24
9	+-----	1	-1	-1	-1	-1	75.69	20.80	1.39	27.29	78.97
10	+---++	1	-1	-1	1	1	85.65	16.42	0.58	25.14	88.94
11	+--+--	1	-1	1	-1	1	103.33	20.88	1.21	28.77	106.61
12	+++--	1	-1	1	1	-1	99.37	29.89	1.15	29.16	102.65
13	+++++	1	1	-1	-1	1	79.69	25.90	0.88	31.88	82.97
14	+++--	1	1	-1	1	-1	85.64	21.60	1.33	29.16	88.92
15	+++--	1	1	1	-1	-1	78.64	28.51	1.07	28.62	81.92
16	+++++	1	1	1	1	1	71.36	39.39	0.96	23.63	74.64
17	CP 1	0	0	0	0	0	96.07	29.59	1.26	32.38	78.02
18	CP 2	0	0	0	0	0	94.25	20.44	1.45	31.01	78.02
19	CP 3	0	0	0	0	0	96.28	24.03	1.33	31.56	78.02

Table 2.4.3 Matrix of the experiments and results for the measured responses of fractional factorial design for CBZ HPMC microcrystals.

Exper imen t No.	Pattern	Chitosan (A)	Drug (B)	Feed Rate (C)	Aspiration (D)	Inlet Temp. (E)	Percent drug dissolved	Particle Size (µm)	Wettability Time (min.)	Angle of Repose (°)	Predicted Percent drug dissolved
1	-----	-1	-1	-1	-1	1	62.94	21.48	2.4	33.36	61.82
2	---+-	-1	-1	-1	1	-1	61.26	25.17	2.1	37.19	60.14
3	--++-	-1	-1	1	-1	-1	58.48	31.28	1.96	33.12	57.36
4	---++	-1	-1	1	1	1	65.18	29.78	2.03	37.67	64.06
5	-+----	-1	1	-1	-1	-1	55.42	23.22	2.35	37.21	54.30
6	-+---+	-1	1	-1	1	1	60.44	23.45	2.15	36.72	59.32
7	-++--	-1	1	1	-1	1	78.53	27.59	0.94	20.39	77.41
8	-+++-	-1	1	1	1	-1	83.94	28.96	1.63	37.48	82.82
9	+-----	1	-1	-1	-1	-1	87.04	22.09	1.56	36.73	85.92
10	+---++	1	-1	-1	1	1	96.95	17.44	0.66	16.93	95.83
11	+-+--	1	-1	1	-1	1	81.36	22.18	1.4	30.06	80.24
12	+++-	1	-1	1	1	-1	76.26	31.75	1.35	26.89	75.14
13	++---	1	1	-1	-1	1	92.04	27.52	1.04	24.57	90.92
14	+++-	1	1	-1	1	-1	75.43	22.94	1.6	30.67	74.31
15	++++-	1	1	1	-1	-1	82.47	30.28	1.31	26.77	81.35
16	+++++	1	1	1	1	1	83.31	41.84	1.2	24.31	82.19
17	CP 1	0	0	0	0	0	64.85	31.44	1.62	25.19	73.95
18	CP 2	0	0	0	0	0	71.27	21.72	1.9	31.62	73.95
19	CP 3	0	0	0	0	0	67.85	25.53	1.8	27.73	73.95

Table 2.4.4 Matrix of the experiments and results for the measured responses of fractional factorial design for CBZ chitosan microcrystals.

Exper imen t No.	Pattern	Chitosan (A)	Drug (B)	Feed Rate (C)	Aspiration (D)	Inlet Temp. (E)	Percent drug dissolved	Particle Size (µm)	Wettability Time (min.)	Angle of Repose (°)	Predicted Percent drug dissolved
1	-----+	-1	-1	-1	-1	1	60.55	20.66	2.31	30.00	2.30
2	----+--	-1	-1	-1	1	-1	58.93	24.21	2.01	36.54	2.00
3	---++--	-1	-1	1	-1	-1	56.26	30.09	1.87	35.36	1.86
4	--++++	-1	-1	1	1	1	62.70	28.65	1.92	30.28	1.91
5	-+----	-1	1	-1	-1	-1	53.32	22.34	2.21	35.45	2.20
6	---+++	-1	1	-1	1	1	58.14	22.56	2.01	34.00	2.00
7	----++	-1	1	1	-1	1	75.54	26.54	0.87	31.25	0.86
8	---++-	-1	1	1	1	-1	80.75	27.86	1.50	30.25	1.49
9	+-----	1	-1	-1	-1	-1	83.73	21.25	1.42	27.89	1.41
10	+++--	1	-1	-1	1	1	93.27	16.78	0.59	25.69	0.58
11	++---+	1	-1	1	-1	1	78.26	21.34	1.24	29.40	1.23
12	+---++	1	-1	1	1	-1	73.36	30.54	1.18	29.80	1.17
13	++---+	1	1	-1	-1	1	88.54	26.47	0.90	32.58	0.89
14	++---+	1	1	-1	1	-1	72.56	22.07	1.36	29.80	1.35
15	++++--	1	1	1	-1	-1	79.33	29.13	1.09	29.25	1.08
16	++++++	1	1	1	1	1	80.14	40.25	0.98	24.15	0.97
17	CP 1	0	0	0	0	0	62.38	30.24	1.29	33.09	1.45
18	CP 2	0	0	0	0	0	68.56	20.89	1.48	31.69	1.45
19	CP 3	0	0	0	0	0	65.27	24.56	1.36	32.25	1.45

2.4.2.4.1. Effect of formulation independent variables on Particle size and percent drug dissolved

Particle size analysis for all experiments was found to have direct relationship with Na-CMC, HPMC and chitosan concentration. It may be attributed to increase in saturation level of solution polymer and drug. Rise in saturation of solution to be spray dried generally produce particles of greater size due to increase in cohesive force of droplets formed during spraying (Adler and Lee, **1999**). Since particle size has direct relationship with drug dissolution, decrease in particle size led to increased drug dissolution due to increase in surface area available for wetting.

But it should also be noted that high level of did not have significant effect on reduction of microcrystals size. This shows that an optimum concentration of polymer helped in controlling the particle size of microcrystals. Na-CMC, HPMC and chitosan have physical properties like moisture retaining, swelling and distributing ability. These properties usually help in wetting of drug microcrystals thereby promoting their dissolution. However increase in chitosan concentration also resulted in decrease in wetting time of microcrystals formed, probably due to decrease in surface area available of particles.

Results also showed that increase in feed rate increased the particle size of microcrystals. Increase in feed rate for spray drying promoted particle growth because of excessive liquid supply and larger droplet size (Maury, *et al.*, **2005**). Literature also has reported that feed rate for spray drying has reflective effect on particle size, since it determined the moisture or liquid content and the droplet size of binder solution (Rambali, *et al.*, **2001**, Vertommen and Kinget, **1997**).

Increase in inlet temperature of inlet air during spray drying decreased the particle size of microcrystals formed since the moisture content of spraying solution was also decreased due to rapid evaporation of liquid. Particle growth has direct relationship with spray rate or feed rate and inverse relationship to the inlet air temperature (Menon, *et al.*, **1996**). Scaled estimates, standard error, 't' ratio and probability for percent drug dissolved of the model analyzed are shown Table 2.4.5, Table 2.4.6 and Table 2.4.7.

CBZ Na-CMC microcrystals showed particle size distribution in the range of 16.42 to 39.39 μm , CBZ HPMC microcrystals showed 17.44 to 41.84 μm whereas CBZ chitosan showed in the range of 16.78 to 40.25 μm . Comparatively illustrating CBZ Na-CMC showed narrow particle size distribution.

CBZ Na-CMC microcrystals showed percent drug dissolved in the range of 61.75 to 103.33, CBZ HPMC microcrystals showed 55.42 to 96.95 whereas CBZ chitosan showed in the range of 58.93 to 93.27. Comparatively illustrating CBZ Na-CMC showed good drug dissolution enhancement.

Table 2.4.5 Model results for Scaled estimates, std error, t ratio and probability of percent drug dissolved and particle size as dependant variables for CBZ Na- CMC microcrystals.

Results for percent drug dissolved of CBZ Na- CMC microcrystals				
Term	Estimate	Std Error	t Ratio	Prob> t
Intercept	78.02	4.38	17.80	0.00
HPMC	10.18	4.78	2.13	0.12
Drug	-2.42	4.78	-0.51	0.65
Feed Rate	2.47	4.78	0.52	0.64
Aspiration	1.44	4.78	0.30	0.78
Inlet Temp.	0.88	4.78	0.18	0.87
HPMC*Drug	-3.67	4.78	-0.77	0.50
HPMC*Feed Rate	0.78	4.78	0.16	0.88
Drug*Feed Rate	-3.45	4.78	-0.72	0.52
HPMC*Aspiration	-0.85	4.78	-0.18	0.87
Drug*Aspiration	-0.39	4.78	-0.08	0.94
Feed Rate*Aspiration	-1.44	4.78	-0.30	0.78
HPMC*Inlet Temp.	-0.79	4.78	-0.17	0.88
Drug*Inlet Temp.	-1.96	4.78	-0.41	0.71
Feed Rate*Inlet Temp.	-0.53	4.78	-0.11	0.92
Aspiration*Inlet Temp.	-3.63	4.78	-0.76	0.50

Table 2.4.6 Model results for Scaled estimates, std error, t ratio and probability of percent drug dissolved and particle size as dependant variables for CBZ HPMC microcrystals.

Results for percent drug dissolved of CBZ HPMC microcrystals				
Term	Estimate	Std Error	t Ratio	Prob> t
Intercept	73.95	1.61	46.03	0.00
HPMC	9.29	1.75	5.31	0.01
Drug	1.38	1.75	0.79	0.49
Feed Rate	1.13	1.75	0.64	0.57
Aspiration	0.28	1.75	0.16	0.88
Inlet Temp.	2.53	1.75	1.44	0.24
HPMC*Drug	-2.43	1.75	-1.39	0.26
HPMC*Feed Rate	-4.63	1.75	-2.65	0.08
Drug*Feed Rate	4.49	1.75	2.56	0.08
HPMC*Aspiration	-1.65	1.75	-0.94	0.42
Drug*Aspiration	-0.95	1.75	-0.54	0.63
Feed Rate*Aspiration	0.70	1.75	0.40	0.72
HPMC*Inlet Temp.	1.53	1.75	0.87	0.45
Drug*Inlet Temp.	-0.40	1.75	-0.23	0.84
Feed Rate*Inlet Temp.	-1.62	1.75	-0.93	0.42
Aspiration*Inlet Temp.	-1.40	1.75	-0.80	0.48

Table 2.4.7 Model results for Scaled estimates, std error, t ratio and probability of percent drug dissolved and particle size as dependant variables for CBZ Chitosan microcrystals.

Results for percent drug dissolved of CBZ Chitosan microcrystals				
Term	Estimate	Std Error	t Ratio	Prob> t
Intercept	71.13	1.55	46.03	0.00
Chitosan	8.94	1.68	5.31	0.01
Drug	1.33	1.68	0.79	0.49
Feed Rate	1.08	1.68	0.64	0.57
Aspiration	0.27	1.68	0.16	0.88
Inlet Temp.	2.43	1.68	1.44	0.24
Chitosan*Drug	-2.34	1.68	-1.39	0.26
Chitosan*Feed Rate	-4.46	1.68	-2.65	0.08
Drug*Feed Rate	4.32	1.68	2.56	0.08
Chitosan*Aspiration	-1.59	1.68	-0.94	0.42
Drug*Aspiration	-0.91	1.68	-0.54	0.63
Feed Rate*Aspiration	0.68	1.68	0.40	0.72
Chitosan*Inlet Temp.	1.47	1.68	0.87	0.45
Drug*Inlet Temp.	-0.38	1.68	-0.23	0.84
Feed Rate*Inlet Temp.	-1.56	1.68	-0.93	0.42
Aspiration*Inlet Temp.	-1.35	1.68	-0.80	0.48

2.4.2.4.2. Effect of formulation independent variables on Wettability time and Angle of repose

Wettability time for microcrystals had a direct relationship with particle size of microcrystals. Due to this all the factors governing particle size had same effect on wettability time. As mentioned previously increase in feed rate resulted in increase particle size of microcrystals. Feed rate has the same effect on particle size distribution also. However particle size distribution measurement was not the part of study, it showed effect on angle of repose of microcrystals which is a flowability measurement tool. High feed rate during the process lead to disorderly growth of particles since equal drying of liquid from droplet surfaces was not ensured, leading to local overwetting (Vertommen and Kinget, 1997).

CBZ Na-CMC microcrystals showed wettability time in the range of 0.58 to 1.97 min, CBZ HPMC microcrystals showed 0.66 to 2.40 min whereas CBZ chitosan microcrystals showed in the range of 0.59 to 2.31 min. Comparatively illustrating the lowest wettability time was observed for OCBZ Na-CMC microcrystals.

Results for Contact angle of pure drug powder and optimized batch of microcrystals showed that there was significant improvement in hydrophilicity of microcrystals produced.

Figure 2.4.13 shows the uniform stable dispersion of optimized batches of microcrystals in water which is also a measure of wettability of dispersed phase.

CBZ Na-CMC microcrystals showed angle of repose in the range of 25.14° to 35.76° , CBZ HPMC microcrystals showed in the range of 16.93° to 37.67° , whereas CBZ chitosan microcrystals showed in the range of 24.15° to 36.54° . The narrow angle of distribution range was observed for OCBZ Na-CMC microcrystals which exemplifies that product obtained from Na CMC is more uniform and flowable.

2.4.2.4.3. Interaction between the factors

The ANOVA results are depicted in Table 2.4.5, Table 2.4.6 and Table 2.4.7 which gives idea about the significant effect of variables individually and in combination with each other. Here instead of using normal probability function 't' ratio, which lists the test statistics for the hypothesis that each parameter is zero. It is the ratio of the parameter estimate to its standard error. If the hypothesis is true, then this statistic has a Student's t-distribution. Looking for a 't' ratio greater than 2 in absolute value is a common rule of thumb for judging significance because it approximates the 0.05 significance level. Also the term 'Prob > |t|' lists the observed significance probability calculated from each 't' ratio. It is the probability of getting, by chance alone, a 't' ratio greater (in absolute value) than the computed value, given a true hypothesis. Often, a value below 0.05 (or sometimes 0.01) is interpreted as evidence that the parameter is significantly different from zero.

The results showed that Na-CMC compared to HPMC and chitosan has imperative effect on percent drug dissolved, particle size, wettability time and angle of repose whereas drug concentration, feed rate, percent aspiration and inlet temperature during spray drying has significant effect on particle size, wettability time and angle of repose.

Thermal Analysis and XRPD Studies

Figure 2.4.7 shows thermogram for pure crystalline carbamazepine characterized by a single, sharp melting endotherm at 194.43 °C with small endothermic peak at 170.86 which can be attributed to presence of small amount of polymorphic form of carbamazepine. Thermograms for CBZ HPMC and CBZ chitosan microcrystals showed considerable decrease in the energy change of the melting endotherm, attributable to a great extent of reduction in crystallinity of drug.

Figure 2.4.8 showed prominent diffraction peaks in the range of 8 – 30 °2 θ during XRPD studies. Thermogram of CBZ Na-CMC microcrystals revealed broadening of melting endotherm of the CBZ. Consequently, there was significant decrease in intensity of major CBZ crystalline peaks (12.5, 16, 20, 26, and 28 °2 θ) in diffractogram of CBZ Na-CMC, CBZ HPMC and CBZ chitosan microcrystals which suggests a favorable interaction between CBZ and carrier Na-CMC. The partial loss of crystallinity of drug observed may also be attributed to physical presence of Na-CMC.

SEM studies performed gave a strong support to the results of DSC and XRPD.

Figure 2.4.7 DSC thermograms for CBZ NACMC, CBZ HPMC and CBZ chitosan microcrystals.

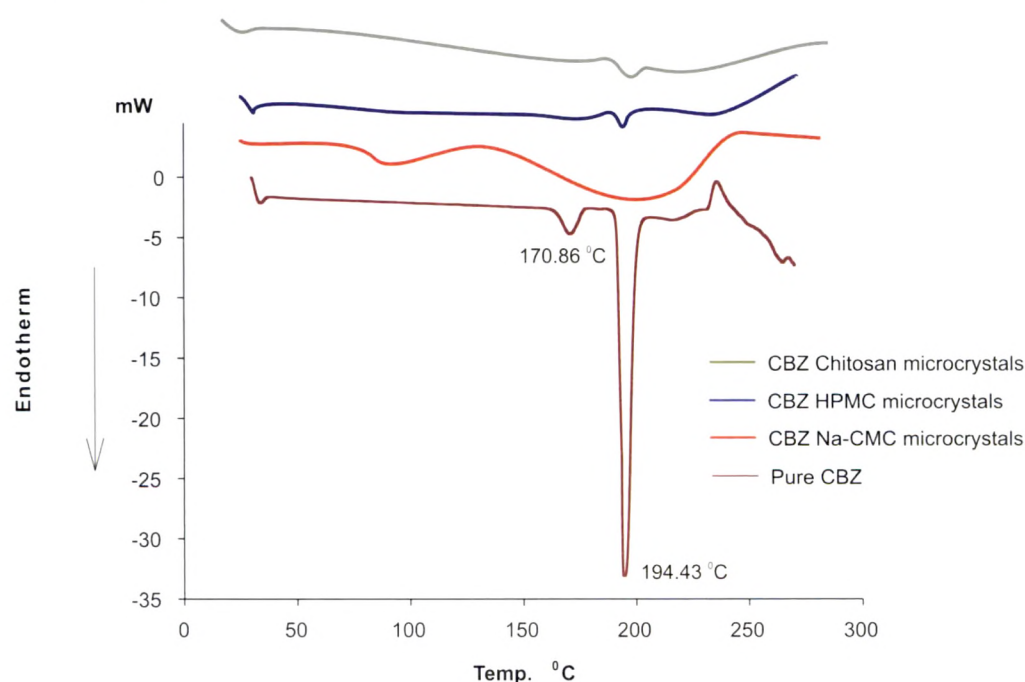
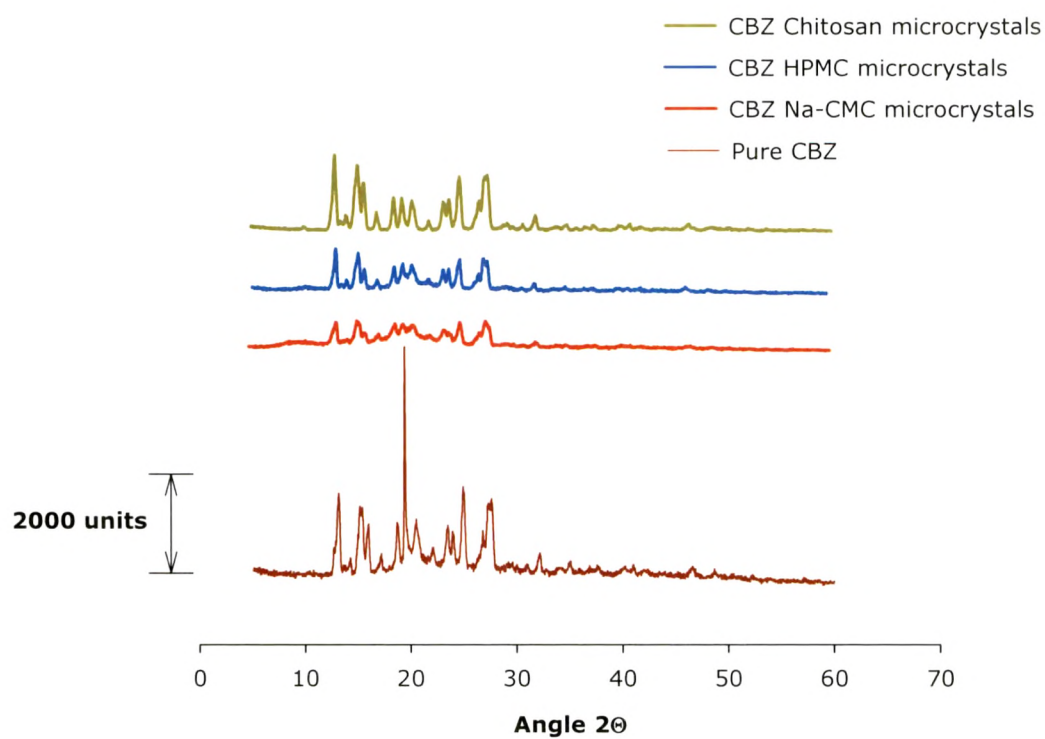


Figure 2.4.8 XRPD results for Pure drug, Chitosan, Physical mixture and Optimized batch of microcrystals.



2.4.2.4.4. SEM studies

The microphotographs of pure CBZ and optimized batch of microcrystals are shown in Figure 2.4.9, Figure 2.4.10, Figure 2.4.11 and Figure 2.4.12. Pure drug was observed in the form of a mixture of some large crystals ranging from 20 - 600 μm) with microparticles. Microcrystals formed in various batches of experimental design revealed significant changes in particle shape and surface topography due to impact of spray drying process. However in figure only images of optimized batch are shown. For all the 3 polymers the microcrystals appeared as smooth spherical agglomerates with slight particle aggregation as well as residual crystals, to a small extent adhered to particles.

Figure 2.4.9 SEM image of Pure crystalline CBZ.



Figure 2.4.10 SEM image of optimized batch of microcrystals of CBZ with Na CMC.

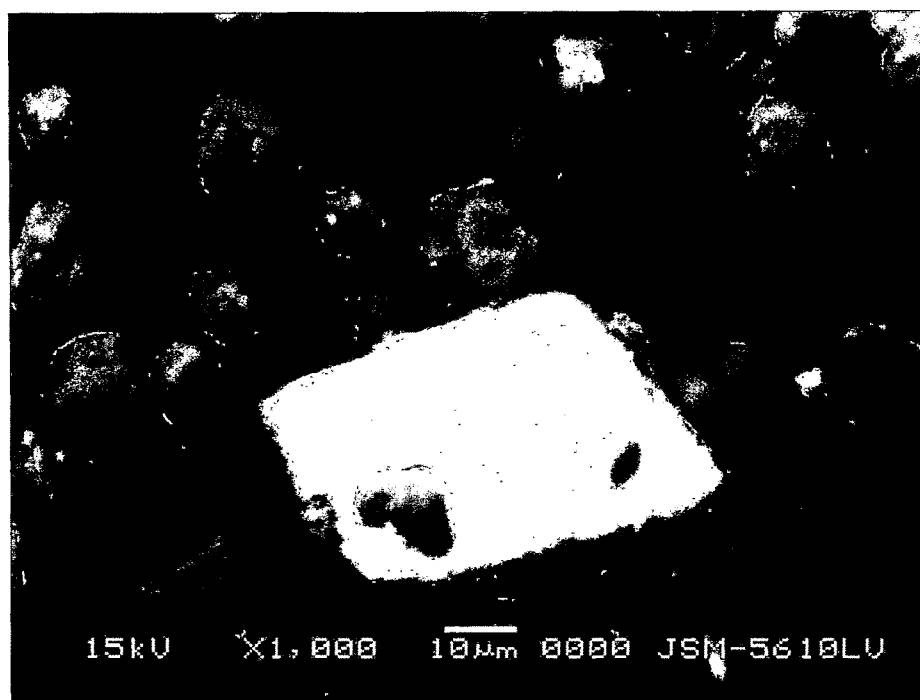


Figure 2.4.11 SEM image of optimized batch microcrystals of CBZ with HPMC.

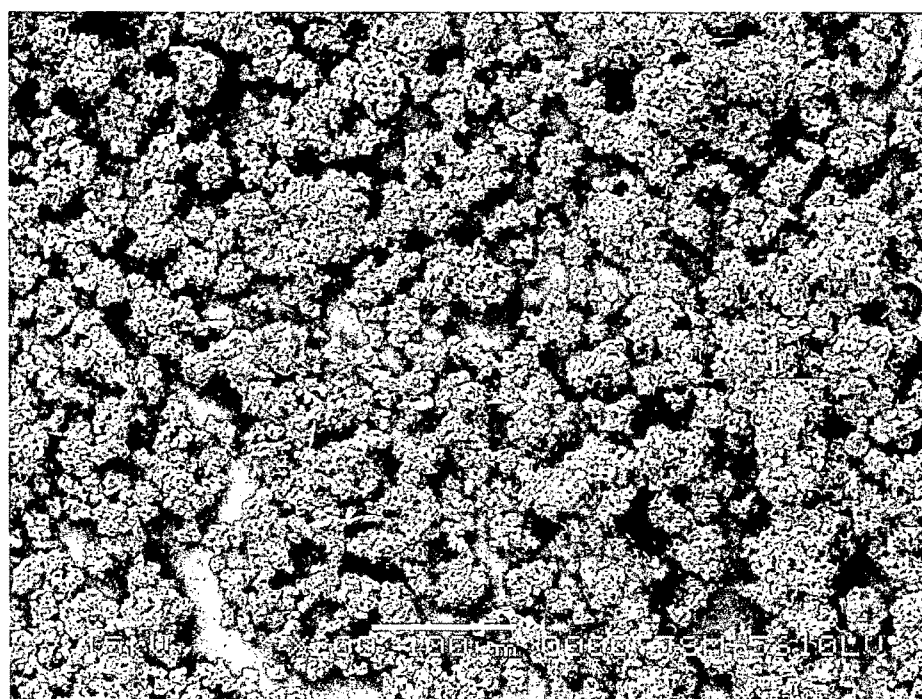


Figure 2.4.12 SEM image of optimized batch microcrystals of CBZ with chitosan.

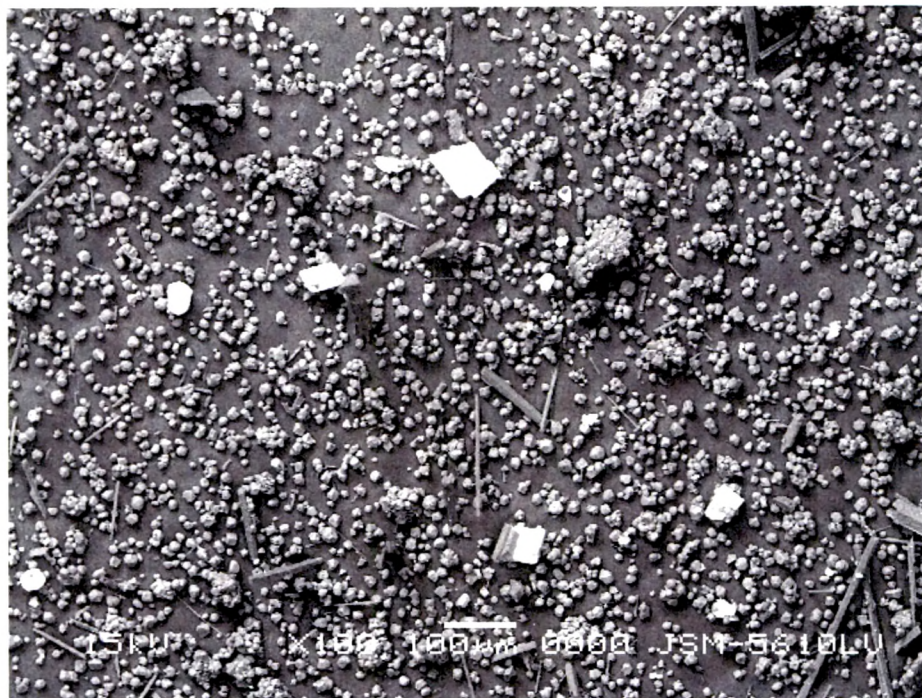
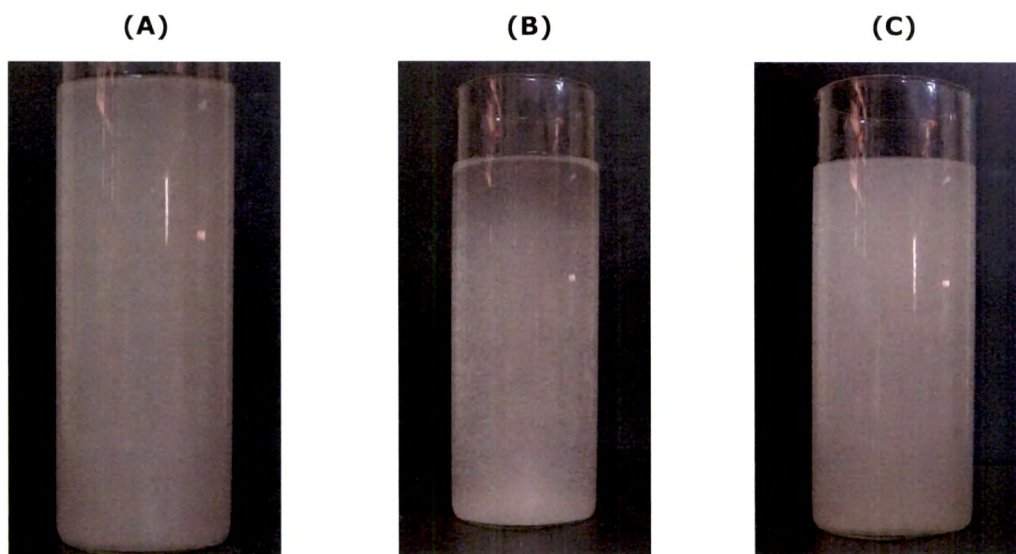


Figure 2.4.13 Microcrystal dispersion of (A) CBZ Na-CMC, (B) CBZ HPMC and (C) CBZ chitosan microcrystals.



2.4.2.5. Microcrystals of Oxcarbamazepine

Figure 2.4.14, Figure 2.4.15 and Figure 2.4.16 shows the leverage plots of predicted and actual values for the experimental design with percent drug dissolved, particle size, wettability time and angle of repose as responses for microcrystals of OCBZ with Na-CMC, HPMC and Chitosan respectively. The points on a leverage plot for simple regression are actual data coordinates, and the horizontal line for the constrained model is the sample mean of the response. But when the leverage plot is for one of multiple effects, the points are no longer actual data values. The horizontal line then represents a partially constrained model instead of a model fully constrained to one mean value. The response values of all the experiments (except for 2 of 3 centre points) lie between the confidence intervals of the leverage plot. Also the confidence region for the line of fit does contain the horizontal line of the mean; this predicts that effects (dependent variables) are significant.

Table 2.4.8 gives quantitative solubility data for OCBZ microcrystals. OCBZ Na-CMC microcrystals were found to have highest solubility for OCBZ compared to other microcrystals.

Table 2.4.8 Quantitative solubility data for pure OCBZ, in different microcrystals and polyethylene glycol 600.

	Solvents		Microcrystals		
	Water	PEG 600	Na-CMC	HPMC	Chitosan
Solubility of OCBZ (g/100mL)	0.0101	0.1964	0.2703	0.2413	0.2340

Figure 2.4.14 Actual vs. Predicted values for (A) percent drug dissolved, (B) particle size, (C) wettability time, (D) angle of repose for OCBZ Na-CMC microcrystals.

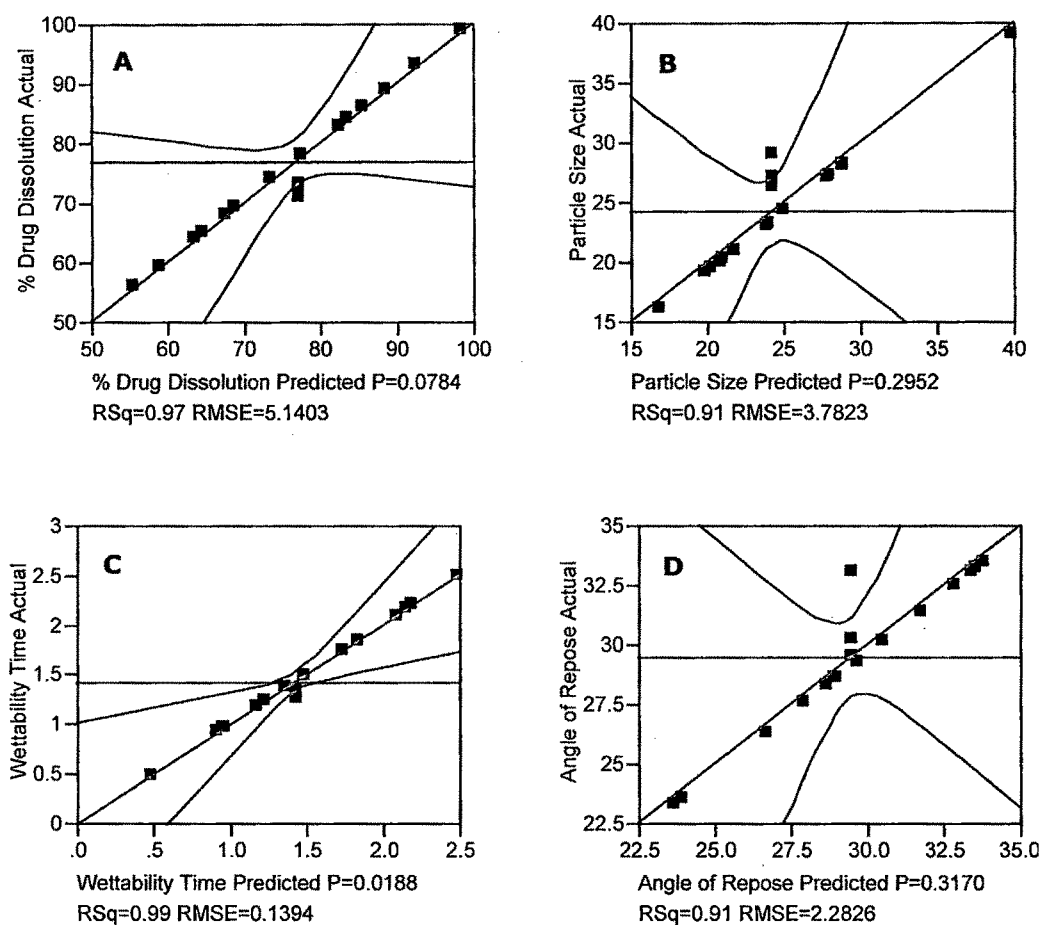


Figure 2.4.15 Actual vs. Predicted values for (A) percent drug dissolved, (B) particle size, (C) wettability time, (D) angle of repose for OCBZ-HPMC microcrystals.

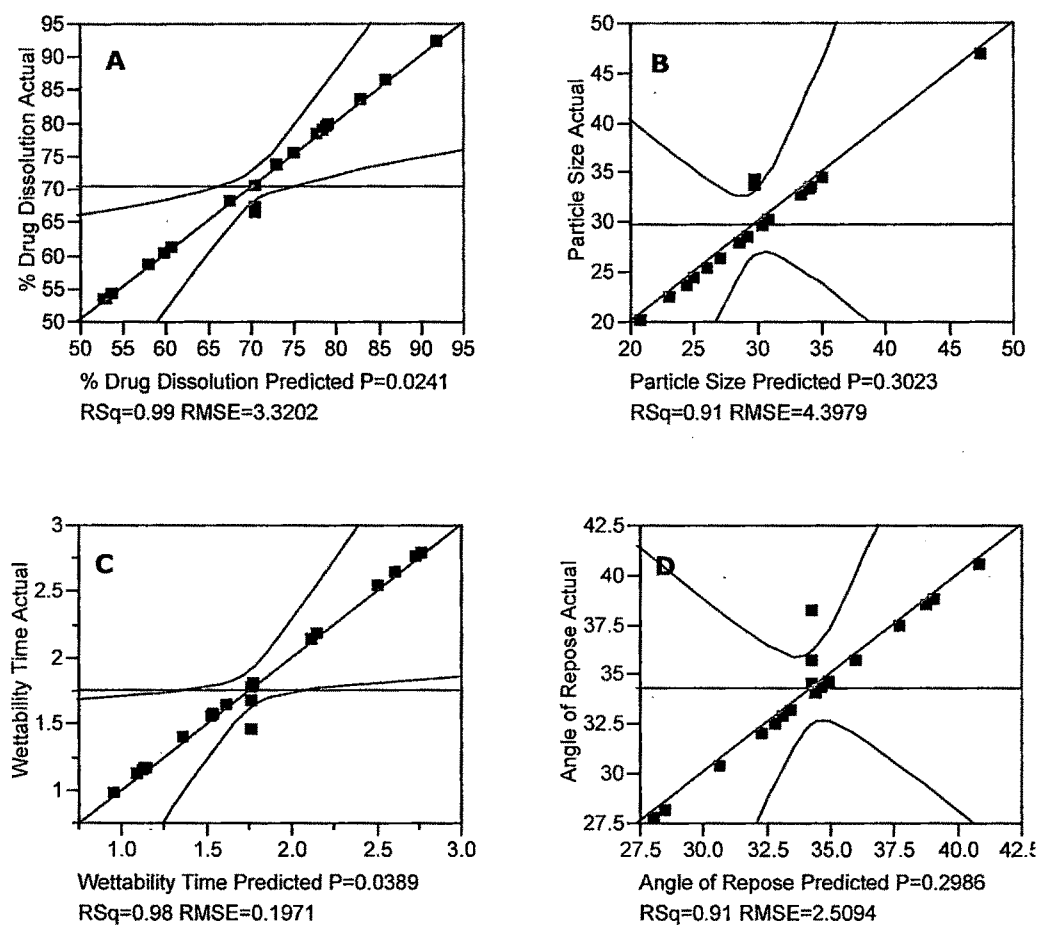
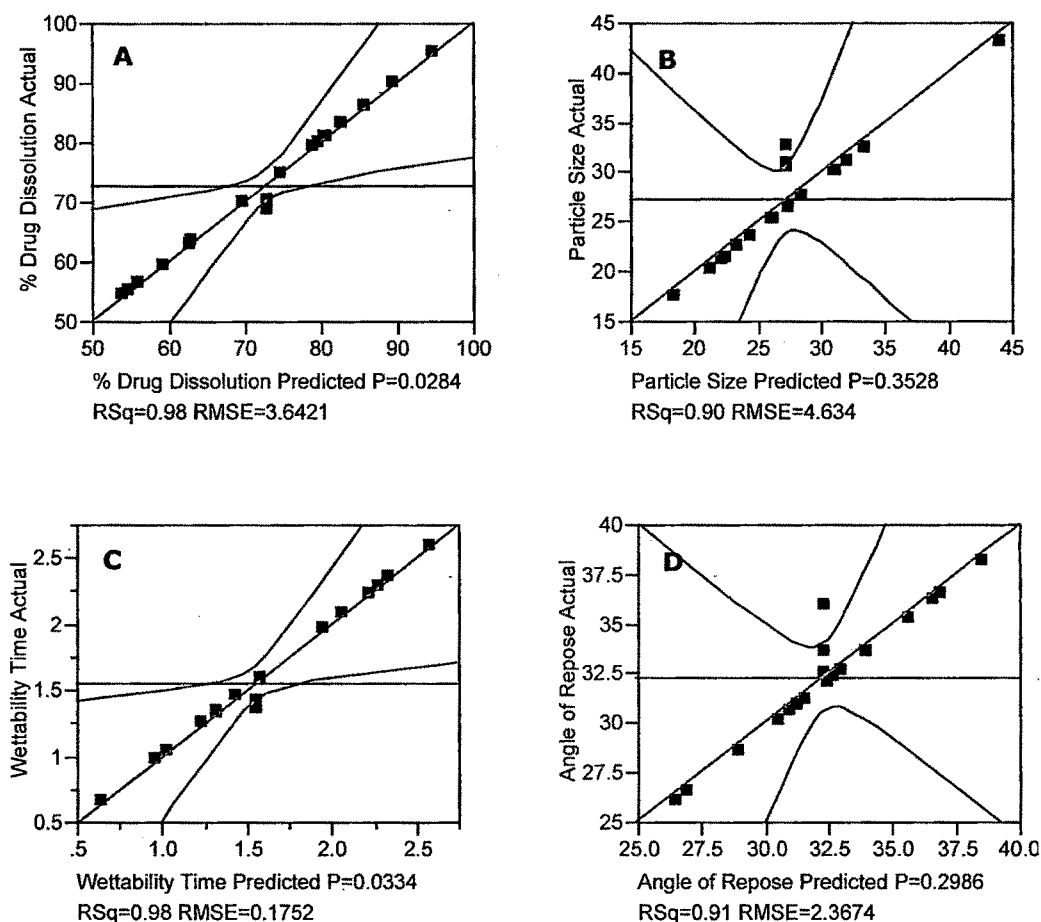


Figure 2.4.16 Actual vs. Predicted values for (A) percent drug dissolved, (B) particle size, (C) wettability time, (D) angle of repose for OCBZ Chitosan microcrystals.



The computed profiles of the effect of all independent variables over dependent variables of the microcrystals are shown in Figure 2.4.17, Figure 2.4.18 and Figure 2.4.19. These profiles when analyzed suggest that all the profiles have significant effect on percent drug dissolution wettability time and angle of repose in more or less prototype. The optimization parameters for spray drying process also have significant effect on product quality, such as increasing in feed rate increases particle size of product considerably. However it did not show any statistically significant effect on percent drug dissolution. Increase in inlet temperature of the system showed decrease in the angle of repose of product which is a flowability indicator. The probable reason for it can be traced to complete drying of the product (i.e. lesser moisture or water content of product). However increase in inlet temperature also showed decrease in percent drug dissolution. It may be hypothesized due to immediate or rapid drying of drug and polymer which leads to incomplete interaction among them. Aspiration did not show any significant effect on the designated dependent variables but it showed momentous effect on morphological characteristics of the product.

Figure 2.4.17 Computed profile for all the dependant variables for OCBZ Na-CMC microcrystals.

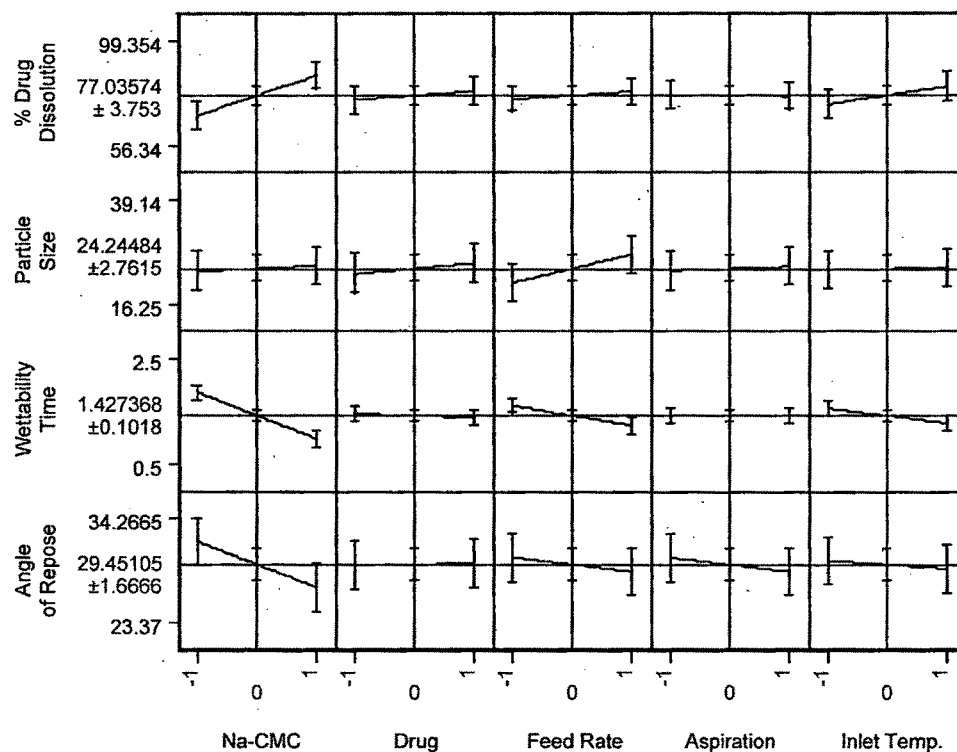


Figure 2.4.18 Computed profile for all the dependant variables for OCBZ HPMC microcrystals.

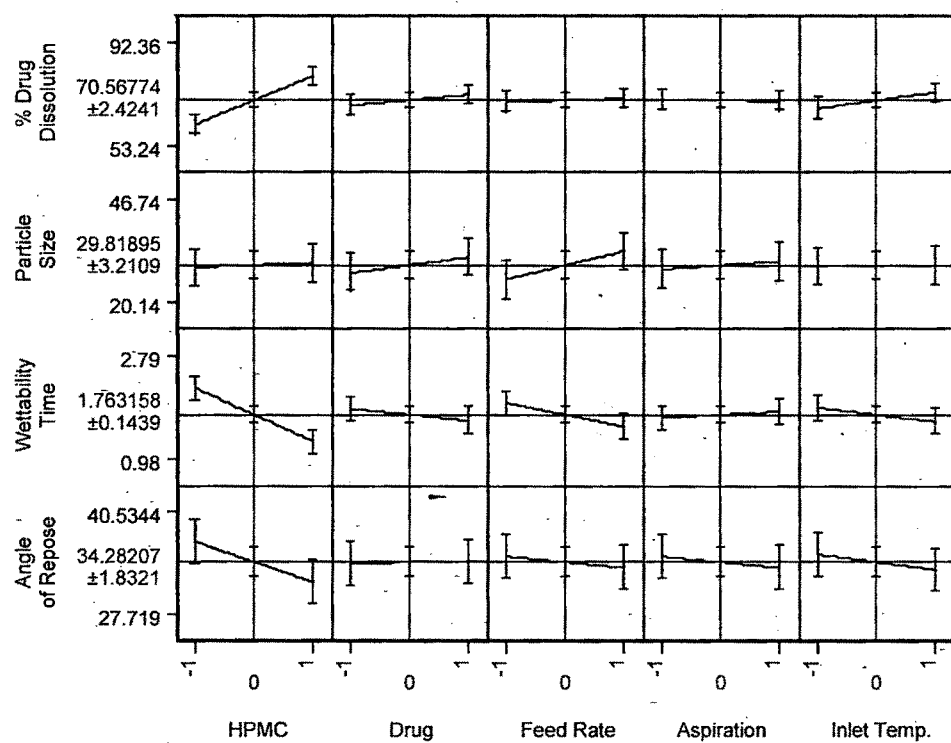


Figure 2.4.19 Computed profile for all the dependant variables for OCBZ Chitosan microcrystals.

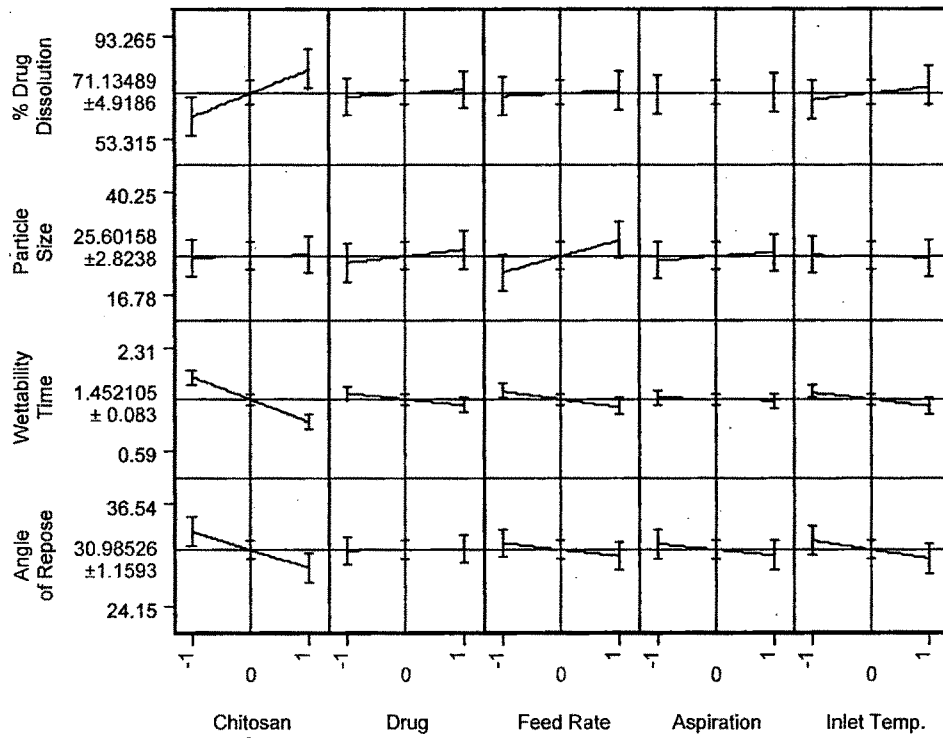


Table 2.4.9 Matrix of the experiments and results for the measured responses of fractional factorial design for OCBZ Na-CMC microcrystals.

Experi ment No.	Pattern	Chitosan (A)	Drug (B)	Feed Rate (C)	Aspiration (D)	Inlet Temp. (E)	Percent drug dissolved	Particle Size (µm)	Wettability Time (min.)	Angle of Repose (°)	Predicted Percent drug dissolved
1	----+	-1	-1	-1	-1	1	69.58	20.14	2.21	31.45	68.71
2	---+-	-1	-1	-1	1	-1	59.67	20.36	2.17	33.25	58.80
3	--++-	-1	-1	1	-1	-1	64.25	28.25	1.75	33.14	63.38
4	---++	-1	-1	1	1	1	68.15	27.36	1.85	30.21	67.28
5	-+---	-1	1	-1	-1	-1	56.34	23.15	2.50	32.57	55.47
6	-++--	-1	1	-1	1	1	65.24	20.14	2.10	33.47	64.37
7	-+++-	-1	1	1	-1	1	86.15	23.37	0.98	29.34	85.28
8	-+++-	-1	1	1	1	-1	89.15	21.01	1.50	28.67	88.27
9	+-----	1	-1	-1	-1	-1	89.33	19.57	1.24	26.34	88.45
10	+++++	1	-1	-1	1	1	99.35	16.25	0.50	23.37	98.48
11	+---+	1	-1	1	-1	1	84.21	19.24	0.97	28.35	83.34
12	+---+	1	-1	1	1	-1	74.36	28.17	1.19	26.34	73.49
13	+++++	1	1	-1	-1	1	93.24	24.37	0.97	30.21	92.37
14	+++++	1	1	-1	1	-1	78.14	20.36	1.38	28.63	77.27
15	+++++	1	1	1	-1	-1	83.14	27.14	0.97	27.64	82.27
16	+++++	1	1	1	1	1	86.24	39.14	0.93	23.61	85.37
17	CP 1	0	0	0	0	0	71.25	29.14	1.27	33.14	77.04
18	CP 2	0	0	0	0	0	73.25	26.35	1.29	29.57	77.04
19	CP 3	0	0	0	0	0	72.65	27.14	1.35	30.27	77.04

Table 2.4.10 Matrix of the experiments and results for the measured responses of fractional factorial design for OCBZ HPMC microcrystals.

Exper imen t No.	Pattern	Chitosan (A)	Drug (B)	Feed Rate (C)	Aspiration (D)	Inlet Temp. (E)	Percent drug dissolved	Particle Size (µm)	Wettability Time (min.)	Angle of Repose (°)	Predicted Percent drug dissolved
1	----+	-1	-1	-1	-1	1	61.27	25.36	2.54	34.31	60.78
2	---+-	-1	-1	-1	1	-1	53.24	24.34	2.76	40.53	52.75
3	--++-	-1	-1	1	-1	-1	54.21	33.25	2.14	38.73	53.72
4	---++	-1	-1	1	1	1	60.28	32.67	2.18	34.08	59.79
5	-+---	-1	1	-1	-1	-1	53.47	28.45	2.79	38.48	52.98
6	-+++-	-1	1	-1	1	1	58.47	26.34	2.64	37.39	57.98
7	-+++-	-1	1	1	-1	1	75.48	27.89	1.12	34.61	74.99
8	-+++-	-1	1	1	1	-1	79.68	29.64	1.80	33.15	79.19
9	+-----	1	-1	-1	-1	-1	83.54	22.34	1.39	30.36	83.05
10	+++++	1	-1	-1	1	1	92.36	20.14	0.98	27.72	91.87
11	++-++	1	-1	1	-1	1	78.97	23.64	1.56	31.99	78.48
12	++-++	1	-1	1	1	-1	68.25	34.39	1.57	32.51	67.76
13	++-++	1	1	-1	-1	1	86.39	30.14	1.17	35.66	85.90
14	++-++	1	1	-1	1	-1	73.64	26.34	1.65	32.51	73.15
15	++-++	1	1	1	-1	-1	78.31	33.36	1.16	32.83	77.82
16	+++++	1	1	1	1	1	79.35	46.74	1.15	28.17	78.86
17	CP 1	0	0	0	0	0	66.31	34.31	1.45	38.16	70.57
18	CP 2	0	0	0	0	0	70.33	33.58	1.67	34.50	70.57
19	CP 3	0	0	0	0	0	67.24	33.64	1.78	35.67	70.57

Table 2.4.11 Matrix of the experiments and results for the measured responses of fractional factorial design for OCBZ chitosan microcrystals.

Exper imen t No.	Pattern	Chitosan (A)	Drug (B)	Feed Rate (C)	Aspiration (D)	Inlet Temp. (E)	Percent drug dissolved	Particle Size (μm)	Wettability Time (min.)	Angle of Repose ($^\circ$)	Predicted Percent drug dissolved
1	-----+	-1	-1	-1	-1	1	63.57	21.57	2.36	32.37	62.96
2	-----+	-1	-1	-1	1	-1	55.27	21.36	2.24	38.24	54.66
3	---+---	-1	-1	1	-1	-1	56.47	32.58	1.98	36.54	55.86
4	---+++	-1	-1	1	1	1	63.21	30.17	2.09	32.15	62.60
5	-+----	-1	1	-1	-1	-1	54.57	25.40	2.60	36.30	53.96
6	-+---+	-1	1	-1	1	1	59.67	23.64	2.30	35.27	59.06
7	-++--+	-1	1	1	-1	1	79.45	25.28	0.99	32.65	78.83
8	-+++-	-1	1	1	1	-1	83.24	26.58	1.60	31.27	82.63
9	+-----	1	-1	-1	-1	-1	86.24	20.38	1.34	28.64	85.63
10	+++--	1	-1	-1	1	1	95.31	17.59	0.67	26.15	94.70
11	++---	1	-1	1	-1	1	80.12	22.57	1.35	30.18	79.51
12	++--+	1	-1	1	1	-1	70.14	31.26	1.26	30.67	69.53
13	++---+	1	1	-1	-1	1	90.01	27.59	0.98	33.64	89.40
14	+++-	1	1	-1	1	-1	75.15	23.65	1.46	30.67	74.54
15	++++--	1	1	1	-1	-1	81.03	30.28	1.05	30.97	80.41
16	++++++	1	1	1	1	1	81.26	43.26	1.05	26.58	80.64
17	CP 1	0	0	0	0	0	68.96	32.67	1.36	36.00	72.81
18	CP 2	0	0	0	0	0	70.57	30.54	1.40	32.55	72.81
19	CP 3	0	0	0	0	0	69.07	30.98	1.42	33.65	72.81

Effect of formulation independent variables on Particle size and percent drug dissolved

OCBZ Na-CMC microcrystals showed particle size distribution in the range of 16.25 to 39.14 μm , OCBZ HPMC microcrystals showed 16.25 to 46.74 μm whereas OCBZ chitosan showed in the range of 17.59 to 43.26 μm . Comparatively illustrating OCBZ Na-CMC showed narrow particle size distribution.

OCBZ Na-CMC microcrystals showed percent drug dissolved in the range of 56.34 to 99.35, OCBZ HPMC microcrystals showed 53.24 to 92.36 whereas OCBZ chitosan showed in the range of 54.57 to 95.31. Comparatively illustrating OCBZ Na-CMC showed good drug dissolution enhancement.

Table 2.4.12 Model results for Scaled estimates, std error, t ratio and probability of percent drug dissolved and particle size as dependant variables for OCBZ Na- CMC microcrystals.

Results for percent drug dissolved of CBZ Na- CMC microcrystals				
Term	Estimate	Std Error	t Ratio	Prob> t
Intercept	77.04	1.18	65.32	0.00
HPMC	8.09	1.29	6.30	0.01
Drug	1.80	1.29	1.40	0.26
Feed Rate	1.55	1.29	1.20	0.31
Aspiration	-0.37	1.29	-0.29	0.79
Inlet Temp.	3.61	1.29	2.81	0.07
HPMC*Drug	-2.61	1.29	-2.03	0.14
HPMC*Feed Rate	-5.56	1.29	-4.33	0.02
Drug*Feed Rate	4.92	1.29	3.83	0.03
HPMC*Aspiration	-1.11	1.29	-0.86	0.45
Drug*Aspiration	0.36	1.29	0.28	0.80
Feed Rate*Aspiration	0.39	1.29	0.30	0.78
HPMC*Inlet Temp.	1.15	1.29	0.89	0.44
Drug*Inlet Temp.	-0.60	1.29	-0.47	0.67
Feed Rate*Inlet Temp.	-1.88	1.29	-1.46	0.24
Aspiration*Inlet Temp.	-1.40	1.29	-1.09	0.35

Table 2.4.13 Model results for Scaled estimates, std error, t ratio and probability of percent drug dissolved and particle size as dependant variables for OCBZ HPMC microcrystals.

Results for percent drug dissolved of CBZ HPMC microcrystals				
Term	Estimate	Std Error	t Ratio	Prob> t
Intercept	70.57	0.76	92.65	0.00
HPMC	9.04	0.83	10.90	0.00
Drug	2.04	0.83	2.46	0.09
Feed Rate	0.76	0.83	0.91	0.43
Aspiration	-0.40	0.83	-0.48	0.66
Inlet Temp.	3.01	0.83	3.63	0.04
HPMC*Drug	-2.72	0.83	-3.28	0.05
HPMC*Feed Rate	-4.64	0.83	-5.59	0.01
Drug*Feed Rate	4.35	0.83	5.24	0.01
HPMC*Aspiration	-1.30	0.83	-1.57	0.21
Drug*Aspiration	0.08	0.83	0.10	0.93
Feed Rate*Aspiration	0.47	0.83	0.57	0.61
HPMC*Inlet Temp.	1.15	0.83	1.39	0.26
Drug*Inlet Temp.	-1.19	0.83	-1.43	0.25
Feed Rate*Inlet Temp.	-1.31	0.83	-1.58	0.21
Aspiration*Inlet Temp.	-1.06	0.83	-1.27	0.29

Table 2.4.14 Model results for Scaled estimates, std error, t ratio and probability of percent drug dissolved and particle size as dependant variables for OCBZ Chitosan microcrystals.

Results for percent drug dissolved of CBZ Chitosan microcrystals				
Term	Estimate	Std Error	t Ratio	Prob> t
Intercept	72.81	0.84	87.14	0.00
Chitosan	8.99	0.91	9.87	0.00
Drug	2.13	0.91	2.34	0.10
Feed Rate	0.94	0.91	1.04	0.38
Aspiration	-0.51	0.91	-0.56	0.61
Inlet Temp.	3.16	0.91	3.47	0.04
Chitosan*Drug	-2.67	0.91	-2.94	0.06
Chitosan*Feed Rate	-5.22	0.91	-5.73	0.01
Drug*Feed Rate	4.75	0.91	5.22	0.01
Chitosan*Aspiration	-1.43	0.91	-1.57	0.21
Drug*Aspiration	-0.20	0.91	-0.22	0.84
Feed Rate*Aspiration	0.61	0.91	0.67	0.55
Chitosan*Inlet Temp.	1.11	0.91	1.22	0.31
Drug*Inlet Temp.	-1.11	0.91	-1.21	0.31
Feed Rate*Inlet Temp.	-1.51	0.91	-1.66	0.20
Aspiration*Inlet Temp.	-1.20	0.91	-1.32	0.28

2.4.2.5.1. Effect of formulation independent variables on Wettability time and Angle of repose

OCBZ Na-CMC microcrystals showed wettability time in the range of 0.5 to 2.5 min, OCBZ HPMC microcrystals showed 0.98 to 2.79 min whereas OCBZ chitosan microcrystals showed in the range of 0.67 to 2.60 min. Comparatively illustrating the lowest wettability time was observed for OCBZ Na-CMC microcrystals.

Results for Contact angle of pure drug powder and optimized batch of microcrystals showed that there was significant improvement in hydrophilicity of microcrystals produced. Figure 2.4.26 shows the uniform stable dispersion of optimized batches of microcrystals in water which is also a measure of wettability of dispersed phase.

OCBZ Na-CMC microcrystals showed angle of repose in the range of 23.37° to 33.47° , OCBZ HPMC microcrystals showed in the range of 27.72° to 40.53° , whereas OCBZ chitosan microcrystals showed in the range of 26.15° to 38.24° . the narrow angle of distribution range was observed for OCBZ Na-CMC microcrystals which exemplifies that product obtained from Na CMC is more uniform and flowable.

2.4.2.5.2. Interaction between the factors

The ANOVA results are depicted in Table 2.4.12, Table 2.4.13 and Table 2.4.14 which gives idea about the significant effect of variables individually and in combination with each other. Here instead of using normal probability function 't' ratio, which lists the test statistics for the hypothesis that each parameter is zero. It is the ratio of the parameter estimate to its standard error. If the hypothesis is true, then this statistic has a Student's t-distribution. Looking for a 't' ratio greater than 2 in absolute value is a common rule of thumb for judging significance because it approximates the 0.05 significance level. Also the term 'Prob > |t|' lists the observed significance probability calculated from each 't' ratio. It is the probability of getting, by chance alone, a 't' ratio greater (in absolute value) than the computed value, given a true hypothesis. Often, a value below 0.05 (or sometimes 0.01) is interpreted as evidence that the parameter is significantly different from zero.

In case of OCBZ microcrystals also results showed that Na-CMC compared to HPMC and chitosan has imperative effect on percent drug dissolved, particle size, wettability time and angle of repose whereas drug concentration, feed rate, percent aspiration and inlet temperature during spray drying has significant effect on particle size, wettability time and angle of repose.

2.4.2.5.3. Thermal Analysis and XRPD Studies

Figure 2.4.20 shows thermogram for pure crystalline carbamazepine characterized by a single, sharp melting endotherm at 232.19 °C. Thermograms for OCBZ HPMC and OCBZ chitosan microcrystals showed considerable decrease in the energy change of the melting endotherm, attributable to a great extent of reduction in crystallinity of drug. Whereas thermogram for OCBZ Na-CMC microcrystals showed almost complete disappearance of melting endotherm owing to conversion of most of the OCBZ from crystalline nature to amorphous one.

Figure 2.4.21 showed prominent diffraction peaks in the range of 8 – 30 °2 θ during XRPD studies. Pure OCBZ crystalline material showed prominent peaks at 23.5, 14.5, 12, 10 and 4 °2 θ . Consequently, there was significant decrease in intensity of major OCBZ crystalline peaks in diffractogram of OCBZ Na-CMC, OCBZ HPMC and OCBZ chitosan microcrystals. The most decrease observed was among OCBZ Na-CMC microcrystal which suggests a favorable interaction between OCBZ and carrier Na-CMC. The partial loss of crystallinity of drug observed may also be attributed to physical presence of Na-CMC.

SEM studies performed gave a strong support to the results of DSC and XRPD.

Figure 2.4.20 DSC thermograms for OCBZ Na-CMC, OCBZ HPMC and OCBZ chitosan microcrystals.

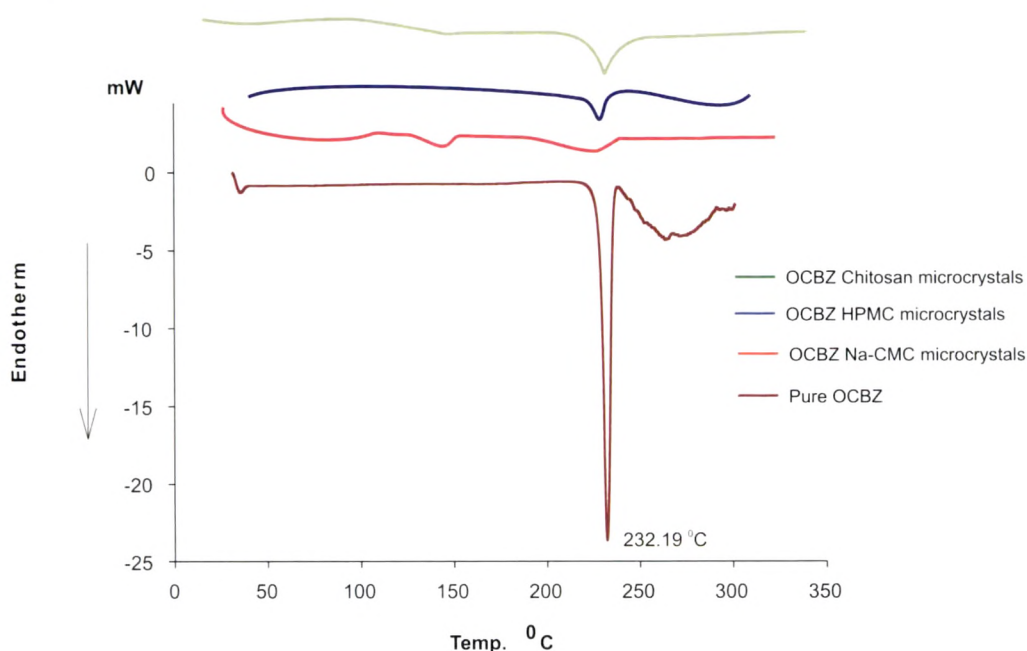
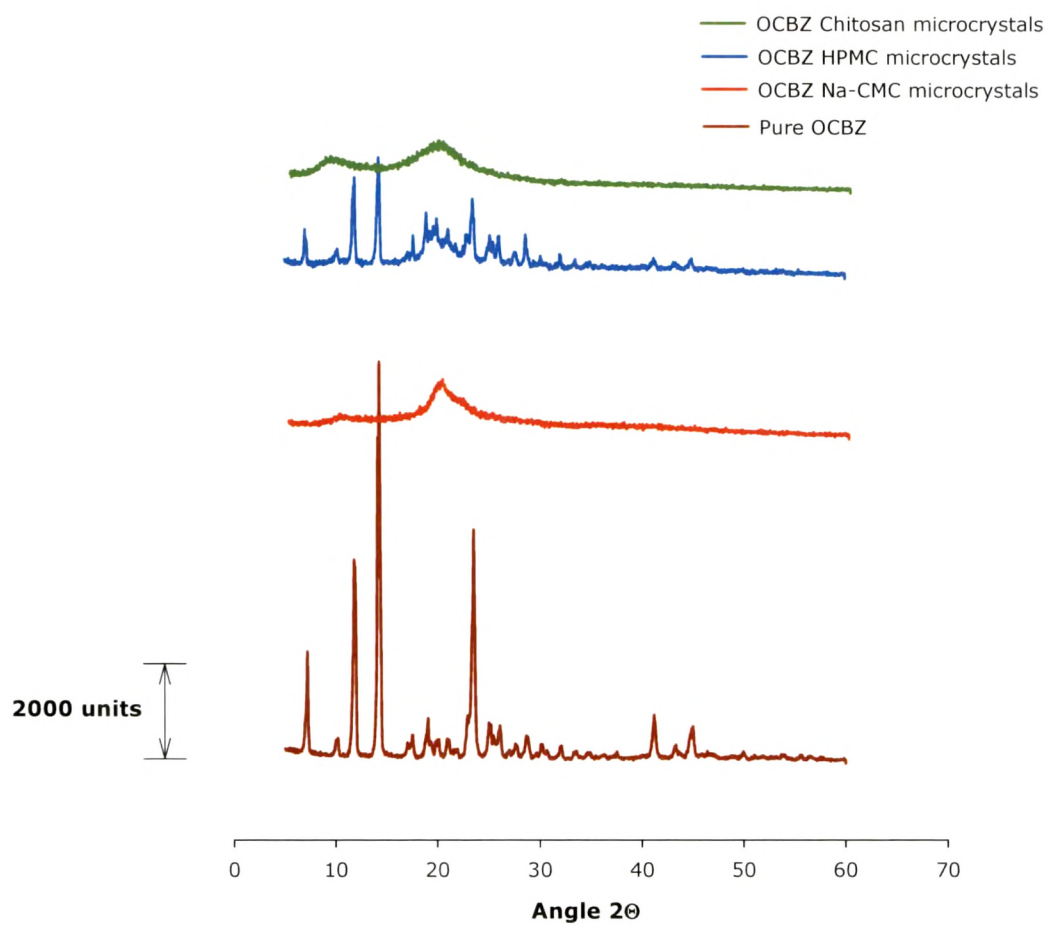


Figure 2.4.21 XRPD results for Pure drug, Chitosan, Physical mixture and Optimized batch of microcrystals.



2.4.2.5.4. SEM studies

The microphotographs of pure OCBZ and optimized batch of microcrystals of OCBZ Na-CMC, OCBZ HPMC and OCBZ chitosan are shown in Figure 2.4.22, Figure 2.4.23, Figure 2.4.24 and Figure 2.4.25 respectively. Pure drug was observed in the form of a mixture of some large crystals ranging from 20 - 600 μm) with microparticles. Microcrystals formed in various batches of experimental design revealed significant changes in particle shape and surface topography due to impact of spray drying process. However in figure only images of optimized batches are shown. For all the 3 polymers the microcrystals appeared as smooth spherical agglomerates with slight particle aggregation as well as residual crystals, to a small extent adhered to particles.

Figure 2.4.22 SEM image of Pure crystalline OCBZ.



Figure 2.4.23 SEM image of optimized batch of microcrystals of OCBZ with Na CMC.

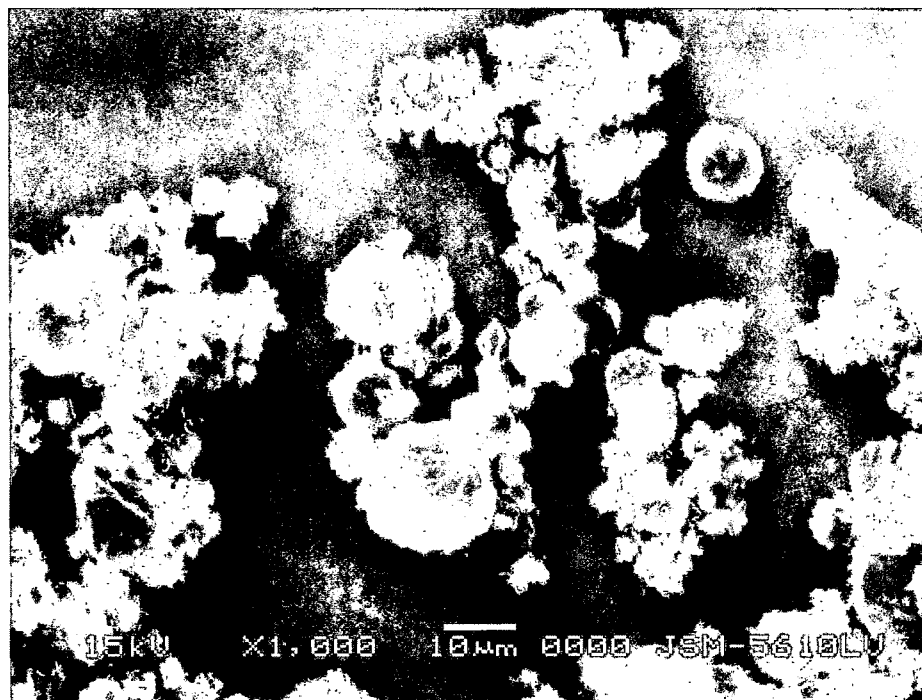


Figure 2.4.24 SEM image of optimized batch microcrystals of OCBZ with HPMC.

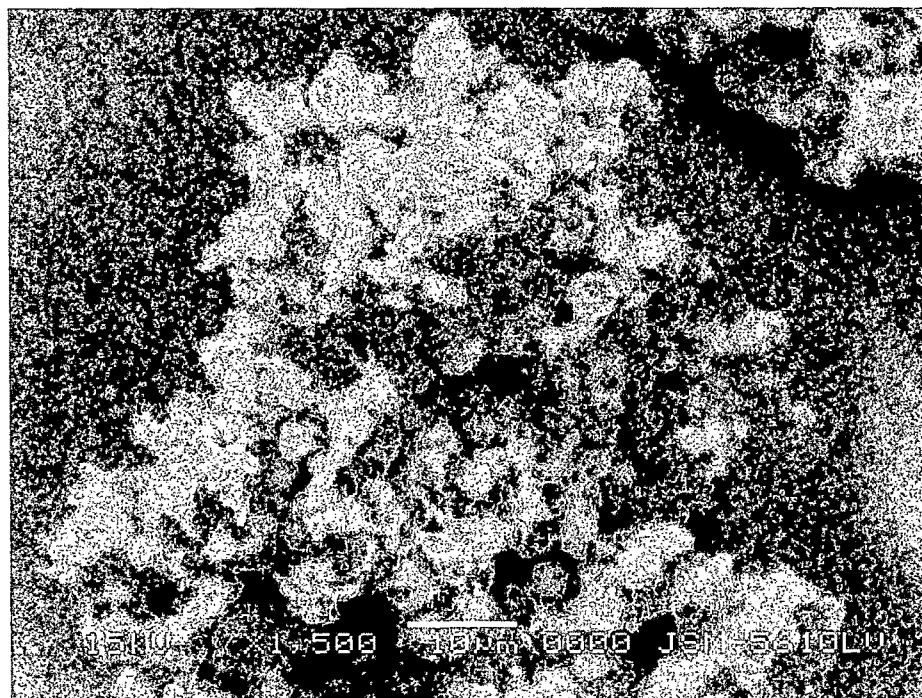


Figure 2.4.25 SEM image of optimized batch microcrystals of OCBZ with chitosan.

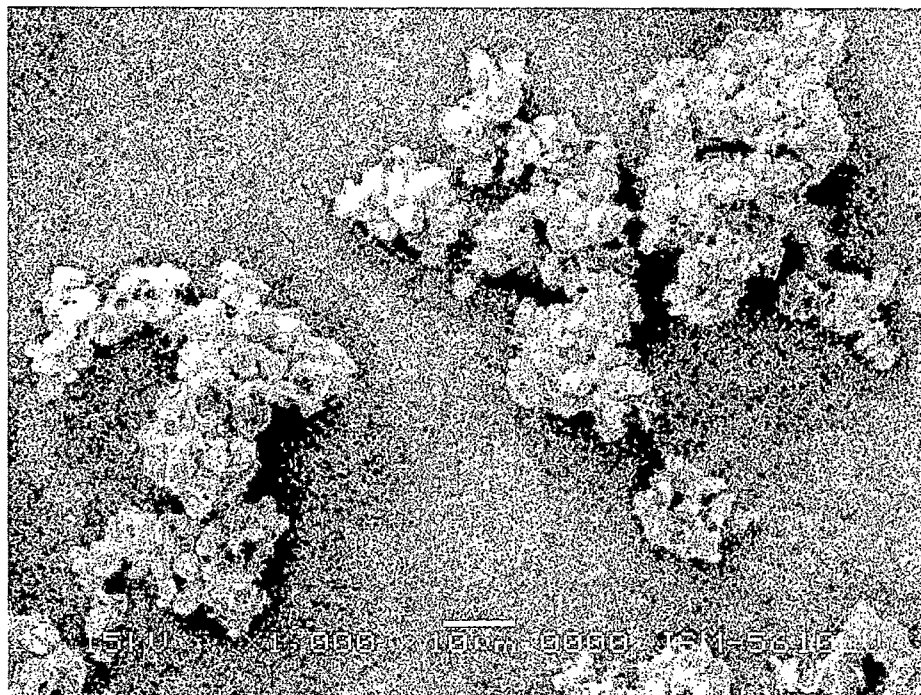
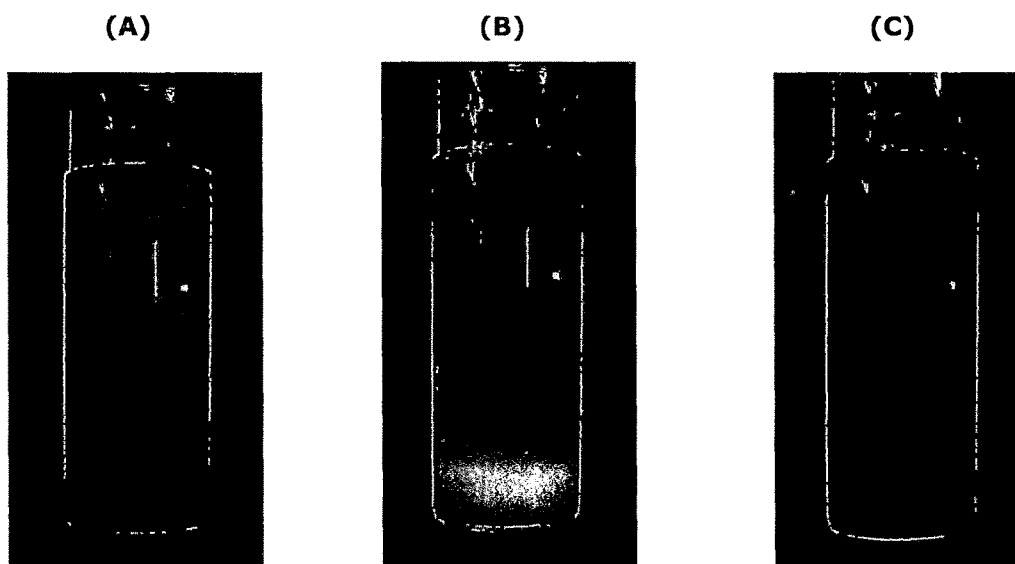


Figure 2.4.26 Microcrystal dispersion of (A) CBZ Na-CMC, (B) CBZ HPMC and (C) CBZ chitosan microcrystals.

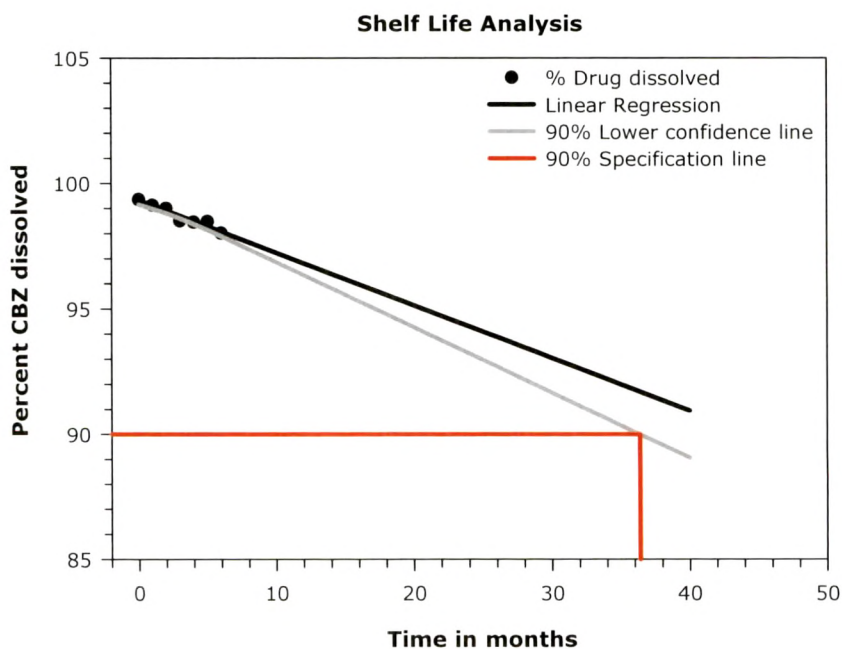


2.4.2.6. Stability studies for CBZ and OCBZ microcrystals systems

Microcrystals of CBZ and OCBZ with Na-CMC showed promising drug dissolution results, hence they were subjected to stability studies. Powders of these microcrystals were packaged in high density polyethylene (HDPE) bottles with polypropylene (PP) caps (foamed polyethylene and pressure sensitive liner). The systems were subjected to stability testing according to the International Conference on Harmonization guidelines for zone III and IV. The packed containers of prepared microcrystals were kept for accelerated ($40^{\circ}\pm 2^{\circ}\text{C}/75\pm 5\%$ relative humidity) and long term ($30^{\circ}\pm 2^{\circ}\text{C}/65\pm 5\%$ relative humidity) stability in desiccators with saturated salt solution for up to 6 months. Long term stability samples were to be analyzed only if samples for accelerated studies ($40^{\circ}\pm 2^{\circ}\text{C}/75\pm 5\%$ RH) fail in analysis. A visual inspection (for coloration of microcrystals content), dissolution testing and pure drug content estimation was carried out every 30 days for the entire period of stability study.

Stability data of microcrystals was extrapolated using linear regression tool for the determination of shelf life of product. Figure 2.4.27 shows the extrapolated accelerated stability data for shelf-life calculation of CBZ Na-CMC microcrystals. The calculated shelf life was found to be 36.36 months (2.98 years).

Figure 2.4.27 Extrapolation of accelerated stability data of CBZ Na-CMC microcrystals for shelf-life calculation.



Similarly for OCBZ Na-CMC microcrystals stability data of was extrapolated using linear regression tool for the determination of shelf life of product. Figure 2.4.28 shows the extrapolated accelerated stability data for shelf-life calculation of OCBZ Na-CMC microcrystals. The calculated shelf life was found to be 26.77 months (2.20 years).

Figure 2.4.28 Extrapolation of accelerated stability data of OCBZ Na-CMC microcrystals for shelf-life calculation.

